Journal of Research of the National Bureau of Standards Vol. 49, No. 4, October 1952 Research Paper 2358

Mass Spectra of the Tetramethyl Compounds of Carbon Silicon, Germanium, Tin, and Lead [1]

Vernon H. Dibeler

Mass spectra of $C(CH_3)_4$, $Si(CH_3)_4$, $Ge(CH_3)_4$, $Sn(CH_3)_4$, and $Pb(CH_3)_4$ were obtained with a Consolidated 21–103 mass spectrometer. Isotopic abundances of carbon, silicon, germanium, tin, and lead were obtained from the observed spectra and used to calculate the monoisotopic spectra. The mass spectra of the Group IV tetramethyls are qualitatively similar. The principal ion in each case results from the dissociation of one methyl group. The molecule ion and ions resulting from the dissociation of hydrogen atoms are rare. Hydrides of the atom ions and the mono-, di-, and tri-methyl ions were observed. Some evidence is pointed out for the possible formation of the CH_3^+ ion and the $C_2H_3^+$ ion in neopentane as hydrides of the central carbon atom.

1. Introduction

A previous paper [1] [2] reported the mass spectra of several organolead and organomercury compounds. A brief discussion was given of the dissociation processes in the mass spectrometer and of the applicability of these molecules to the isotopic analysis of the metallic elements. The results of a similar study of the Group IV tetramethyl compounds are reported here.

Although the mass spectra of both neopentane and lead tetramethyl have been reported previously [1, 2], significant instrumental modifications have since been made, so that these spectra were remeasured to simplify direct comparison with the other compounds.

The isotopic abundance of germanium, tin, and lead were first measured by Aston [3] by using the alkyl compounds of these elements. Because of hydride formation during the ionization and dissociation processes, recent measurements have been made on inorganic halide compounds of these elements. The low vapor pressure of the tin and lead halides, however, introduces experimental difficulties not encountered when using the metal alkyls. Furthermore, this research and others recently reported [1, 4] indicate that, in spite of the necessary corrections to the spectra for ions resulting from dissociation processes and hydride formation, isotopic abundances of the metals can be measured with a precision comparable to that obtained from measurements on inorganic halides.

2. Experimental Details

Mass spectra were obtained with a Consolidated 21–103 mass spectrometer. The energy of the ionizing electrons was nominally 70 volts and the temperature of the ion source was 250° C. The metastable suppressor, which also acts as a virtual slit at the collector end of the analysor, was adjusted to give a resolution of about 1 in 300. Routine techniques and procedures were used to obtain all the data.

Liquid samples were introduced into the reservoir through a glass frit covered with liquid gallium. Neopentane and silicon tetramethyl were introduced by evaporation from liquid stored in glass ampoules with internal break seals. The pressure of the samples in the reservoir was measured with a micromanometer [5].

The neopentane was National Bureau of Standards Standard Sample 299, with a stated purity of 99.96 ± 0.02 mole percent.

Silicon tetramethyl was kindly supplied by the General Electric Research Laboratory. A trace of methyl bromide was the only impurity of the material observed in the mass spectrum.

Germanium tetramethyl was prepared from methyl magnesium bromide and germanium tetrachloride in dibutyl ether. The final product, obtained in low yield, contained only a few tenths of a mole percent impurities, principally butyl ether. A second preparation from zinc dimethyl and germanium tetrachloride [6] gave nearly quantitative yields of high-purity product.

Tin tetramethyl was kindly supplied by the Metal and Thermit Corporation, New York. Total impurities, principally toluene, diethyl ether, and benzene, were estimated to be less than 2 mole percent.

Lead tetramethyl, obtained from the Ethyl Corporation, was the same sample as that previously described [1].

3. Results

In order to compare the relative probabilities of the various dissociation processes in these molecules, it is first necessary to calculate the spectra that would be obtained if all the constituent elements were monoisotopic (that is, the monoisotopic spectrum). For this purpose the isotopic abundances of the elements, except hydrogen, are best calculated from the observed spectra. These values, calculated as described below and summarized in table 2, are compared with previously reported values.

Table 1 presents in brief form portions of the polyisotopic spectra [3] of the tetramethyl compounds to illustrate the calculations of the isotopic abundances and of the monoisotopic spectra. Excepting the

[1] Presented at the Pittsburgh Conference on Analytical Chemistry and Applied Spectroscopy, March 1952.

[2] Figures in brackets refer to references at the end of the paper.

[3] The detailed polyisotopic spectra of neopentane and lead tetramethyl have been published, and the spectra of the silicon, germanium, and tin compounds will be submitted for publication in reference [2].

UNIVERSITY OF MICHIGAN LIBRARIES

spectrum of neopentane, the contributions of ions containing C^{13} and D atoms have been subtracted as described below. Thus the organometallic compounds are polyisotopic with respect to the central metallic atom only. The relative ion abundances are given in the conventional way, that is, relative to the most abundant ion.

It is possible to calculate the C^{12}/C^{13} abundance ratio in neopentane from the ion abundances in the C_4 group by assuming a value for the abundance of deuterium. Except for a negligible correction, all of the 55 peak (column 1, table 1) is attributed to the $C_4^{12}H_7^+$ ion. A sufficiently accurate calculation of the contribution of the $C^{13}C_3^{12}H_7^+$ ion to the 56 peak is obtained by multiplying the abundance of the 55 peak (3.06) by an approximate value for the C^{13} abundance times the number of carbon atoms, $(3.06)(0.01)(4)=0.12$. This contribution is subtracted from the 56 peak (3.80) to give the abundance of the $C_4^{12}H_8^+$ ion (3.68). Similarly, the correction to the 57 peak for the $C^{13}C_3^{12}H_8^+$ ion is given by $(3.68)(0.01)(4)=0.15$, and the corrected abundance of the $C_4^{12}H_9^+$ ion is $100-0.15=99.85$. Next, the small but measurable contribution of the $C_4^{12}H_8D^+$ ion to the 58 peak is calculated by assuming an H/D ratio of 6700 [7]. This corresponds to a deuterium abundance of 0.0149 atom percent. Thus the contribution $(99.85)(0.000149)(9)=0.13$ is subtracted from the 58 peak (4.53) to give the abundance of the $C^{13}C_3^{12}H_9^+$ ion (4.40). The observed C^{13} abundance is therefore 1.10 percent of the C^{12} abundance. This corresponds to 1.08_8 atom percent C^{13}.

By using the observed C^{13} abundance and the deuterium abundance given above, the monoisotopic spectrum of neopentane has been obtained (column 2, table 3) by subtracting from the polyisotopic spectrum the separate contributions of ions containing C^{12} and D atoms and ions containing C^{13} and H atoms. It can be shown that contributions of ions containing more than one C^{13} atom or ions containing C^{13} and D atoms have a negligible effect on these calculations. The organometallic spectra given in table 1 were similarly corrected for contributions of ions containing C^{13} and D atoms. However, the monoisotopic spectra with respect to the metal ions were calculated in the more precise way previously illustrated in detail for lead [1].

TABLE 1. *Partial polyisotopic spectra of the Group IV tetramethyl compounds for 70-v electrons*

m/e	$C(CH_3)_4$	m/e	$Si(CH_3)_4$	m/e	$Ge(CH_3)_4$	m/e	$Sn(CH_3)_4$	m/e	$Pb(CH_3)_4$
27	16.98	28	3.52	70	4.37	112	0.61	204	1.82
28	2.85	29	7.91	71	6.43	113	.33	205	0.17
29	35.77	30	0.78	72	5.83	114	.42	206	36.78
30	0.82	31	3.71	73	10.34	115	.45	207	31.70
				74	10.06	116	9.08	208	73.65
41	43.78	42	4.20	75	11.56	117	9.76	209	6.62
42	3.18	43	15.98	76	1.77	118	17.56		
43	1.60	44	3.82	77	2.80	119	13.61	217	0.07
44	0.52	45	12.55			120	23.07	218	.64
		46	0.69	85	13.67	121	11.21	219	4.29
54	.23	47	.41	86	4.28	122	2.95	220	5.70
55	3.06			87	21.86	123	1.60	221	53.00
56	3.80	58	2.06	88	9.94	124	3.39	222	43.26
57	100.0	59	2.42	89	26.39	125	2.06	223	90.84
58	4.53	60	0.17	90	2.54			224	0.90
				91	8.91	157	3.01		
71	0.02	71	.42	92	0.10	158	0.02	249	2.56
72	.01	72	.92			159	2.06	250	0.49
		73	100.0	114	.33	160	1.43	251	52.44
		74	4.97	115	56.64	161	45.03	252	41.11
		75	3.25	116	0.45	162	24.18	253	100.0
				117	75.61	163	74.71	254	1.00
		88	0.77	118	21.82	164	27.45		
		89	.04	119	100.0	165	100.0	266	0.11
		90	.03	120	0.17	166	0.32	267	.08
				121	21.15	167	14.29	268	.22
						168	0.22		
				134	0.41	169	17.77		
						170	0.07		

TABLE 2.—*Summary of isotopic abundances used in computing the monoisotopic spectra of the Group IV tetramethyl compounds*

Carbon	C^{12}/C^{13}
This research	91.0±0.5 [a]
CO_2, petroleum [8]	91.2
CO_2, limestone [8]	88.3

Silicon	Si^{28}	Si^{29}	Si^{30}
This research	92.41±0.3	4.57±0.05	3.01±0.05
Bainbridge and Nier [7]	92.27±0.09	4.68±0.05	3.05±0.03

Germanium	Ge^{70}	Ge^{72}	Ge^{73}	Ge^{74}	Ge^{76}
This research	20.64±0.2	27.50±0.3	7.72±0.08	36.43±0.3	7.71±0.08
Bainbridge and Nier [7]	20.55	27.37	[b] 7.67	36.74	7.67

Tin	Sn^{112}	Sn^{114}	Sn^{115}	Sn^{116}	Sn^{117}	Sn^{118}	Sn^{119}	Sn^{120}	Sn^{122}	Sn^{124}
This research	0.99±0.05	0.68±0.03	0.36±0.03	14.49±0.1	7.71±0.08	24.09±0.2	8.59±0.08	32.52±0.3	4.77±0.05	5.81±0.06
Bainbridge and Nier [7]	.95	.65	.34	14.24	7.57	24.01	8.58	32.97	4.71	5.98

Lead	Pb^{204}	Pb^{206}	Pb^{207}	Pb^{208}
This research	1.32±0.02	26.67±0.2	20.50±0.2	51.50±0.3
Reference [1] (21–102 MS)	1.31	26.79	20.55	51.35

[a] Estimated limit to instrumental errors possibly present.
[b] The value of 7.61% for Ge^{73} given in [7] is the result of a misprint in the original reference, as noted by Graham, et al. [12].

The partial spectrum of silicon tetramethyl is given in column 2, table 1. As in the carbon compound, the trimethyl ions (m/e=73, 74, and 75) are the most suitable for calculating the isotopic abundance of silicon. As no 76 peak was observed, the absence of a monohydride of the trimethyl ion is assumed. The ratio $Si(CH_3)_3H^+/Si(CH_3)^+_3$ is estimated to be less than 0.002. However, the presence of ions m/e=71 and 72, indicates the necessity of making corrections for contributions of ions resulting from the dissociation of hydrogen atoms. To a good approximation, the abundances of the ions $Si(CH_3)_2CH^+$ and $Si(CH_3)_2CH_2^+$ relative to $Si(CH_3)_3^+$ are given by the ratio of the peaks 71:72:73= 0.0042:0.0092:1.00. As the 75 peak is attributed to $Si^{29}(CH_3)_3^+$ only, multiplying its abundance (3.25) by the above ratios gives the contributions of the $Si^{29}(CH_3)_2CH_2^+$ (0.03) and the $Si^{30}(CH_3)_3CH^+$ (0.01) ions to the 74 and 73 peaks, respectively. Subtracting the 0.03 from the 74 peak (4.97) gives the corrected $Si^{29}(CH_3)_3^+$ ion contribution. Multiplying this by the above ratios gives the ions containing Si^{29} and permits calculation of the corrected $Si^{30}(CH_3)_3^+$ ion. The isotopic abundance of silicon calculated from the trimethyl ions appears in table 2. The monoisotopic spectrum calculated therefrom appears in column 3, table 3.

The partial polyisotopic spectrum of germanium tetramethyl is given in column 3, table 1. Again, the isotopic abundance is calculated from the trimethyl ions (m/e=115 to 121). As no m/e221= was observed, the absence of a monohydride of the trimethyl ion was assumed. The ratio $Ge(CH_3)_3H^+/Ge(CH_3)_3^+$ was estimated less than 0.001. The presence of a 114 peak, however, indicated the dissociation of one hydrogen atom with an approximate abundance ratio $Ge(CH_3)_2CH_2^+/Ge(CH_3)_3^+$= 0.0058. Using this value the contributions of the isotopic ions of $Ge(CH_3)_3^+$ and of $Ge(CH_3)_2CH_2^+$ were obtained. However, a small residual remained on the m/e=120 peak corresponding to a monohydride ratio of $Ge(CH_3)_3H^+/Ge(CH_3)^+_3$=0.0005. This small correction was included, and the isotopic abundance was calculated as described for silicon. The observed values are given in table 2. The monoisotopic spectrum appears in column 4, table 3.

The partial spectrum of tin tetramethyl is given in column 4, table 1. Because of the large number of isotopes and the possibility of overlapping of ions containing different numbers of carbon atoms, the abundances of the tin isotopes were calculated from the Sn^+ ions at m/e=112 to 124. This results in some loss in precision. A first approximation of the SnH^+/Sn^+ ratio is given by the ratio of peaks 125/124. Starting from m/e=116 the corrected abundances of Sn^{117}, Sn^{118}, Sn^{119}, and Sn^{120} are calculated. Then the ratio 121/120=0.561 gives the more nearly correct value for the relative abundance of the monohydride ion. There are four points at which to compare the computed with the observed values. At m/e=113, the computed and observed abundances of $Sn^{112}H^+$ are 0.34 and 0.33, respectively. At m/e=121, the computed and observed values of $Sn^{120}H^+$ are 11.20 and 11.21, respectively. At m/e=123, the $Sn^{122}H^+$ values are 1.64 and 1.60, and at m/e=125, the $Sn^{124}H^+$ values are 2.00 and 2.06. The agreement between computed and observed abundances is considered good, as errors are cumulative. The isotopic abundance of the tin isotopes are given in table 2, and the monoisotopic spectrum is summarized in column 5, table 3.

Portions of the polyisotopic spectrum of lead tetramethyl are given in column 5, table 1. The method of calculating the isotopic abundance from the Pb^+ ions and the derivation of the monoisotopic spectrum have been described [1]. The isotopic abundances given in table 2 are not compared with values reported by other workers because of the well-known variation of abundance with origin of the sample. The source of the lead used in the present sample is not known.

TABLE 3.—*Monoisotopic spectra of the tetramethyl compounds of carbon, silicon, germanium, tin, and lead for 70-v electrons*

Ion [a]	Relative abundance				
	$C(CH_3)_4$	$Si(CH_3)_4$	$Ge(CH_3)_4$	$Sn(CH_3)_4$	$Pb(CH_3)_4$
C	0.10	0.04	0.16	0.26	0.25
CH	.25	.18	.32	.71	.78
CH_2	1.25	.82	1.27	2.72	2.98
CH_3	9.27	5.07	5.41	11.8	12.4
X		3.51	7.52	20.2	71.3
XH		7.73	11.2	11.3	6.65
XH_2		0.28	0.14		
XH_3		3.45	.47		
XC		0.08	0.47	0.34	0.80
XCH	0.14	1.03	.32	1.58	3.46
XCH_2	1.94	4.21	4.54	7.26	6.80
XCH_3	17.0	15.7	22.7	36.1	90.9
XCH_4	2.47	18.6	0.47	0.27	0.90
XCH_5	35.8	11.9	5.20		
XC_2	0.05	0.17	0.14		0.03
XC_2H	.86	2.66	1.13		.13
XC_2H_2	2.01	0.46	0.05		
XC_2H_3	17.3	2.58	.86		.06
XC_2H_4	1.31	0.25	.05		
XC_2H_5	43.8	1.75	.91	0.22	.55
XC_2H_6	1.70	1.97	6.30	22.6	25.3
XC_2H_7	1.53	2.26	1.43	1.42	.45
XC_3	0.02	0.02			
XC_3H	.26	.21			
XC_3H_2	1.34	.27			
XC_3H_3	1.41	.18			
XC_3H_4	0.29	.02			
XC_3H_5	1.48	.07			
XC_3H_6	0.16	.28			
XC_3H_7	3.06	.41			
XC_3H_8	3.67	.90	0.58	0.96	1.00
XC_3H_9	100.0	100.0	100.0	100.0	100.0
XC_3H_{10}			0.05	0.33	0.95
XC_3H_{11}	0.01	0.78	.42	.84	.22

[a] *X* represents the central atom of each of the five compounds.

4. Discussion

4.1. Measurements of Isotopic Abundance

The uncertainties indicated in table 2 are estimated errors probably present in the recording system only. For the principal isotopes, the reproducibility was at least a factor of 10 better than the estimated error. The purpose of comparing the present results with previously reported values is merely to show the extent of agreement of values obtained by using organometallic compounds and routine operating

UNIVERSITY OF MICHIGAN LIBRARIES

procedures with values obtained in other laboratories by using inorganic compounds and specialized techniques.

Nier and Gulbransen [8] and Murphey and Nier [9] have demonstrated the variation in the natural abundance of C^{13} with the source of material. Apparently C^{13} is concentrated in limestone, whereas C^{12} is concentrated in plant material. Although the exact origin of the neopentane sample is not known, it very probably contained carbon from petroleum sources only. The observed value of the C^{12}/C^{13} ratio is consistent with this probability. The ratio is also consistent with values obtained from a variety of hydrocarbons, most of them certainly from petroleum sources, measured routinely in the Bureau's Mass Spectrometry Laboratory over a period of several years.

The isotopic abundances of silicon, germanium, and tin are in good agreement with the values for these elements adopted by Bainbridge and Nier [7]. This is particularly interesting in view of the possible complexity of the dissociation processes of the organometallic compounds compared with the inorganic molecules usually measured. In the case of the organometallics, it is apparently possible to make the corrections for the contributions of ions containing C^{13} and D atoms, of hydride ions, and of ions resulting from the dissociation of H atoms with a precision comparable with the uncertainty in recording the mass spectra. Furthermore, routine operating procedures and techniques devised for standard gas analysis apparently provide a degree of reproducibility and accuracy comparable with that of previously published results.

The present value for the isotopic abundance of lead is a remeasurement of the same sample previously measured [1] with a Consolidated 21–102 instrument. Although major modifications were made to the ion source and ion collector in the interval between the two series of measurements, the values agree within the estimated error. Because of the well-known variation in the isotopic abundance of lead, it is not very instructive to compare observed values of a sample of unknown origin with previously reported data. The present results, probably for lead of mixed origins, are within the range of isotopic abundances reported by Nier and coworkers [10] for lead from various ores.

Some advantages of using lead alkyls rather than inorganic lead halides for isotopic abundance measurements have been discussed [1, 4]. For example, no appreciable background of lead tetramethyl remains in the ion source and analyzer tube after a very few minutes of pumping. Furthermore, in the sample-handling system used in this work less than 0.1 percent of the original sample remains in the reservoir or on the walls after five minutes of evacuation. Isolating the reservoir from the pumps at this point causes no appreciable increase in background in one-half hour. This would seem to indicate that by exercising reasonable caution, memory effects are considerably less of a problem in the case of the lead tetramethyl than in the case of lead halides. Also, the deposition of metallic lead on insulators and other parts of the ion source is not an important factor in the case of lead alkyls. The introduction of lead tetramethyl for several hours of operation produces no noticeable effects on the operation of the ion source.

Unfortunately, the formation of hydrides rules out the use of organometallic compounds in a search for rare isotopes. Also, precise correction for hydride contributions depends on previous knowledge of the absence of an isotope with a mass number equal to that of the hydride of a relatively abundant isotope.

4.2 Dissociation Processes

The mass spectra of the five compounds are qualitatively similar. The very low relative abundance of the molecule ion and the maximum abundance of the trimethyl ion are characteristic of molecules exhibiting this type of symmetry. The abundances of ions resulting from the dissociation of two, three, and four methyl groups increase in fairly regular fashion with increasing atomic number of the central atom. This is particularly apparent in the abundances of the ions $C^+ < Si^+ < Ge^+ < Sn^+ < Pb^+$. The decreasing resemblance to the hydrocarbon spectrum is also apparent with increasing atomic number. The spectra of tin and lead tetramethyl are simpler than those of silicon and germanium, containing fewer hydride ions and ions resulting from the dissociation of hydrogen atoms.

Monohydrides of the metal atoms were observed in all of the organometallics. In addition, di- and trihydrides of the silicon and germanium atom ions were observed. The abundance of the trihydride ions increases from zero for tin and lead to 3.45 for SiH_3^+, whereas the abundance of the methyl ion decreases from 12.4 in lead tetramethyl to 5.07 in silicon tetramethyl. The abundance of the CH_3^+ ion in neopentane (9.27) indicates that some of the methyl ions in this compound may originate as trihydrides of the central carbon atom. Hydrides of the monomethyl ions were also observed in the organometallic compounds. The abundances of the dihydrides, XCH_3^+, in carbon, silicon, and germanium (like the XCH_3^+ ions) decrease with increasing atomic number of the central atom. In the metal alkyls, these ions can only be accounted for by rearrangement of hydrogen atoms. The abundance of the $C_2H_3^+$ ion in neopentane (35.8) compared with $Si(CH_3)H_2^+$ (11.9) and $Ge(CH_3)H_2^+$ (5.20) and zero for the corresponding tin and lead ions again indicates that at least part of the $C_2H_3^+$ results from the rearrangement of hydrogen atoms. This is in disagreement with the experimental evidence reported by Langer and Johnson [11] indicating that rearrangement of methyl groups is the source of these ions. Rearrangements of methyl radicals to give hydrocarbon ions containing two carbon atoms were observed in all of the metal alkyl spectra except silicon tetramethyl, in which Si^+ ions partially interferred. In each case, however, the most abundant of these ions ($m/e=27$) was less than 1 percent of the trimethyl ion and their relative abundances showed no

elation to the ethane spectrum or to the analogous ons in neopentane.

Unlike the monomethyl hydrides, the abundance f the dimethyl hydrides, $X(CH_3)_2H^+$, is a maximum or $Si(CH_3)_2H^+$. Furthermore, the abundance of the rimethyl hydrides, $X(CH_3)_3H^+$, increase with increasing atomic number of the central atom. The omplicated manner in which the abundance of ydride ions varies may depend on steric effects of he several methyl groups surrounding the central tom.

Except for the rare tetramethyl ions and the monoydride of the trimethyl ions of germanium, tin, and ead, a maximum number of three atoms and/or ethyl groups attached to the central atom is the eneral rule. This would suggest that ionization ccurs by the loss of a bonding electron between the entral atom and a methyl group.

The author gratefully acknowledges helpful discussions and continual encouragement given by Dr. Fred L. Mohler throughout the course of this work.

5. References

[1] V. H. Dibeler and F. L. Mohler, J. Research NBS **47**, 337 (1951) RP2259.
[2] API tables of mass spectral data, Carnegie Institute of Technology, Pittsburgh, Pa.
[3] F. W. Aston, Mass spectra and isotopes, 2d ed. (Longmans, Green & Co., New York, N. Y., 1941).
[4] C. B. Collins, J. R. Freeman, and J. T. Wilson, Phys. Rev. **82**, 966 (1951).
[5] V. H. Dibeler and F. Cordero, J. Research NBS **46**, 1 (1951) RP2167.
[6] J. H. Lengel and V. H. Dibeler, J. Am. Chem. Soc. **74**, 2683 (1952).
[7] K. T. Bainbridge and A. O. Nier, Relative isotopic abundances of the elements, Preliminary Report No. 9, National Research Council, Washington, D. C.
[8] A. O. Nier and E. A. Gulbransen, J. Am. Chem. Soc., **61**, 697 (1939).
[9] B. F. Murphey and A. O. Nier, Phys. Rev. **59**, 771 (1941).
[10] A. O. Nier, R. W. Thompson, and B. F. Murphey, Phys. Rev. **60**, 112 (1941).
[11] A. Langer and P. Johnson, Symposium on the use of isotopes in petroleum chemistry, Chicago Meeting of the American Chemical Society, 1950.
[12] R. P. Graham, J. Macnamara, I. H. Crocker, and R. B. MacFarlane, Canadian J. Chem. **29**, 90 (1951).

Washington, June 19, 1952.

UNIVERSITY OF MICHIGAN LIBRARIES

Journal of Research of the National Bureau of Standards Vol. 49, No. 4, October 1952 Research Paper 2359

Determination of Planeness and Bending of Optical Flats

Walter B. Emerson

The true contours, undistorted by gravitational bending, were determined for four 10 ⅝-inch-diameter standard optical flats of fused quartz. The bending deflections of these flats were determined by a method based upon the differential bending with thickness of the flats. Bending deflection curves of a flat supported at three points equidistant from the center of the flat and equidistant from each other were obtained. The locus of the bending deflections at the center of a flat, similarly supported but with supports at different distances from the center, approximates a straight line. This paper describes the method used to obtain the true contours and the bending deflection curves of the flats, and compares the bending values so determined with theoretically derived values.

1. Introduction

One activity of the National Bureau of Standards is to determine the deviation from a plane of surfaces of optical flats submitted for calibration. Usually these are disks of fused quartz used as working standards by makers of optical elements. Disks 10 in. in diameter, with specified maximum deviation from a plane of 0.1 fringe (approximately 0.000,001 in.) are frequently submitted. These are tested by interferometric comparison with the Bureau's 10 ⅝-in.-diameter fused quartz standard planes, the contour of which should be known to a few hundredths of a fringe to make the tests valid to the required tolerance.

It is commonly assumed that by intercomparison of three surfaces, the deviation of each surface from a plane may be determined. This is true if the flats are similarly supported and are identical except for differences in surface contour. Otherwise, consideration must be given to the deflection of each flat when supported in its position of test. Even in the case of support of the lower flat in mercury, some bending attributable to nonuniform distribution of forces by the weight of the upper flat and by surface-tension effects at the edge of the lower flat is to be expected. The theory of the bending of circular plates has been developed by Nádai [1, 2, 3][1] and Timoshenko [4], and from these theoretical considerations an equation was formulated for circular plates supported at the vertices of an inscribed equilateral triangle whereby the gravitational bending deflection along a diametric line parallel to two of the supports may be determined with respect to a plane passing through the points of support. The results, based on a value $\nu=0.14$ for Poisson's ratio, are plotted as a dimensionless function from which the bending along a given diameter of a quartz plate may be readily determined.

In addition to deflections caused by bending, deflections are present because of shearing stresses and stress normal to the face of the plate. When these stresses are all taken into account for the case of a plate simply supported at the edges, Timoshenko [4] gives the following equation for the lateral deflection:

$$w=\frac{q}{64D}(a^2-r^2)\left(\frac{5+\nu}{1+\nu}a^2-r^2\right)+\frac{qh^2}{8D}\frac{3+\nu}{6(1-\nu^2)}(a^2-r^2), \tag{1}$$

[1] Figures in brackets indicate the literature references at the end of this paper.

where

w=lateral deflection,
q=lateral pressure,
D=flexural rigidity$=Eh^3/12\ (1-\nu^2)$,
E=Young's modulus,
a=plate radius,
r=distance from center,
h=plate thickness,
ν=Poisson's ration.

For plates acted on by gravitational forces, the lateral pressure is given by

$$q=\rho g h, \tag{2}$$

where ρ is the density and g the acceleration of gravity. Substituting (2) into (1) and replacing D by $Eh^3/12\ (1-\nu^2)$ gives

$$w=\left(\frac{1}{h^2}\right)\frac{\rho g}{16E}3(1-\nu^2)(a^2-r^2)\left(\frac{5+\nu}{1+\nu}a^2-r^2\right)+\frac{\rho g}{4E}(3+\nu)(a^2-r^2). \tag{3}$$

It is seen that the first term in this equation varies inversely as the thickness squared and the second term is independent of thickness. Relations similar to (3), but depending differently on r, apply when the plate is supported by other means than simple support. One can express the deflection of the plate as

$$w=\frac{1}{h^2}f_b(r)+f_s(r), \tag{4}$$

where the functions f_b, for bending, and f_s, for shear and lateral pressure depend only on the means of support

It should be pointed out that eq (3) does not include the effect of local deformation near points of concentrated load. These will be shown to be small, by measurement, for the plates tested.

Relationship (4) furnishes a basis for determining the true contour, undistorted by bending, shear, and lateral pressure effects, of the surfaces of optical flats.

A method for determining the *true contour* and the *bending* (the first term in relation (4)) of optical flats is presented and this method is applied to determinations of contour and to evaluation of the bending of four optical flats, and compares the bending values so determined with the values obtained according to theory.

UNIVERSITY OF MARYLAND LIBRARIES

2. Methods

2.1 Determination of True Contours

If a circular plate, resting on supports at the vertices of an inscribed equilateral triangle, supports a similar plate on supports directly above those for the lower plate, the surfaces of the plates tend to sag. If the surfaces were originally plane, the upper surface of the lower plate will now be concave, *and* the adjacent surface of the upper plate will be convex by an equal amount if the plates are of equal thickness, and by a greater amount if the upper plate is thinner. With three transparent plates of like material, properties, and diameter the *true contour* of their surfaces (that is, if the plates were supported uniformly and did not bend) may be determined by intercomparison of the plates, but no knowledge of the amount the plates bend will be obtainable. However, intercomparison of a series of plates that differ only in thickness will yield not only the true contour of the surfaces but also an evaluation of the change in contour (bending deflection) of the surfaces caused by the weight of the plates.

The following fused-quartz optical flats having a nominal diameter of 10 5/8 in. were available for intercomparison in this investigation:

Flat number	Diameter	Thickness (t)	t^3
	Inches	*Inches*	
1	10.66	1.428	2.039
2	10.61	1.626	2.644
3	10.59	2.50	6.250
4	10.58	2.50	6.250

Flats 1 and 2, which have served as standard planes at the Bureau for the past 30 years, contain numerous strias and inclusions, and the quality of their materials is inferior to that of flat 3, which was recently purchased, and also of flat 4, which was loaned for this investigation by the maker of flat 3. Flats 3 and 4 are slightly wedge-shaped, and the listed thickness is the average of measurements at several places around the circumference. For the purpose of this investigation, flats 3 and 4 are considered identical, except for difference in contour.

Based on the relationship that the bending deflection varies inversely as the square of the thickness, the deflection of flat 1 will be 1.30 times that of flat 2 and 3.07 times that of 3 or 4; the deflection of flat 2 will be 2.36 times that of 3 or 4.

By intercomparing flats 1, 2, and 3 in the relative positions shown in figure 1 (series 1) the true contour of flat 1 may be obtained directly from interferometric measurements of the sum of the contours of adjacent surfaces of the supported flats.

Let:

Each flat be supported at three points equidistant from the center and equidistant from each other; the supports for the upper flat be directly above those for the lower flat; the algebraic sum of the contours of adjacent surfaces be measured along a diametric line parallel to two of the supports of each flat;

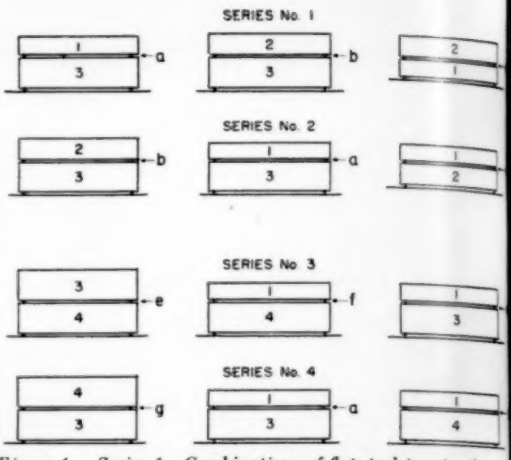

Figure 1. Series 1—Combinations of flats to determine the true contour of Numbers 1, 2, 3, and 4.

C_1; C_2; C_3 = true contours, undistorted by bending, of flats 1, 2, and 3;

a; b; c = measured sum of the contours of 1 on 3; 2 on 3; and 2 on 1, respectively;

$\pm D$ = bending deflection of flat 3 (also of 4);

$\pm D_1$ = bending deflection of flat 1 = $\pm 3.07\ D$;

$\pm D_2$ = bending deflection of flat 2 = $\pm 2.36\ D$;

S = shearing deflection of each plate;

+value = downward deflection;

−value = upward deflection.

Then:

$$C_1+D_1+S+C_3-D-S=a$$

$$C_2+D_2+S+C_3-D-S=b$$

$$C_2+D_2+S+C_1-D_1-S=c$$

and:

$$C_1=\frac{a-b+c}{2}$$

$$C_2-0.71D=\frac{-a+b+c}{2}$$

$$C_3+2.07D=\frac{a+b-c}{2}$$

Whereas C_1 is obtained directly in terms of measurable quantities a, b, c, values for C_2 and C_3 cannot be determined from these measurements unless the bending deflection D is known. Determinations that require correction for D will be referred to as *indirect determinations.*

Similarly, series 2, 3, and 4, figure 1, yield direct values of C_2, C_3, and C_4, respectively, and yield also indirect values of C_1, C_3, and C_4.

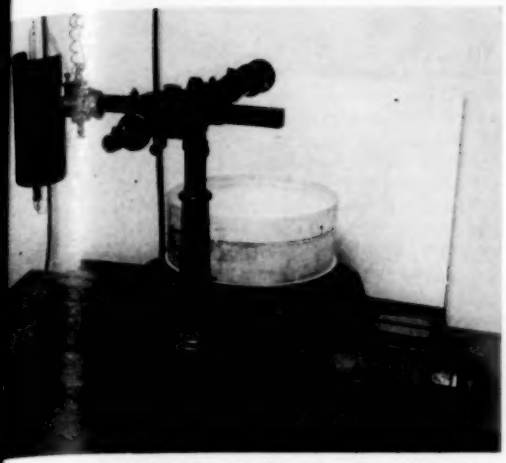

URE 2. *Setup for the determinations of contour and bending.*

2.2. Determination of Bending Deflection

Since the bending deflection (given by the first rm of eq (4) varies inversely as the thickness squared e bending deflections D_1 and D of flats 1 and 3, spectively, may be determined from measurements the sum of the contours with flat 1 above and eneath flat 3. If the measured values are a with t 1 above and a' with flat 3 above:

$$+3.07D+S+C_2-D-S=a; \quad C_1+C_3+2.07D=a; \tag{5}$$

nd

$$+D+S+C_1-3.07D-S=a'; \quad C_1+C_3-2.07D=a'. \tag{6}$$

rom eq (5) and (6),

$$14D=a-a'; \; D=0.242\ (a-a'); \; D_1=0.743\ (a-a').$$

Had a thinner flat, 0.75 in. thick, been available r comparison with flat 3, the value $(a-a')$, from e measurements would equal 20.2 times the deflecon of flat 3, thus increasing appreciably the accuracy the determinations of bending.

3. Procedure for Comparing the Flats

One flat was supported, with its optical surface up, three 1/8-in.-diameter paper disks spaced equidisnt from the center of the flat and equidistant from ch other on the glass plate shown in figure 2. A cond flat, with its optical surface down, was supted on the first flat by three similar disks directly ove the supports of the lower flat. The combinaon was placed on a movable carriage beneath a ulfrich viewing instrument [5]. By means of a and crank operating through reduction gears, the mbination could be moved slowly and smoothly ross the field of the viewing instrument, which

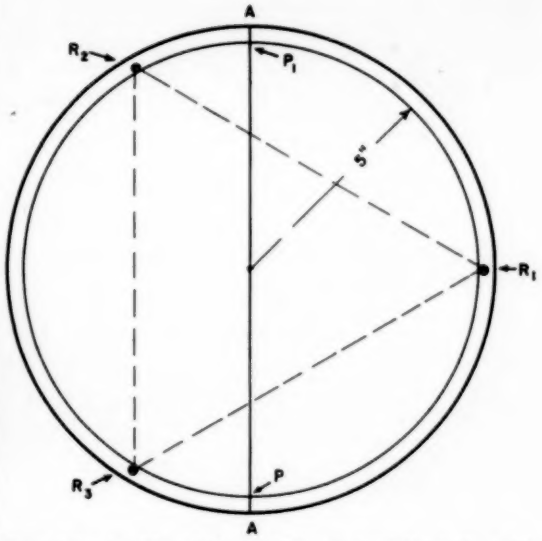

FIGURE 3. *Position of diametric line* A-A *relative to the points of support, and of points* P *and* P_1 *between which the measurements were made.*

served both as a source of monochromatic light and as a means for measuring deviations of the resulting fringes from a straight line, that is, the algebraic sum of the contours of adjacent surfaces. Desired fringe widths were obtained by selecting paper disks of proper relative thickness. Widths corresponding to 300 divisions of the micrometer head of the viewing instrument proved satisfactory in this work.

Measurements for each combination of flats were made between points P and P_1, figure 3, which are 5 in. from the center and lie on a definite diametric line AA that is parallel to supports R_2 and R_3. The sum of the contours was determined for the inner 10-in. diameter surface of the flats rather than for the entire surface because of irregularities in the outlying area that might affect the accuracy of measurements.

The deviation of a fringe from a straight line passing through the intersections of that fringe with the circumference of the 10-in. surface was measured in terms of divisions of the micrometer head of the viewing instrument. The number of divisions thus measured (given the proper sign to indicate the direction of curvature) divided by the divisions between successive fringes is the algebraic sum of the contours in terms of fringes. Determinations were made at eleven points along the diameter.

Comparisons were made in a temperature-controlled room with the flats enclosed in an insulated container (not shown in fig. 2) covered inside and outside with aluminum-coated paper. By uncovering a small opening in the top of the container, fringes were observed and measured. The usual procedure was to set up the flats during the forenoon, measure the combination several times in the afternoon when thermal conditions were stabilized, and

repeat the observations the following morning, thus completing one set of observations. The flats were then reset and the procedure repeated. The final values for the contours are based on an average of five sets of observations for each combination of flats. The maximum deviation of the individual sets from the mean for a given combination in no case exceeded 0.017 fringe for measurements at the center; and the average deviation from the mean was 0.005 fringe.

4. Measurements and Results

4.1 True Contours

a. Direct Determinations

To test the validity of the methods described in section 2.1 for determining the true contours of the four standard flats, the differences a, b, c, d, e, f, g (fig. 1, series 1, 2, 3, and 4) were determined by interferometric comparison when the flats were supported at three points located as follows:

5.06 in. (0.95 × radius r) from the center

3.5 in. (0.66 × radius r) from the center.

From these measurements the true contours of the flats were obtained from equations

$$C_1=\frac{a-b+c}{2},\quad C_2=\frac{b-a+d}{2},$$

$$C_3=\frac{e-f+a}{2},\quad C_4=\frac{-a+f+g}{2}.$$

Additional values were obtained with the flats supported at 0.95r by substituting flat 2 for flat 1 in series 3 and 4, and flat 4 for flat 3 in series 1 and 2.

The resulting determinations of the true contour of flat 1 are given in table 1. The two determinations at 0.95r, columns 2 and 3, differ by only a few units in the third decimal place. Column 4 gives the mean of the determinations at 0.95r. The contour determined with supports at 0.66r are given in column 5. Column 6 gives the difference between the contours determined for the two conditions of support, and indicates that true contours obtained by this method are nearly the same whether determined with supports at 0.95r or at 0.66r. Column 7 gives the mean of the direct determinations of true contour for these two supports.

The magnitude of the differences given in columns 4 and 6 for this flat are representative of those similarly obtained for flats 2, 3, and 4.

b. Indirect determinations

Intercomparison of the various combinations in section 2.1 for different positions of the supports yields some equations that include terms 0.71D, 1.36D, or 2.07D, where D is the bending deflection of 2.5-in.-thick flats 3 or 4 at points between P and P_1, figure 3, relative to the bending deflection at points P, P_1. Values for D were obtained from determinations described in section 4.2. The magnitude of D will depend upon the position of the supports and the place of measurement. By substituting the values thus determined for D in the equations that include a term for the bending deflection, additional values of the true contours of the four flats were obtained.

TABLE 1. *True contour (in fringes) of the central 10-in.-diameter surface of optical flat 1 by direct and indirect methods*

+value=convexity; −value=concavity

Distance from P	Direct determinations						Indirect determinations (corrected for bending term)										
	Position of supports				Difference 4−5	Mean 4 and 5	Position of supports							Difference 11−14	Mean 11 and 14	Difference 7−16	Contour (mean 7 and 16)
	0.95r		Mean 2 and 3	0.66r			0.95r				0.66r						
							For corresponding bending terms—			Mean 8, 9 and 10	For corresponding bending terms—		Mean 12 and 13				
							(2.07D)	(0.71D)	(0.71D)		(2.07D)	(0.71D)					
1	2	3	4	5	6	7	8	9	10	11	12	13	14	15	16	17	18
Inches																	
0.0	0.000	0.000	0.000	0.000	0.000	0.000	0.000	0.000	0.000	0.000	0.000	0.000	0.000	0.000	0.000	0.000	0.000
.5	−.021	−.019	−.020	−.021	+.001	−.021	−.023	−.027	−.025	−.025	−.024	−.027	−.026	+.001	−.026	−.005	−.033
1.5	−.069	−.055	−.057	−.061	−.006	−.059	−.062	−.068	−.064	−.065	−.067	−.072	−.070	+.005	−.068	+.004	−.066
2.5	−.084	−.081	−.083	−.079	−.004	−.081	−.077	−.080	−.077	−.078	−.082	−.085	−.084	+.003	−.081	.000	−.081
3.5	−.111	−.112	−.112	−.104	−.008	−.108	−.107	−.108	−.109	−.108	−.110	−.114	−.112	+.004	−.110	+.002	−.109
4.5	−.137	−.135	−.136	−.133	−.003	−.135	−.136	−.135	−.133	−.135	−.135	−.136	−.136	+.001	−.136	+.001	−.136
5.0	−.132	−.128	−.130	−.129	−.001	−.130	−.128	−.129	−.125	−.128	−.130	−.129	−.130	+.002	−.129	−.001	−.130
5.5	−.127	−.127	−.127	−.125	−.002	−.126	−.124	−.124	−.125	−.124	−.127	−.127	−.127	+.003	−.126	.000	−.126
6.5	−.108	−.110	−.109	−.108	−.001	−.109	−.109	−.102	−.105	−.105	−.110	−.110	−.110	+.005	−.108	−.001	−.109
7.5	−.079	−.077	−.078	−.072	−.006	−.075	−.074	−.075	−.073	−.074	−.074	−.074	−.074	.000	−.074	−.001	−.075
8.5	−.053	−.053	−.053	−.055	+.002	−.054	−.053	−.050	−.049	−.051	−.054	−.054	−.054	+.003	−.053	−.000	−.054
9.5	−.022	−.021	−.022	−.024	+.002	−.023	−.024	−.022	−.021	−.022	−.026	−.026	−.026	+.004	−.024	+.001	−.023
10.0	.000	.000	.000	.000	.000	.000	.000	.000	.000	.000	.000	.000	.000	.000	.000	.000	.000

The indirect determinations for flat 1 with supports at $0.95r$ are given in table 1, columns 8, 9, 10, and with supports at $0.66r$, in columns 12, and 13. Columns 11 and 14 give the means of determinations at $0.95r$ and $0.66r$, respectively. Column 15 gives the difference between the mean values at $0.95r$ and $0.66r$. As with the direct determinations, the individual indirect determinations differ from their respective mean values in the third decimal place, and likewise the differences in their mean values are small notwithstanding the large differences in bending term values applied in the equations. Column 16 gives the mean of the indirect determinations for the flats supported at $0.95r$ and at $0.66r$. The small differences between the direct values (col. 7 and the indirect vlaues (col. 16) shown in column 17 are attributed to experimental errors. Equally small differences between direct and indirect values were obtained for flats 2, 3, and 4. Column 18 gives the true contour of flat 1, and is taken as the average of the direct and indirect determinations. The true contours of the four standard flats are shown in figure 4.

4.2 Bending of Flats

The bending deflection was determined from comparisons of flats 1 and 3 by the method described in section 2.2.

These flats were supported as previously on 1/8-in.-diameter paper disks at three points equidistant from the center of the flat and equidistant from each other. The deviation of a fringe from a straight line was measured for the inner 10-in.-diameter surfaces along a diametric line parallel to two of the supports of each flat: first with flat 1 above; and second with flat 3 above. The measured deviations were a and a', respectively.

To determine the effect on bending when the flats were supported at different distances from the center, tests were made with supports at the following distances: 1.0 in. ($0.19r$); 1.5 in. ($0.28r$); 2.5 in. ($0.47r$); 3.5 in. ($0.66r$); 4.25 in. ($0.80r$); 5.06 in. ($0.95r$)

The bending deflection of flat 1 was calculated from equation $D_1 = 0.743\ (a - a')$, except for the $0.19r$ support, for which no value of a' was determined.[2] The deflection for this support was calculated from $D_1 = 1.483[a - (C_1 + C_3)]$, using the values previously determined for C_1 and C_3.

Figure 5 gives the bending curves for the inner 10-in. surface of flat 1 supported at different distances from the center. The bending deflection at the center changed from a downward (+) deflection of 0.143 fringe for supports at $0.95r$ to an upward (−) deflection of 0.278 fringe for supports at $0.19r$. Inspection of the curves indicated that the bending deflection of a flat supported at $0.70r$ would be quite small. Determinations were then made for this condition. The results, which are shown with the other curves in figure 5, indicate that the bending along the diametric line does not exceed 0.01 fringe for flat 1. The bending of thicker flats 3 and 4 when supported at $0.70r$ could be considered negligible.

The bending deflections at the center of the surface of flat 1 when plotted for the different supports appear to fall approximately on a straight line, figure 6. By projecting the line to intersect the circumfer-

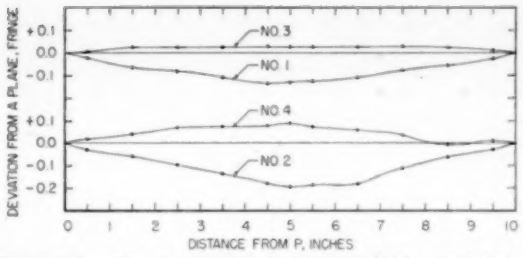

FIGURE 4. *True contours of the four standard optical flats.*
(+ Value indicates convexity; − value indicates concavity).

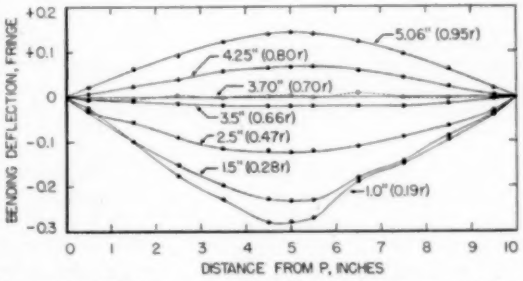

FIGURE 5.—*Bending curves for flat Number 1 supported at different distances from its center.*
(+Value=downward deflection; −value=upward deflection)

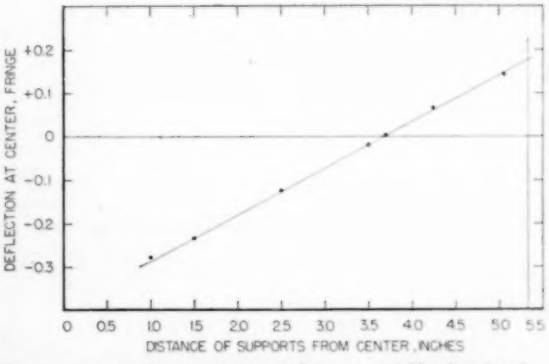

FIGURE 6.—*Bending deflection at the center of Number 1 relative to points P, P₁ 5 in. from the center, for supports at different distances from the center.*

[2] Support near the center appears to be a severe condition that might cause permanent change in the flat, and therefore should, in general, be avoided. Previous tests of flats supported 0.5 in. from the center gave a pronounced peak distortion at the center. In the present instance, flats 1 and 3 were supported for 1 day at $0.19r$. A month later, when the flats were supported at $0.95r$ and compared, the measured values for a and a' differed from previous values by approximately −0.03 fringe, thus indicating either a permanent or temporary differential change in the flats. During the following month, the flats were supported at $0.95r$, that is, in a position in which the deflection is in a direction opposite to that with supports near the center. At the end of the month measured values of a and a' approached closely the original values, indicating that the change may have been caused wholly or in part by plastic flow of the fused quarts. As a subject for investigation, it appears important to determine, with flats other than the Bureau's standard planes, the nature of the changes in contour that occur when flats are supported in extreme positions.

ence of this 10.66-in.-diameter flat, the bending deflection that would result, if the flat were supported at its edge, is obtained. The best value for the bending deflection, W_E, at the center of flat 1 with respect to points on the diametric line 5 in. from the center (that is, for the inner 10-in. surface) when the flat is supported at its edge appears to be

$$W_E = 0.177 \text{ fringe} = 2.05 \times 10^{-6} \text{ in.}$$

The data given in figures 5 and 6 may have application when very accurate comparisons of a standard flat and a test flat of less diameter are required. The test flat in this case may rest on supports at 0.70 of its radius to give minimum bending, and the supports for the standard may be placed in vertical alignment with these. The true contour of the standard may then be corrected by the bending data to give its contour in the position of test.

5. Comparison of Theoretical and Experimental Values for Bending Deflection

Figure 7 is the theoretical curve for the bending deflection at the center of a 10-in. diameter inner surface of flat 1 along AA with respect to a plane defined by the three symmetrically spaced points of support BBB of a uniformly loaded fused-quartz plate.

Constants for flat 1:[3] $a = 5.33$ in.; $h = 1.428$ in.; $P = 10.18$ lb; $E = 10.15 \times 10^6$ psi; $\nu = 0.14$.

From figure 7, $w(Eh^3/Pa^2)$ at the center of flat 1 $(r/a = 0)$ with respect to a plane through the points of support is 0.424; or

$$w = 4.15 \times 10^{-6} \text{ in.} \qquad (7)$$

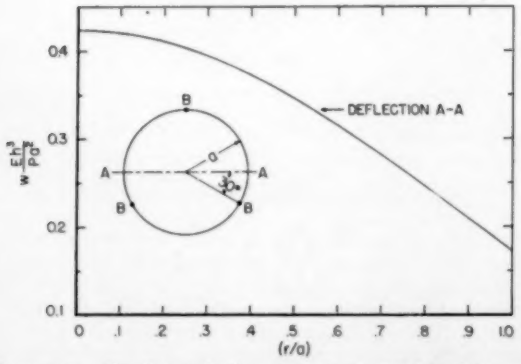

FIGURE 7. *Bending deflection of uniformly loaded plate supported at three equally spaced points on circumference BBB.*

E, Modulus of elasticity; P, weight of plate; a, radius of plate; h, thickness of plate; r, distance from center; ν, 0.14, Poisson's ratio for fused quartz; w, deflection along A–A relative to BBB.

[3] Values for E and ν are those considered by Sosman [6] as the best values for fused quartz.

Similarly, $w(Eh^3/Pa^2)$ at a point along AA 5 in. from the center $(r/a = 0.94)$ is 0.195; or

$$w_1 = 1.91 \times 10^{-6} \text{ in.} \qquad (8)$$

The difference between (7) and (8), or w_T is the bending deflection at the center of flat 1 with respect to points P and P_1 on AA that are 5 in. from the center; or $w_T = 2.24 \times 10^{-6}$ in. The corresponding deflection w_E determined experimentally (section 4.2) is $w_E = 2.05 \times 10^{-6}$ in.; that is, the theoretical value is between 9 and 10 percent greater than that determined experimentally.

In order to determine the relative shapes of theoretical and experimental bending curves for comparable conditions of support, the deflections given in figure 5 for the bending curve of flat 1 supported at $0.95r$ were increased by the ratio 177/143 (see section 4.2) to approximate the condition of edge support for which the theory applies.

Figure 8 shows that the theoretical and the experimental bending curves are similar in shape but differ in magnitude of the deflections. The values derived by theory average about 11 percent greater than those obtained by the method used in this investigation.

This agreement between the theoretical and the experimental values for bending appears satisfactory in view of the many factors that might influence either result. The experimental values would be affected by small differences in setting the flats, errors of measurement, insufficient number of measurements taken to integrate small local variations in optical surfaces as noted by Saunders [7] and the use of supports of finite size rather than point supports. Likewise, the theoretical values would be different were other values used for E and ν. The values determined for these elastic constants of fused quartz by different observers vary appreciably as shown in a summary by Sosman [6]. He states "A study of the assemblage as a whole will show there

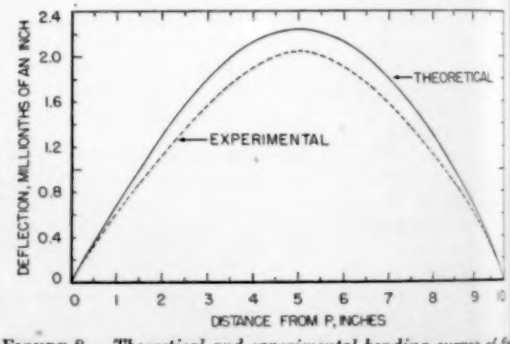

FIGURE 8.—*Theoretical and experimental bending curves of flat Number 1 supported at three equally spaced points on its circumference. The curves give the difference in the bending deflection at points along a diametric line that is parallel to two of the supports and the deflection at points on the same line that are 5 in. from the center of the flat. Bending deflections relative to the points of support may be obtained by increasing the theoretical values 1.91×10^{-6} in. and by increasing the experimental values 1.7×10^{-6} in.*

not much consistency, either in the theory or experiment among the various values. Part of the reason, I feel sure, is that the usual specimen of fused silica is not structurally isotropic, as we have been assuming, but is to a greater or less degree anisotropic." From this consideration alone, the values of σ and E used to calculate the theoretical bending may not apply to the standard flats.

Substitution of the theoretical value for bending for the experimental value would change the true contour at the center of flat 1, as given in table 1 for supports at $0.95r$, by 0.01 fringe in those cases where corrections of 2.07D are applied, and would initiate to some extent the excellent agreement of direct and indirect determinations of contour. The determined bending deflection values may, therefore, be more applicable to the present flats and their conditions of test than the theoretical ones.

6. Effect of Supports of Finite Size

When flats supported on balls are compared, a series of interference fringes concentric about the point of contact of support and surface is visible, indicating an appreciable deformation of the surface concentrated at the point of contact. The reason for using 1/8-in-diameter paper supports in the present work was to distribute the load over a larger area and thereby avoid damage to the flats. Local distortion of the surface surrounding the disks for about 3/32 in. beyond the supports was evident when viewing the fringes. At the edge of a disk, the surface of the flat was depressed about 0.3 fringe. It is quite reasonable that the deflection may be somewhat less when flats are supported on the disks rather than points, thus giving a lower value than that required by theory. To test this, from consideration of contour, bending, shear, local deformation at the supports, and thickness of the flats, the following equation was derived, in which contour, shear, and the effect of the supports are eliminated.

$$\frac{D_{\text{in.}}}{t_z^2}=\frac{1}{2}\frac{\dfrac{b'-b}{t_z-t_x}-\dfrac{a'-a}{t_y-t_x}}{\dfrac{t_x+t_y}{t_y^2}-\dfrac{t_x+t_z}{t_z^2}},$$

in which $D_{\text{in.}}$ is the bending deflection of a plate 1 in. thick and t_x, t_y, t_z=thickness of plates X, Y, Z, and $D_{\text{in.}}/t_z^2$ is the bending deflection of X. From comparisons of X and Y: a is the deviation of a fringe from a straight line, with X above, and a' is the deviation of a fringe from a straight line, with Y above. From comparisons of X and Z: b is the measured deviation, with X above, and b' is the measured deviation, with Z above.

The difference between the values for bending previously determined and those by this method was less than the experimental error of this method. No effect of local deformation on the bending deflection was therefore indicated by these experiments.

The excellent agreement between contours obtained with support at $0.95r$ and at $0.66r$, table 1, indicates that local deformation near the supports had negligible effect on the contour measurements.

7. Conclusion

Precise calibration of optical flats requires that account be taken of the surface distortion that results when the flats are supported in their position of test. For a 10 5/8-in.-diameter, 1 7/16-in.-thick fused-quartz optical flat supported at three equally spaced points at its edge, the gravitational bending deflection at the center of the flat with respect to its points of support will be approximately 4×10^{-6} in. To reduce this to 1×10^{-6} in. (0.1 fringe) would require a thickness of 2.9 in. on the basis of theoretical computations, which agree quite closely with experimental determinations. The bending deflection will increase appreciably for larger flats because it varies directly as the fourth power of the radius. For three-point support, bending is small and at a minimum when the supports lie on the circumference of a circle having a radius 0.7 that of the flat.

Whenever two flats of the same material and diameter but of different thicknesses are available and can be similarly supported during comparison, the bending deflection of each flat may be determined by the described methods. Likewise, if three flats of the same material and diameter are available, very precise determinations of the true contours, undistorted by bending of their surfaces, may be determined.

The author expresses his deep appreciation to Samuel Levy of the Engineering Mechanics Section of the Bureau for his cooperation in the theoretical determinations of the deflection of plates that were used in this investigation and for his many helpful suggestions.

8. References

[1] A. Nádai, Die Verbiegungen in einzelmen Punkten unterstuetzter kreisfoermiger Platten, Physik. Z. **23,** (1922).
[2] A. Nádai, Theorie der Plattenbiegung und ihre experimentelle Best˜tigung, Z. angew. Math. Mech. **2,** 381–394, (1922).
[3] A. Nádai, Elastische Platten (Berlin, J. Springer, p. 196, 1925).
[4] S. Timoshenko, Theory of plates and shells, p. 61–63; 80; 271. (McGraw-Hill Book Co., Inc., New York and London, 1940).
[5] C. Pulfrich, Z. Instr. **18,** 261, (1898).
[6] R. B. Sosman, Properties of silica, 437 (The Chemical Catalog Co., Inc., New York, N. Y., 1927).
[7] J. B. Saunders, Contour mapping of optical surfaces with light waves, J. Research NBS **47,** 148 (1951) RP2239.

Washington, May 27, 1952.

Index of Refraction of Magnesium Oxide

Robert E. Stephens and Irving H. Malitson

The index of refraction of magnesium oxide crystal has been measured for wavelengths from 0.36 to 5.35 microns. In the visible region, measurements were made at three temperatures, close to 20°, 30°, and 40° C. Thermal coefficients were computed for this range of temperatures for nine wavelengths.

1. Introduction

In 1935, shortly after moderate sized artificially rown crystals of magnesium oxide became available, o papers were published dealing with the optical roperties of this material.[1] [2]

Strong and Brice measured the index of refraction f two prisms, cut from the same crystal, by photoraphic and visual means over the range from 2536 o 7065 A. Barnes, Brattain, and Seitz investigated he transmittance and reflectance of this material n the infrared region from approximately 1 to approxmately 30 μ. They published a curve showing the ndex of refraction as calculated by means of the resnel reflection equations from the measured eflectance.

Some time ago two small prisms of magnesium xide crystals of excellent optical quality were sent o the National Bureau of Standards by Elias Burtein of the Naval Research Laboratory for measureents of the index of refraction and the thermal oefficients of the index of refraction. These prisms, lthough rather small, were of high optical quality nd entirely adequate for precision measurements of ndex in the visible region of the spectrum.

Because of the high sensitivity of the lead sulfide hotoconducting cell in the region from about 0.3 to bout 2.6 μ, it was found practicable to measure the ndex of refraction for several ultraviolet and infrared nes of the mercury and cadmium spectra with good ccuracy. Beyond 2.6 μ it was possible, by using ide slits and a Golay pneumatic detector, to get ata of fair accuracy at the wavelengths of several bsorption bands of polystyrene and carbon dioxide. Due to the limitations of the apparatus, the range of he measurements was from 0.36117 μ (cadmium) to 35 μ (polystyrene). According to the results referred to in footnotes 1 and 2, magnesium oxide is efully transparent from 0.2200 to 9 μ.

2. Measurements in the Visual Range

The index of refraction in the visible range was easured by means of a precision spectrometer by he minimum-deviation method. This was done at hree temperatures near 20°, 30°, and 40° C for each f nine wavelengths, which, with their emitting lements, are listed in table 1.

[1] John Strong and R. T. Brice, Optical properties of magnesium oxide, J. Opt. oc. Am. 25, 307 (1935).
[2] Barnes, Brattain, and Seitz, On the structure and interpretation of the infrared bsorption spectra of crystals, Phys. Rev., 2d series, 48, 582 (1935).

TABLE 1. *Spectrum lines used for index measurements*

Designation	Source	Wavelength
		A
A′ mean	Potassium	7678.58
	Helium	7065.20
	...do	6678.15
C	Hydrogen	6562.8
D mean	Sodium	5892.62
e	Mercury	5460.74
F	Hydrogen	4861.33
g	Mercury	4358.35
h	...do	4046.56

By differencing all the observed indexes and the observed temperatures, thermal coefficients of index were computed for the ranges 20° to 30° C and 30° to 40° C. These coefficients were averaged to obtain the coefficients for 30° C. The coefficients for 30° C were plotted as a function of wavelength and smoothed values were read from a curve. Then, assuming linearity of the coefficients over the temperature range, the thermal coefficients of index were computed for 20°, 25°, 30°, 35°, and 40° C at each of the wavelengths. These values are presented in table 2.

TABLE 2. *Thermal coefficients of index of refraction of magnesium oxide,* $\Delta n \times 10^6/°C$

Wavelength	20° C	25° C	30° C	35° C	40° C
A					
7679	13.6	13.7	13.8	13.9	14.0
7065	14.1	14.2	14.3	14.4	14.5
6678	14.4	14.5	14.6	14.7	14.8
6563	14.5	14.6	14.7	14.8	14.9
5893	15.3	15.4	15.5	15.6	15.7
5461	15.9	16.0	16.1	16.2	16.3
4861	16.9	17.0	17.1	17.2	17.3
4358	18.0	18.1	18.2	18.3	18.4
4047	18.9	19.0	19.1	19.2	19.3

By the use of the table of coefficients, small corrections in index were made to all observed values of index, so that the corrected values correspond to exact temperatures of 20°, 30°, and 40° C. The corrected observed indexes, averaged for the two prisms, are listed in table 3. The indexes of prism II, however, were larger than those of prism I by 24×10^{-6}.

The corrected observed indexes, table 3, for 20° and 40° C were reduced to indexes at 30° C by means of the coefficients in table 2, and the resulting indexes were averaged with the corrected observed values at 30°. The following four-constant Ketteler-Helm-

TABLE 3. *Observed index of refraction of magnesium oxide corrected to 20°, 30°, and 40° C*

(Average for two prisms)

Wavelength	20° C	30° C	40° C
A			
7679	1.728677	1.728805	1.728940
7065	1.730977	1.731109	1.731272
6678	1.732721	1.732871	1.733008
6563	1.733299	1.733444	1.733592
5893	1.737319	1.737485	1.737631
5461	1.740729	1.740887	1.741044
4861	1.747040	1.747233	1.747407
4358	1.754652	1.754832	1.755010
4047	1.760990	1.761174	1.761371

holtz dispersion equation was fitted to the resulting averaged indexes:

$$n^2=2.957019-0.0101373\lambda^2+\frac{0.0216485}{\lambda^2-0.0158650}. \quad (1)$$

In this equation the wavelength in microns is used.

The accuracy of fit of this equation is shown in table 4, which lists the averaged corrected observed indexes, the indexes computed by the equation, and the differences.

TABLE 4. *Comparison of indexes computed by equation (1) with observed values*

All are for 30° C.

Wavelength	Averaged corrected observed index	index computed by equation (1)	Difference observed minus computed
A			
7679	1.728810	1.728807	$+3\times10^{-6}$
7065	1.731119	1.731113	+6
6678	1.732866	1.732867	−1
6563	1.733445	1.733447	−2
5893	1.737478	1.737478	0
5461	1.740886	1.740883	+3
4861	1.747233	1.747232	+1
4358	1.754830	1.754836	−6
4047	1.761178	1.761178	0

With the computed indexes at 30° C and the temperature coefficients of table 2 it is possible to construct a table of indexes of refraction of magnesium oxide for various temperatures between 20° and 40° C and for selected wavelengths between 4000 and 7800 A. The computed values 20°, 30°, and 40° C for the nine wavelengths actually used in the visual range and two others, at 5085 and 6438 a (cadmium lines), are listed in table 5.

In table 5 the averaged values of the residuals observed minus computed at 20°, 30°, and 40° C. are +1, 0, and -1×10^{-6}, respectively; and at only 1 of the 27 observed points does the residual exceed 9×10^{-6}.

Seven of the wavelengths for which Strong and Brice measured the index of magnesium oxide are among those of table 5. For comparison with the results of Strong and Brice, we have computed the index for 23° C, the temperature at which their measurements were made, using the Δn's of table 5. These are tabulated, with those of Strong and Brice,

TABLE 5. *Index of refraction of magnesium oxide at 20° and 40° C, at 11 selected wavelengths*

Wavelength	Index at— 20° C	Δn	Index at— 30° C	Δn	Index at— 40° C
A					
7679	1.728670	137	1.728807	139	1.728946
7065	1.730971	142	1.731113	144	1.731257
6678	1.732722	145	1.732867	147	1.733014
6563	1.733301	146	1.733447	148	1.733595
6438	1.733956	148	1.734104	150	1.734254
5893	1.737324	154	1.737478	156	1.737634
5461	1.740723	160	1.740883	162	1.741045
5085	1.744415	165	1.744580	167	1.744747
4861	1.747062	170	1.747232	172	1.747404
4358	1.754655	181	1.754836	183	1.755019
4047	1.760988	190	1.761178	192	1.761370
Abbe number, ν	53.58	---	53.50	---	53.42

in table 6. For further comparison, the differences the average of the differences, second differences and the average of the second differences are shown. These appear to show a systematic difference index of 37×10^{-5} between the samples measured Strong and Brice and those reported here.

TABLE 6. *Comparison of National Bureau of Standards indexes with those of Strong and Brice for magnesium oxide*

Wavelength	n NBS (23° C)	n Strong and Brice (23° C)	Difference	Second difference
A				
4047	1.761045	1.76137	32×10^{-5}	-5×10^{-5}
4358	1.754709	1.75510	39	+2
4861	1.747113	1.74744	33	−4
5461	1.740771	1.74122	45	+8
5893	1.737370	1.73789	52	+15
6563	1.733345	1.73364	29	−8
7065	1.731014	1.73127	26	−11
		Average...	37	8

Strong and Brice also measured the index magnesium oxide at 2° C for two wavelengths, 6 and 4861 A. The resulting thermal coefficients the 2° to 23° C range were 1.14×10^{-5} and 1.47×10 respectively, compared to 1.46×10^{-5} and 1.70×10 respectively, obtained in the present work for t 20° to 30° C range; and 1.48×10^{-5} and 1.72×1 for the 30° to 40° C range. Although our resu show that the thermal coefficient increases w temperature the rate is insufficient to account the difference between these coefficients and th of Strong and Brice.

The Abbe numbers obtained by Strong and Bri 53.80 at 2° C and 53.55 at 23°, compare favora with those reported here.

3. Measurements in the Infrared and Ultraviolet Range

The indexes in the infrared and ultraviolet regio were measured by the minimum-deviation metho The minimum deviation was measured in a Ze spectrometer of the Wadsworth type with concav mirrors for collimating and collecting. These mirro are of off-axis portions of paraboloids and their figu is such that their definition and resolving power

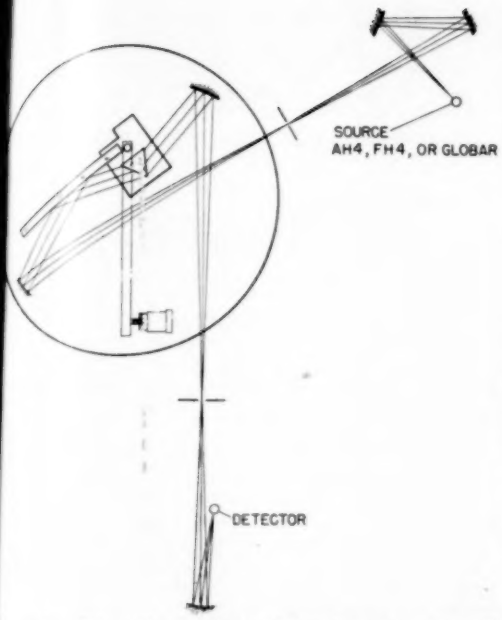

IGURE 1. *Schematic drawing of infrared spectrometer with source and detector.*

xcellent. The prism table and Wadsworth mirror re rotated by means of a lever and a tangent screw, he position of the screw being indicated by a longiudinal scale and divided head. The instrument and ccessories are shown schematically in figure 1.

The angular position of the prism table has been xpressed as a function of scale reading by means of a ollimator, a telescope, and two small plane mirrors ounted together, with a small angle between them. his angle was stepped off repeatedly until the entire ale had been covered. From the data so obtained table of corrections was made. These corrections ere plotted on a graph, and the corrections used ere read from a smooth curve fitted to the plotted oints. The calibration was carried to the nearest econd of angle.

The minimum deviations of prisms I and II were oo small to be used in the Zeiss spectrometer, and he combination of both prisms gave deviations that ere too large. Consequently, the angle of prism I as reduced by grinding and polishing. At the ame time, prism II, which had become dull, was esurfaced. These two were then mounted together n a base plate forming a composite prism with an ffective angle of 49°59′34″.

For the ultraviolet and the infrared to 2.4 μ a lead ulfide photoconducting cell was used as the detector. For longer wavelengths, a Golay pneumatic detector as used. The responses were amplified (the Golay mplifier and chopper were used with both detectors) nd indicated or recorded by an electronic self-alancing potentiometer. A synchronous motor with

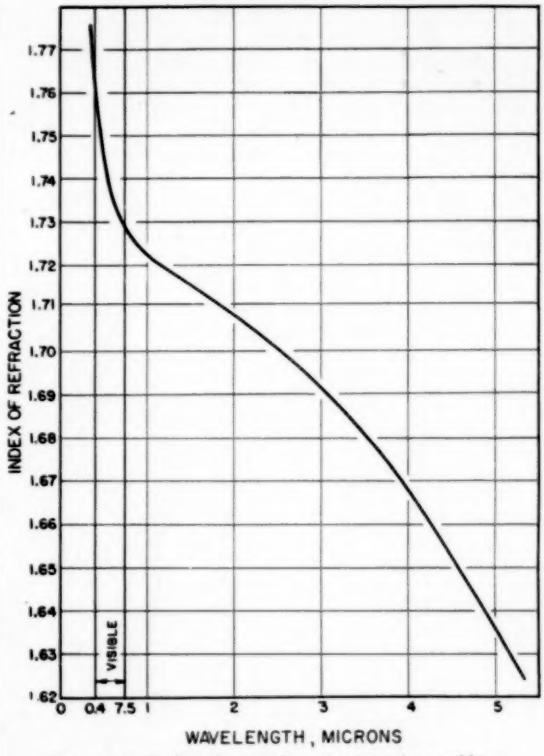

FIGURE 2. *Index of refraction of magnesium oxide at 23.3° C.*

suitable gears was used to drive the spectrometer screw. As the chart in the potentiometer was also driven by a synchronous motor, the resulting chart gave response as a function of spectrometer position. The exploratory work by means of which the spectrum lines and absorption bands were identified and their approximate scale readings located was done by means of these charts. The scale readings corresponding to the peaks of absorption by which the five longest wavelengths were identified were read from the charts. However, hand settings for maximum response on the emission lines of the spectrum of mercury were made repeatedly, and the results were averaged to obtain higher precision.

The prism was placed upon the spectrometer table, leveled by placing shims under one corner, and turned by hand to the position of minimum deviation. A visible spectrum line was used for the adjustment. After these adjustments had been made, the physical detector was put in place to receive the flux from the exit slit.

With the spectrometer used it was not possible to observe the undeviated beam, consequently the angle of minimum deviation could not be measured directly. For flux to reach the exit slit, it must have been deviated between 37° and 57°. The difference in minimum deviation between an invisible line and

a visible one was measured on this spectrometer and added to the deviation for the visible line to obtain the angle of minimum deviation for the invisible line. The minimum deviation for the visible line was measured with high accuracy on another spectrometer by visual means. Several visible lines were used and the results averaged to obtain better accuracy.

The indexes resulting from these measurements are presented in table 7. These data are also presented graphically in figure 2.

TABLE 7. *Index of refraction of magnesium oxide for wavelengths in the infrared and ultraviolet at 23.3° C*

Wavelength	Source	Index of refraction
Microns		
0.36117	Cd	1.77318
.365015	Hg	1.77186
1.01398	Hg	1.72259
1.12866	Hg	1.72059
1.36728	Hg	1.71715
1.52952	Hg	1.71496
1.6932	Hg	1.71281
1.7092	Hg	1.71258
1.81307	Hg	1.71108
1.97009	Hg	1.70885
2.24929	Hg	1.70470
2.32542	Hg	1.70350
3.3033	Polystyrene	1.68526
3.5078	do	1.68055
4.258	CO_2	1.66039
5.138	Polystyrene	1.63138
5.35	do	1.62404

Several four- and five-constant equations have been fitted to the data for the entire wavelength range. The best is the following five-constant one which was fitted by least squares:

$$n^2=2.956362-0.01062387\lambda^2-0.0000204968\lambda^4+\frac{0.02195770}{\lambda^2-0.01428322}$$

where λ is in microns. Admittedly the fit is not excellent. In particular, in the visible region, where the observed indexes are probably accurate within a few units in the sixth decimal place, the values computed by this formula differ systematically from those computed with eq (1) by as much as $\pm 5\times10^{-5}$. In general, however, considering the whole range of wavelength, it is probable that no further improvement of eq (2) is justified because the indexes in the ultraviolet and infrared are less accurately determined than those in the visible region. Although the indexes for the sharp emission lines of cadmium and mercury are probably accurate to a few units in the fifth decimal place, some of those identified by means of the relatively broad absorption bands of polystyrene and carbon dioxide may be inaccurate in the fourth decimal place.

WASHINGTON, July 14, 1952.

nal of Research of the National Bureau of Standards Vol. 49, No. 4, October 1952 Research Paper 2361

efractivity of Potassium Bromide for Visible Wavelengths[1]

Robert J. Spindler and William S. Rodney[2]

Values of the index of refraction of potassium bromide were determined independently on two high-precision spectrometers by the method of minimum deviation for 11 spectral lines at temperatures near 17°, 24°, and 27° C. The instruments are described, and the methods used in obtaining results valid in the sixth decimal place of index are discussed. Temperature coefficients of index were determined, and a small linear variation was found with respect to wavelength [1][3]. With the values of dn/dt so obtained, the experimental data were reduced to a common temperature, averaged, and a four-constant Ketteler-Helmholtz dispersion equation fitted to the data and adjusted by least squares. The refractive indices of potassium bromide for the particular prism used are intermediate between the values reported by Harting [2] and Forrest [3]. Reduced to 23° C for comparison, the results for sodium light are Harting, 1.55983; National Bureau of Standards, 1.55978; and Forrest, 1.55971. Another prism measured at NBS yielded 1.55983, and an obviously defective prism gave 1.55889. Small differences in dispersion were also detected.

1. Introduction

Potassium bromide is of interest to designers of tical instruments because of its transparancy in the frared region of the spectrum and because of the ssibility of using it in connection with other optical terials for correction of secondary spectrum. he need for precise values of refractive indices in is connection is well known. Although some data refractive indices of potassium bromide in the sual spectral region have been published, the lack agreement among investigators is considerable. he authors of this paper were fortunate in having e opportunity to measure the same sample indeendently on two high-precision spectrometers, reby gaining a satisfactory degree of certitude garding the validity of the results obtained, even the sixth decimal place.

Considerable interest has been displayed by recent vestigators [4, 5] in the thermooptical behavior of e alkali halides, primarily owing to their relatively mple crystalline structure and the information such ta afford to physicists concerning interionic bond engths. Here again, lack of precise data on temrature coefficients has handicapped physicists in eorizing upon such matters. Such considerations ve led one of the authors [1] to an investigation of e dependence of index of refraction of potassium omide upon temperature. The data thus obtained e precise enough to merit attention over the temrature range studied and are presented herein. ch data are necessary, furthermore, when reporting xth-decimal-place values of indices of crystals whose mperature coefficients are as large as those of otassium bromide.

Investigation of the indices of different samples of e same crystalline material in the same laboratory always of interest because of the information proded concerning control in the manufacturing process. Such information is vitally important to optical designers, as they must know the limits between which materials vary in order to make a proper choice for their design. In this regard, differences of dispersion between samples of the substance are particularly important. Measurements were performed upon three different samples of potassium bromide grown by the Harshaw Chemical Corporation. Two of the samples were finished into 60° prisms, and the third was finished into a 30° prism by the Perkin-Elmer Corporation. The two 60° prisms were made available to the authors by Earle K. Plyler of the Radiometry Section of the National Bureau of Standards. The prism measured upon two spectrometers at three temperatures was one of these. The 30° prism was made available to the authors by Stanley S. Ballard and the Polaroid Corporation.

2. Description of Apparatus

2.1. Watts Spectrometer

One of the spectrometers (fig. 1) was made by E. R. Watts & Son, Ltd., of London, and is based on the original National Physical Laboratory design described in detail in the literature [6]. The collimator and telescope objectives have focal lengths of 60 cm and 40 cm, and clear apertures of 9 cm and 4 cm, respectively. An auxiliary telescope, identical in every respect to the rotating telescope, and mounted on a pedestal that may be clamped to the circular base, is furnished with the instrument. It may be used for a variety of purposes, including adjustment of collimation, measurement of prism angles by the substitution method, and measurement of the error in the 90° deviation of optical squares.

The collimator slit of the instrument is provided with a device for opening and closing the slit jaws symmetrically. A graduated drum is attached to the slit-width adjusting screw in order that slit widths can be recorded and repeated when necessary. Two parallel vertical lines bisected by a horizontal line are etched upon a glass plate that is mounted im-

[1] The work described in this paper was carried out in part under the sponsorship the U. S. Air Force and U. S. Army Signal Corps.
[2] Some of the results reported in this paper were submitted by William S. dney as partial fulfillment of the requirements for the degree of Master of ence at The Catholic University of America, Washington, D. C., 1951.
[3] Numbers in brackets refer to literature reference :a :the end of this paper.

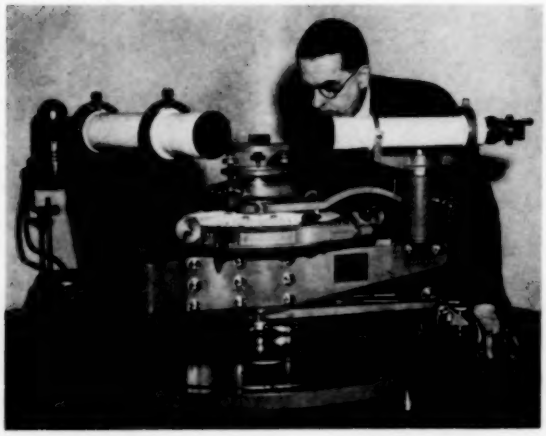

FIGURE 1. *Watts spectrometer.*

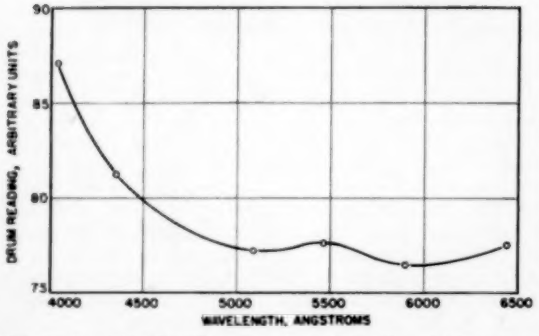

FIGURE 2. *Tube lengths for perfect collimation of telescope of Watts spectrometer.*

mediately behind the slit, that is, upon the source side. In adjusting collimation and making pointings, focus is made upon these lines in order that wide slits may be used to obtain sufficient intensity and to reduce chromatic parallax, as recommended by Guild [7].

Both telescopes are provided with rotatable eyepiece micrometers, permitting rapid and accurate determination of small angles and pyramidal errors of prisms. Several eyepieces of various powers are provided, and one of the Gauss type is used for leveling and autocollimation.

A removable table containing two slides that travel in superimposed ways at right angles to each other was constructed for the prism table of the instrument. The slides are actuated by slow-motion screws and greatly facilitate centering the prism with respect to collimator and telescope objectives.

Both telescopes and the collimator are provided with a rack-and-pinion device for focusing purposes. A graduated circular drum is mounted upon the pinion gear and positions of the rack may be noted by means of the graduations. By means of a monochromator manufactured by the Carl Zeiss Co. of

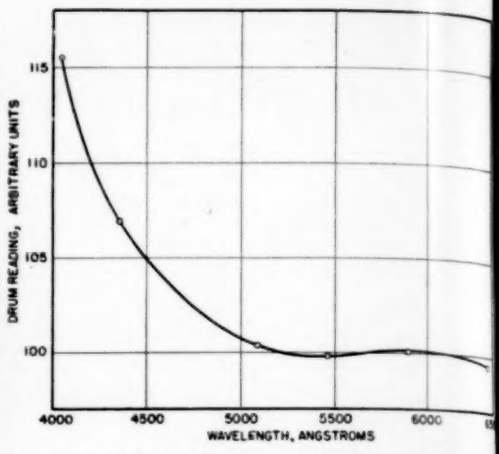

FIGURE 3. *Tube lengths for perfect collimation of auxili telescope of Watts spectrometer.*

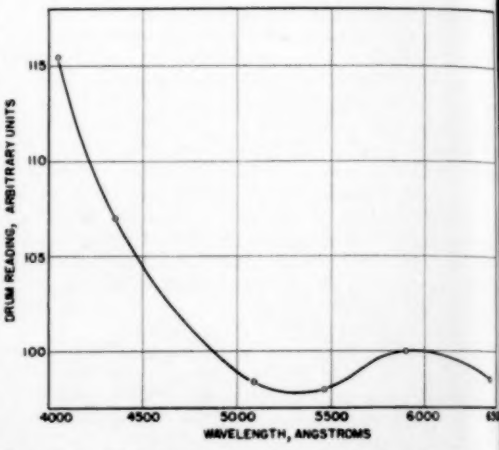

FIGURE 4. *Tube lengths for perfect collimation of collimat Watts spectrometer.*

Jena, fitted with a flint-glass prism as dispersi agent, several spectral lines of a cadmium-mercu FH–4 lamp were separated and used as sources illuminate the collimator slit. All three tube lengt were adjusted for truly parallel monochromat light of each particular wavelength by the us method of focusing upon each other in pairs, described by Glazebrook [8]. The drum readin were recorded, and the results are shown in figur 2, 3, and 4. With the aid of these data the collimat and telescope may be adjusted for truly paral monochromatic light. If the prism has appreciab power, owing, for example, to curved surfaces, th will be evidenced by the modification of telesco tube length necessary for sharp focus of the co mator-slit image.

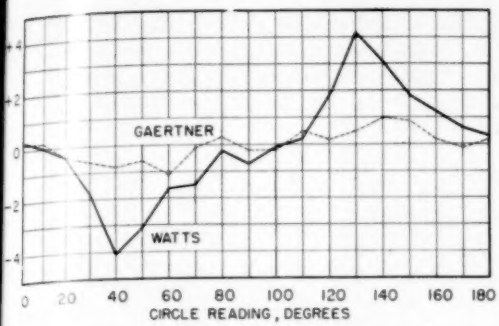

URE 5. *Error in the mean of opposite 90° angles as a function of circle orientation.*

The microscopes are mounted on a ring that may rotated independently around the circle. This eatly facilitates the reading of the microscopes, for eir positions may be so adjusted as to eliminate e troublesome cases where the microscopes are accessible for certain telescope orientations. The icrometer screws make 1 revolution per minute of c, and the drums are graduated to read half-conds directly. The elimination of parallax was fected by proper focusing, and the tube length of ch microscope was adjusted to insure proper mag-ification so that 5 revolutions of the drum covered e average of a few 5-min intervals ruled upon the rcle.

The divided circle is ruled on the periphery of a 5-in. cylindrical drum and is graduated to 5-min tervals. A complete calibration of the circle grad-tions has not been made, but a test showing the ror in the mean of readings for opposite angles used by positional errors of the degree graduations s been made at 10° intervals completely around e circle. For convenience, the size of the opposite gles was chosen to be 90°. The results of this test e shown in figure 5. The maximum value of 4.2 c is uncomfortably large, but as is more or less well nown [9], the effect of positional error of the circle arkings upon measurements can be satisfactorily inimized in the average, provided a systematic ogram of observations using proper orientations of e circle is followed.

Errors of subintervals of the degree intervals were etermined by measurements on four 1° intervals ar 0°, 90°, 180°, and 270°, respectively. These easurements show that there is a periodic error that epeats six times in each degree interval and has an mplitude of approximately 1 sec. The periodic ature of these errors is such that their effect will be rgely minimized in the average of two microscopes y making their angular displacement 179°55′ in-ead of exactly 180°. Thus in figure 6 the errors of e degree subintervals as seen under microscope A re shown by the solid line. If corresponding inter-als of the circle pass under microscopes A and B imultaneously, the degree subinterval errors seen nder microscope B would be identical with those en under A, and no reduction would be possible by

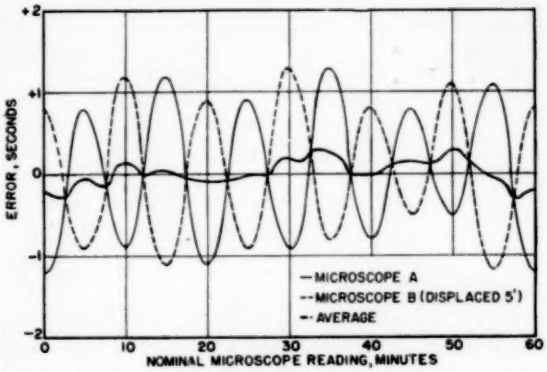

FIGURE 6. *Error of degree subintervals as a function of microscope reading on initial graduation of each 5-minute subinterval (Watts spectrometer).*

averaging A and B. If, however, the phase relationship of the error is altered by displacing microscope B one-half period (5 min), then the errors of the degree subintervals, as they will appear under B, are shown by the dotted line in figure 6. The residual error after averaging both microscopes will be reduced to the amount shown by the heavy line.

The report of an examination by the National Physical Laboratory of the circle of a similar spectrometer manufactured by the same firm is of interest because one might suspect the general characteristics of the two circles to be similar, assuming that both were ruled upon the same engine. This report mentions a systematic error that "recurs every ten minutes of arc and which results in a mean disparity of 1.05 ($\pm$0.1) seconds in the alternate spaces between adjacent graduations." This is adequately descriptive of the error of the degree subintervals found for the instrument in the NBS laboratory. The report further states that the main systematic error can be represented "by a periodic error in the graduations of which only half a complete period is comprised within the full circle of the scale. The beginning and end of this half-period coincides closely with the zero graduation." Designating by θ an angle measured from the scale zero, the report further states "The error is zero for θ=0°, 180°, or 360° and has a maximum value of +1.95 seconds for θ=90° or 270°. The error is positive for all values of θ, the errors of the second half of the scale (180° to 360°) being a repetition of those of the first half without change of sign." "The rms value of the random component of the error of position of a graduation is 0.60 $\pm$0.07 seconds."

The test performed here on the circle of the Bureau's instrument does not yield directly comparable information, but it is of interest to estimate the results that would probably be obtained by testing the circle referred to in the NPL report in the same manner in which the circle mounted in the instrument in the Bureau's laboratory was tested. The periodicity of the systematic error is the same for both circles. In making a 90° opposite-angle test on the circle

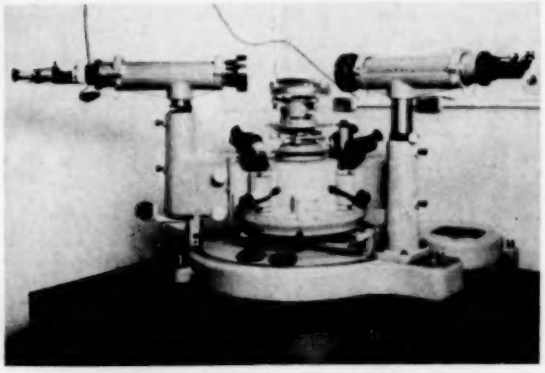

FIGURE 7. *Gaertner spectrometer.*

described in the NPL report, the error would be 0 for one 90° angle as read between 315° and 45° (the other 90° angle read from 165° to 225°) and +1.95 sec for one 90° angle as read between 0° and 90° (the other 90° angle read between 180° and 270°). The superposed random component of rms=±0.60 sec for line position contributes an rms random component of 0.60 sec for the mean of opposite-angle readings. If it chances that the random component should be as large as twice the rms value for lines used when the first 90° angle is read in the vicinity of 0° to 90°, then an error of +3.2 sec would be found, as compared with +4 sec, the extreme found on the instrument tested here.

Thus it would appear that the over-all quality of the circle reported upon by the NPL may be somewhat higher than the one tested at the NBS. Nevertheless, the characteristics of these circles with respect to magnitude and periodicity of errors are very similar.

2.2. Gaertner Spectrometer

The other spectrometer (fig. 7) was made by the Gaertner Scientific Corp., Chicago, Ill. It is designated as type L–124 and is of recent design. The telescope and collimator each have focal lengths of 50 cm and a clear aperture of 5 cm. Several eyepieces of various powers are provided, including a Gaussian used for leveling and autocollimation. Slow-motion screws are provided for making small angular displacements of the telescope and the divided circle. The collimator slit is provided with an auxiliary prism to facilitate comparison of spectra. A vertical spider thread is mounted in the center of the collimator slit, so that wide slits could be used and pointings made upon the spider thread in order to lessen chromatic parallax [7]. A removable table, similar to the one described in section 2.1, is mounted upon the prism table of the instrument.

The circle, which is of stainless steel, has a diameter of 300 mm. A zone about 1 in. wide near the periphery of the circle was ground and polished optically flat by the Bureau's Optical Shop. Lines separated by 5 min of arc were ruled upon the polished zone by Benjamin L. Page in the Length Section of the National Bureau of Standards. T errors of position of the degree graduations have n been explicitly investigated, but a test of the er of the mean of opposite 90° angles, similar to th described in section 2.1, was made. The results this test are plotted in figure 5. The maximu value of 1.1 sec indicates that the effect of po tional errors of the degree markings are much le serious, approximately one-fourth of those on t Watts instrument. The same systematic progra of observations mentioned in section 2.1 was us in making all determinations on this instrument.

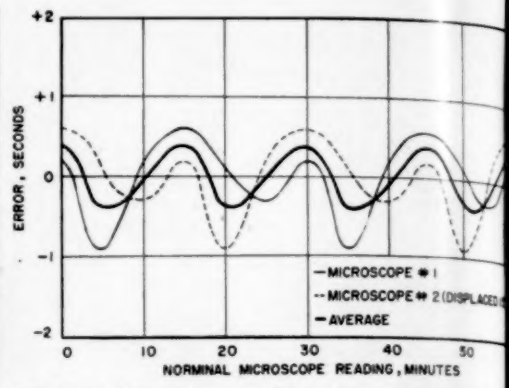

FIGURE 8. *Error of degree subintervals as a function of mi scope reading on initial graduation of each 5-minute sub interval (Gaertner spectrometer).*

The results of an investigation of errors in t degree subintervals are shown in figure 8. T error of the intervals, although not so complete periodic as was the case with the circle of the Wat instrument, appears to repeat itself twice in ea degree interval and has a maximum amplitude 0.9 sec of arc. By making the angular separati of two micrometer microscopes 179°45′ instead exactly 180°, these errors will be largely minimiz in their average, as discussed in section 2.1. Th in figure 8 the errors as seen under microscope 1 a shown by the solid line. If microscope 2 is displace one-half period (15 min) so that the errors se under it are of the amounts indicated by the dott line, the amplitude of the residual error in the ave age of the two will be reduced to a uniform value 0.4 sec, as shown by the heavy line.

3. Experimental Program and Procedur

Index determinations were made at temperatur near 17°, 22°, and 27° C for 11 spectral lines. T sample was kept in a dessicator while not actuall being measured. The relative humidity of the roo in which the measurements were made was regulate so as not to exceed 45 percent. No deterioration the surfaces of the sample became noticeable duri the course of the experiments. Care was taken t allow the sample sufficient time to reach temperatu equilibrium before making deviation measurement

fteen or more hours were allowed for reaching mperatur equilibrium whenever the temperature the sur oundings was changed.

All refra ting-angle determinations were made by toccollima ion, with the Gauss eyepieces supplied ith the nstruments. Measurements at each of e three temperatures failed to demonstrate any mperature dependence of the refracting angle. order to minimize torsional errors of the cone, the rocedure recommended by Tilton [9] was followed, e-half the measurements being made on the angle self and the others on its explement.[4] The differ- nce between the average of these two sets of data as observed to be negligible on both spectrometers 22° C and 27° C but amounted to about 1.5 sec n the Gaertner instrument at the lower tempera- re. The refracting angle was of the order of agnitude of 60°. Symmetrical use of the circle as achieved by using three different orientations splaced 60° from each other for each set of angle easurements.

Measurements of double deviation were made for ch spectral line after the prismatic sample had been entered with respect to the telescope and collimator bjectives. Because the double deviation was always f the order of 90°, two determinations with the rcle orientations 90° apart suffice to cancel approxi- ately the effects of positional errors of the circle ulings. At least two, and sometimes four, indi- idual determinations of double deviation were made n each instrument for each spectral line measured.

The temperature and the humidity of the labora- ory in which the measurements were made were utomatically controlled. The prism temperature as assumed to be the same as that recorded by a ercury thermometer suspended directly over the rism, with the mercury bulb almost in contact. he temperature was recorded at equal time intervals uring the course of the observations by an observer ewing the thermometer through a telescope. The hermometer could be read directly to the nearest enth of a degree, and the hundredths estimated. he thermometer was calibrated by the Bureau's hermometry Section, and the correction applied ver the range used was negligible. Care was taken o shield the thermometer from sources of radiation. he light source was located in a fiberboard con- ainer, and the room was more or less darkened while he observations were being made. Fluctuations in emperature were noted because of the unavoidable roximity of the observer operating the spectro- meter. The average deviation of the recorded emperatures was 0.03° C. The room temperature as adjusted to the desired value, and after sufficient ime had elapsed for equilibrium conditions to pre- ail, the deviation measurements were made.

All indices reported in this paper were corrected to refer to dry air at 760-mm pressure (Hg), and to the air temperature listed, by use of tables and pro- cedures described by Tilton [10]. Temperature coefficients were computed for each of the 11 wave- lengths and plotted. A straight line was passed through these data, and a least-squares adjustment of the constants was made. With the values of dn/dt computed from this equation, (2), all observed data were adjusted to 22° C. A four-constant Ketteler-Helmholtz dispersion equation was fitted to the weighted mean of the observed data and adjusted by the method of least squares.

[4] "Explement" is defined as the angle that must be added to a given angle to produce 360 degrees.

4. Results

Values of refractive index at 22° C were computed for wavelengths ranging from 4000 to 7100 A from the dispersion equation

$$n^2=2.3618102-0.00058072\lambda^2+\frac{0.02305269}{\lambda^2-0.0245381}, \tag{1}$$

and for temperatures ranging from 16° to 28° C from the temperature coefficient equation

$$\frac{dn}{dt}=-(31.742+13.21\lambda)\times10^{-6}, \tag{2}$$

where λ is in microns. These values are listed in table 1. The tabular intervals are so chosen that sixth-decimal-place indices may be obtained by linear interpolation. Table 2 lists light sources, spectral lines, wavelengths, observed and computed indices, and their differences. Table 3 lists values of dn/dt observed and computed and their differences.

Figure 9 shows a comparison of the values reported by other investigators [2, 3, 11, 12, 13]. The ordinates represent differences between the values of other observers and values reported in table 1 of this paper. Christiansen's values, like Sprockhoff's are only for the C, D, and F lines. Gyulai's values were determined on an instrument using a physical detector. He was chiefly interested in the ultraviolet indices, and the visible data represent one extreme of his observations. The most recently reported values are those of Forrest [3] and Harting [2]. The average difference at 20° C between Forrest's values and the authors' is approximately -7×10^{-5} and is constant within $\pm5\times10^{-6}$; and between Harting's values and the authors' the difference is $+4\times10^{-5}$. The constancy in the sixth decimal place between Forrest's values and those of the authors' indicate that the internal precision of both sets of data is very high. The constancy with respect to Harting's data is of the order of one unit in the fifth decimal place, indicating a somewhat lesser degree of precision in his work. The average difference between the values reported by Forrest and by Harting is of the order of one unit in the fourth decimal place. Both these sets of data were determined in comparatively recent times on high-precision spectrometers by using modern techniques, and the differences between the two sets of data are probably caused by varying amounts of impurities in the samples themselves.

TABLE 1. *Refractive indices of potassium bromide*

[Computed from equations 1 and 2]

Wavelength	Refractive index at —												
	16° C	17° C	18° C	19° C	20° C	21° C	22° C	23° C	24° C	25° C	26° C	27° C	28° C
A													
4000	1.591415	1.591378	1.591341	1.591304	1.591267	1.591230	1.591193	1.591156	1.591119	1.591082	1.591045	1.591008	1.590971
4010	1.591101	1.591064	1.591027	1.590990	1.590953	1.590916	1.590879	1.590842	1.590805	1.590768	1.590731	1.590694	1.590657
4020	1.590789	1.590752	1.590715	1.590678	1.590641	1.590604	1.590567	1.590530	1.590493	1.590456	1.590419	1.590382	1.590345
4030	1.590480	1.590443	1.590406	1.590369	1.590332	1.590295	1.590258	1.590221	1.590184	1.590147	1.590110	1.590073	1.590036
4040	1.590174	1.590137	1.590100	1.590063	1.590026	1.589989	1.589952	1.589915	1.589878	1.589841	1.589804	1.589767	1.589730
4050	1.589872	1.589834	1.589797	1.589760	1.589723	1.589686	1.589649	1.589612	1.589575	1.589538	1.589501	1.589464	1.589427
4060	1.589571	1.589534	1.589496	1.589459	1.589422	1.589385	1.589348	1.589311	1.589274	1.589237	1.589200	1.589162	1.589125
4070	1.589273	1.589236	1.589198	1.589161	1.589124	1.589087	1.589050	1.589013	1.588976	1.588939	1.588902	1.588864	1.588827
4080	1.588978	1.588941	1.588904	1.588866	1.588829	1.588792	1.588755	1.588718	1.588681	1.588644	1.588606	1.588569	1.588532
4090	1.588685	1.588648	1.588611	1.588573	1.588536	1.588499	1.588462	1.588425	1.588388	1.588351	1.588313	1.588276	1.588239
4100	1.588395	1.588358	1.588321	1.588283	1.588246	1.588209	1.588172	1.588135	1.588098	1.588061	1.588023	1.587986	1.587949
4110	1.588107	1.588070	1.588033	1.587996	1.587958	1.587921	1.587884	1.587847	1.587810	1.587772	1.587735	1.587698	1.587661
4120	1.587822	1.587785	1.587748	1.587711	1.587673	1.587636	1.587599	1.587562	1.587525	1.587487	1.587450	1.587413	1.587376
4130	1.587539	1.587502	1.587465	1.587428	1.587390	1.587353	1.587316	1.587279	1.587242	1.587204	1.587167	1.587130	1.587093
4140	1.587259	1.587222	1.587185	1.587148	1.587110	1.587073	1.587036	1.586999	1.586962	1.586924	1.586887	1.586850	1.586813
4150	1.586981	1.586944	1.586907	1.586870	1.586832	1.586795	1.586758	1.586721	1.586684	1.586646	1.586609	1.586572	1.586535
4160	1.586706	1.586669	1.586632	1.586595	1.586557	1.586520	1.586483	1.586446	1.586409	1.586371	1.586334	1.586297	1.586260
4170	1.586434	1.586396	1.586359	1.586322	1.586285	1.586247	1.586210	1.586173	1.586136	1.586098	1.586061	1.586024	1.585987
4180	1.586163	1.586125	1.586088	1.586051	1.586014	1.585976	1.585939	1.585902	1.585864	1.585827	1.585790	1.585753	1.585715
4190	1.585895	1.585857	1.585820	1.585783	1.585746	1.585708	1.585671	1.585634	1.585596	1.585559	1.585522	1.585485	1.585447
4200	1.585629	1.585591	1.585554	1.585517	1.585480	1.585442	1.585405	1.585368	1.585330	1.585293	1.585256	1.585219	1.585181
4210	1.585365	1.585328	1.585290	1.585253	1.585216	1.585178	1.585141	1.585104	1.585066	1.585029	1.584992	1.584954	1.584917
4220	1.585103	1.585066	1.585028	1.584991	1.584954	1.584916	1.584879	1.584842	1.584804	1.584767	1.584730	1.584692	1.584655
4230	1.584844	1.584807	1.584769	1.584732	1.584695	1.584657	1.584620	1.584583	1.584545	1.584508	1.584471	1.584433	1.584396
4240	1.584587	1.584550	1.584512	1.584475	1.584438	1.584400	1.584363	1.584326	1.584288	1.584251	1.584214	1.584176	1.584139
4250	1.584332	1.584295	1.584257	1.584220	1.584183	1.584145	1.584108	1.584071	1.584033	1.583996	1.583959	1.583921	1.583884
4260	1.584078	1.584041	1.584003	1.583966	1.583929	1.583891	1.583854	1.583817	1.583779	1.583742	1.583705	1.583667	1.583630
4270	1.583828	1.583791	1.583754	1.583716	1.583679	1.583641	1.583604	1.583567	1.583529	1.583492	1.583454	1.583417	1.583380
4280	1.583579	1.583542	1.583505	1.583467	1.583430	1.583392	1.583355	1.583318	1.583280	1.583243	1.583205	1.583168	1.583131
4290	1.583332	1.583295	1.583258	1.583220	1.583183	1.583145	1.583108	1.583071	1.583033	1.582996	1.582958	1.582921	1.582884
4300	1.583089	1.583051	1.583014	1.582976	1.582939	1.582901	1.582864	1.582827	1.582789	1.582752	1.582714	1.582677	1.582639
4310	1.582846	1.582808	1.582771	1.582733	1.582696	1.582658	1.582621	1.582584	1.582546	1.582509	1.582471	1.582434	1.582396
4320	1.582605	1.582567	1.582530	1.582492	1.582455	1.582417	1.582380	1.582343	1.582305	1.582268	1.582230	1.582193	1.582155
4330	1.582367	1.582329	1.582292	1.582254	1.582217	1.582179	1.582142	1.582105	1.582067	1.582030	1.581992	1.581955	1.581917
4340	1.582130	1.582092	1.582055	1.582017	1.581980	1.581942	1.581905	1.581868	1.581830	1.581793	1.581755	1.581718	1.581680
4350	1.581895	1.581857	1.581820	1.581782	1.581745	1.581707	1.581670	1.581633	1.581595	1.581558	1.581520	1.581483	1.581445
4360	1.581662	1.581625	1.581587	1.581550	1.581512	1.581475	1.581437	1.581399	1.581362	1.581324	1.581287	1.581249	1.581212
4370	1.581431	1.581394	1.581356	1.581319	1.581281	1.581244	1.581206	1.581168	1.581131	1.581093	1.581056	1.581018	1.580981
4380	1.581201	1.581164	1.581126	1.581089	1.581051	1.581014	1.580976	1.580938	1.580901	1.580863	1.580826	1.580788	1.580751
4390	1.580974	1.580937	1.580899	1.580862	1.580824	1.580787	1.580749	1.580711	1.580674	1.580636	1.580599	1.580561	1.580524
4400	1.580748	1.580711	1.580673	1.580636	1.580598	1.580561	1.580523	1.580485	1.580448	1.580410	1.580373	1.580335	1.580298
4410	1.580524	1.580487	1.580449	1.580412	1.580374	1.580337	1.580299	1.580261	1.580224	1.580186	1.580149	1.580111	1.580074
4420	1.580302	1.580265	1.580227	1.580190	1.580152	1.580115	1.580077	1.580039	1.580002	1.579964	1.579927	1.579889	1.579852
4430	1.580083	1.580045	1.580007	1.579970	1.579932	1.579895	1.579857	1.579819	1.579782	1.579744	1.579707	1.579669	1.579631
4440	1.579865	1.579827	1.579789	1.579752	1.579714	1.579677	1.579639	1.579601	1.579564	1.579526	1.579489	1.579451	1.579413
4450	1.579648	1.579610	1.579572	1.579535	1.579497	1.579460	1.579422	1.579384	1.579347	1.579309	1.579272	1.579234	1.579196
4460	1.579433	1.579395	1.579358	1.579320	1.579282	1.579245	1.579207	1.579169	1.579132	1.579094	1.579056	1.579019	1.578981
4470	1.579219	1.579181	1.579144	1.579106	1.579068	1.579031	1.578993	1.578955	1.578918	1.578880	1.578842	1.578805	1.578767
4480	1.579008	1.578970	1.578933	1.578895	1.578857	1.578820	1.578782	1.578744	1.578707	1.578669	1.578631	1.578594	1.578556
4490	1.578798	1.578760	1.578723	1.578685	1.578647	1.578610	1.578572	1.578534	1.578497	1.578459	1.578421	1.578384	1.578346
4500	1.578589	1.578551	1.578514	1.578476	1.578438	1.578401	1.578363	1.578325	1.578288	1.578250	1.578212	1.578175	1.578137
4510	1.578382	1.578344	1.578307	1.578269	1.578231	1.578194	1.578156	1.578118	1.578081	1.578043	1.578005	1.577968	1.577930
4520	1.578177	1.578140	1.578102	1.578064	1.578026	1.577989	1.577951	1.577913	1.577876	1.577838	1.577800	1.577762	1.577725
4530	1.577973	1.577936	1.577898	1.577860	1.577822	1.577785	1.577747	1.577709	1.577672	1.577634	1.577596	1.577558	1.577521
4540	1.577771	1.577734	1.577696	1.577658	1.577620	1.577583	1.577545	1.577507	1.577470	1.577432	1.577394	1.577356	1.577319
4550	1.577571	1.577533	1.577495	1.577457	1.577420	1.577382	1.577344	1.577306	1.577268	1.577231	1.577193	1.577155	1.577117
4560	1.577372	1.577334	1.577296	1.577258	1.577221	1.577183	1.577145	1.577107	1.577069	1.577032	1.576994	1.576956	1.576918
4570	1.577175	1.577137	1.577099	1.577061	1.577024	1.576986	1.576948	1.576910	1.576872	1.576835	1.576797	1.576759	1.576721
4580	1.576979	1.576941	1.576903	1.576865	1.576828	1.576790	1.576752	1.576714	1.576676	1.576639	1.576601	1.576563	1.576525
4590	1.576784	1.576746	1.576708	1.576670	1.576633	1.576595	1.576557	1.576519	1.576481	1.576444	1.576406	1.576368	1.576330
4600	1.576591	1.576553	1.576515	1.576477	1.576440	1.576402	1.576364	1.576326	1.576288	1.576251	1.576213	1.576175	1.576137
4610	1.576399	1.576361	1.576323	1.576285	1.576248	1.576210	1.576172	1.576134	1.576096	1.576059	1.576021	1.575983	1.575945
4620	1.576209	1.576171	1.576133	1.576096	1.576058	1.576020	1.575982	1.575944	1.575906	1.575868	1.575831	1.575793	1.575755
4630	1.576020	1.575982	1.575944	1.575907	1.575869	1.575831	1.575793	1.575755	1.575717	1.575679	1.575642	1.575604	1.575566
4640	1.575833	1.575795	1.575757	1.575720	1.575682	1.575644	1.575606	1.575568	1.575530	1.575492	1.575455	1.575417	1.575379
4650	1.575647	1.575609	1.575572	1.575534	1.575496	1.575458	1.575420	1.575382	1.575344	1.575306	1.575268	1.575231	1.575193
4660	1.575462	1.575424	1.575387	1.575349	1.575311	1.575273	1.575235	1.575197	1.575159	1.575121	1.575083	1.575046	1.575008
4670	1.575279	1.575242	1.575204	1.575166	1.575128	1.575090	1.575052	1.575014	1.574976	1.574938	1.574900	1.574862	1.574825
4680	1.575098	1.575060	1.575022	1.574984	1.574946	1.574908	1.574870	1.574832	1.574794	1.574756	1.574718	1.574680	1.574642
4690	1.574917	1.574879	1.574841	1.574803	1.574765	1.574727	1.574689	1.574651	1.574613	1.574575	1.574537	1.574499	1.574461
4700	1.574738	1.574700	1.574662	1.574624	1.574586	1.574548	1.574510	1.574472	1.574434	1.574396	1.574358	1.574320	1.574282
4710	1.574560	1.574522	1.574484	1.574446	1.574408	1.574370	1.574332	1.574294	1.574256	1.574218	1.574180	1.574142	1.574104
4720	1.574383	1.574345	1.574307	1.574269	1.574231	1.574193	1.574155	1.574117	1.574079	1.574041	1.574003	1.573965	1.573927
4730	1.574208	1.574170	1.574132	1.574094	1.574056	1.574018	1.573980	1.573942	1.573904	1.573866	1.573828	1.573790	1.573752
4740	1.574034	1.573996	1.573958	1.573920	1.573882	1.573844	1.573806	1.573768	1.573730	1.573692	1.573654	1.573616	1.573578

TABLE 1. *Refractive indices of potassium bromide*—Continued

[Computed from equations 1 and 2]

Wavelength	Refractive index at —												
	16° C	17° C	18° C	19° C	20° C	21° C	22° C	23° C	24° C	25° C	26° C	27° C	28° C
A													
4500	1.573861	1.573823	1.573785	1.573747	1.573709	1.573671	1.573633	1.573595	1.573557	1.573519	1.573481	1.573443	1.573405
4600	1.573689	1.573651	1.573613	1.573575	1.573537	1.573499	1.573461	1.573423	1.573385	1.573347	1.573309	1.573271	1.573233
4700	1.573519	1.573481	1.573443	1.573405	1.573367	1.573329	1.573291	1.573253	1.573215	1.573177	1.573139	1.573101	1.573063
4800	1.573350	1.573312	1.573274	1.573236	1.573198	1.573160	1.573122	1.573084	1.573046	1.573008	1.572970	1.572932	1.572894
4900	1.573182	1.573144	1.573106	1.573068	1.573030	1.572992	1.572954	1.572916	1.572878	1.572840	1.572802	1.572764	1.572725
5000	1.573015	1.572977	1.572939	1.572901	1.572863	1.572825	1.572787	1.572749	1.572711	1.572673	1.572635	1.572597	1.572559
5100	1.572850	1.572811	1.572773	1.572735	1.572697	1.572659	1.572621	1.572583	1.572545	1.572507	1.572469	1.572430	1.572392
5200	1.572686	1.572648	1.572609	1.572571	1.572533	1.572495	1.572457	1.572419	1.572381	1.572343	1.572305	1.572266	1.572228
5300	1.572522	1.572484	1.572445	1.572407	1.572369	1.572331	1.572293	1.572255	1.572217	1.572179	1.572141	1.572102	1.572064
5400	1.572360	1.572322	1.572284	1.572245	1.572207	1.572169	1.572131	1.572093	1.572055	1.572017	1.571978	1.571940	1.571902
5500	1.572199	1.572161	1.572123	1.572084	1.572046	1.572008	1.571970	1.571932	1.571894	1.571856	1.571817	1.571779	1.571741
5600	1.572039	1.572001	1.571963	1.571924	1.571886	1.571848	1.571810	1.571772	1.571734	1.571696	1.571657	1.571619	1.571581
5700	1.571881	1.571843	1.571805	1.571767	1.571728	1.571690	1.571652	1.571614	1.571576	1.571537	1.571499	1.571461	1.571423
5800	1.571723	1.571685	1.571647	1.571609	1.571570	1.571532	1.571494	1.571456	1.571418	1.571379	1.571341	1.571303	1.571265
5900	1.571567	1.571529	1.571491	1.571453	1.571414	1.571376	1.571338	1.571300	1.571261	1.571223	1.571185	1.571147	1.571109
6000	1.571411	1.571373	1.571335	1.571297	1.571258	1.571220	1.571182	1.571144	1.571106	1.571067	1.571029	1.570991	1.570953
6100	1.571257	1.571219	1.571181	1.571143	1.571104	1.571066	1.571028	1.570990	1.570951	1.570913	1.570875	1.570837	1.570799
6200	1.571103	1.571065	1.571027	1.570989	1.570950	1.570912	1.570874	1.570836	1.570798	1.570759	1.570721	1.570683	1.570645
6300	1.570952	1.570913	1.570875	1.570837	1.570799	1.570760	1.570722	1.570684	1.570645	1.570607	1.570569	1.570531	1.570492
6400	1.570801	1.570762	1.570724	1.570686	1.570647	1.570609	1.570571	1.570533	1.570494	1.570456	1.570418	1.570380	1.570341
6500	1.570651	1.570612	1.570574	1.570536	1.570498	1.570459	1.570421	1.570383	1.570344	1.570306	1.570268	1.570230	1.570191
6600	1.570502	1.570463	1.570425	1.570387	1.570349	1.570310	1.570272	1.570234	1.570195	1.570157	1.570119	1.570081	1.570042
6700	1.570353	1.570315	1.570276	1.570238	1.570200	1.570161	1.570123	1.570085	1.570046	1.570008	1.569970	1.569931	1.569893
6800	1.570206	1.570168	1.570129	1.570091	1.570053	1.570014	1.569976	1.569938	1.569899	1.569861	1.569823	1.569784	1.569746
6900	1.570060	1.570022	1.569983	1.569945	1.569907	1.569868	1.569830	1.569792	1.569753	1.569715	1.569677	1.569638	1.569600
7000	1.569915	1.569877	1.569838	1.569800	1.569762	1.569723	1.569685	1.569647	1.569608	1.569570	1.569532	1.569493	1.569455
7100	1.569771	1.569733	1.569694	1.569656	1.569618	1.569579	1.569541	1.569503	1.569464	1.569426	1.569387	1.569349	1.569311
7200	1.569628	1.569590	1.569551	1.569513	1.569475	1.569436	1.569398	1.569360	1.569321	1.569283	1.569245	1.569206	1.569168
7300	1.569486	1.569448	1.569410	1.569371	1.569333	1.569294	1.569256	1.569218	1.569179	1.569141	1.569102	1.569064	1.569026
7400	1.569344	1.569306	1.569267	1.569229	1.569191	1.569152	1.569114	1.569076	1.569037	1.568999	1.568960	1.568922	1.568884
7500	1.569204	1.569166	1.569128	1.569089	1.569051	1.569012	1.568974	1.568936	1.568897	1.568859	1.568820	1.568782	1.568744
7600	1.569066	1.569027	1.568989	1.568950	1.568912	1.568873	1.568835	1.568797	1.568758	1.568720	1.568681	1.568643	1.568604
7700	1.568927	1.568888	1.568850	1.568811	1.568773	1.568734	1.568696	1.568658	1.568619	1.568581	1.568542	1.568504	1.568465
7800	1.568790	1.568751	1.568713	1.568674	1.568636	1.568597	1.568559	1.568521	1.568482	1.568444	1.568405	1.568367	1.568328
7900	1.568653	1.568614	1.568576	1.568537	1.568499	1.568460	1.568422	1.568383	1.568345	1.568307	1.568268	1.568230	1.568191
8000	1.568517	1.568478	1.568440	1.568401	1.568363	1.568324	1.568286	1.568248	1.568209	1.568171	1.568132	1.568094	1.568055
8100	1.568382	1.568343	1.568305	1.568266	1.568228	1.568189	1.568151	1.568113	1.568074	1.568035	1.567997	1.567959	1.567920
8200	1.568248	1.568210	1.568171	1.568133	1.568094	1.568056	1.568017	1.567978	1.567940	1.567901	1.567863	1.567824	1.567786
8300	1.568115	1.568077	1.568038	1.568000	1.567961	1.567923	1.567884	1.567845	1.567807	1.567768	1.567730	1.567691	1.567653
8400	1.567983	1.567945	1.567906	1.567867	1.567829	1.567791	1.567752	1.567713	1.567675	1.567636	1.567598	1.567559	1.567521
8500	1.567852	1.567814	1.567775	1.567737	1.567698	1.567660	1.567621	1.567582	1.567544	1.567505	1.567467	1.567428	1.567390
8600	1.567721	1.567683	1.567644	1.567606	1.567567	1.567529	1.567490	1.567451	1.567413	1.567374	1.567336	1.567297	1.567259
8700	1.567592	1.567554	1.567515	1.567477	1.567438	1.567400	1.567361	1.567322	1.567284	1.567245	1.567207	1.567168	1.567130
8800	1.567464	1.567425	1.567386	1.567348	1.567309	1.567271	1.567232	1.567193	1.567155	1.567116	1.567078	1.567039	1.567000
8900	1.567335	1.567297	1.567258	1.567220	1.567181	1.567143	1.567104	1.567065	1.567027	1.566988	1.566950	1.566911	1.566872
9000	1.567209	1.567170	1.567131	1.567093	1.567054	1.567016	1.566977	1.566938	1.566900	1.566861	1.566823	1.566784	1.566745
9100	1.567082	1.567043	1.567004	1.566966	1.566927	1.566889	1.566850	1.566811	1.566773	1.566734	1.566695	1.566657	1.566618
9200	1.566957	1.566918	1.566880	1.566841	1.566802	1.566764	1.566725	1.566686	1.566648	1.566609	1.566570	1.566532	1.566493
9300	1.566832	1.566793	1.566755	1.566716	1.566677	1.566639	1.566600	1.566561	1.566523	1.566484	1.566445	1.566407	1.566368
9400	1.566708	1.566669	1.566631	1.566592	1.566553	1.566515	1.566476	1.566437	1.566399	1.566360	1.566321	1.566283	1.566244
9500	1.566585	1.566546	1.566508	1.566469	1.566430	1.566392	1.566353	1.566314	1.566276	1.566237	1.566198	1.566160	1.566121
9600	1.566463	1.566424	1.566386	1.566347	1.566308	1.566270	1.566231	1.566192	1.566154	1.566115	1.566076	1.566038	1.565999
9700	1.566341	1.566303	1.566264	1.566225	1.566186	1.566148	1.566109	1.566070	1.566032	1.565993	1.565954	1.565915	1.565877
9800	1.566220	1.566182	1.566143	1.566104	1.566065	1.566027	1.565988	1.565949	1.565911	1.565872	1.565833	1.565794	1.565756
9900	1.566100	1.566062	1.566023	1.565984	1.565945	1.565907	1.565868	1.565829	1.565791	1.565752	1.565713	1.565674	1.565636
10000	1.565981	1.565943	1.565904	1.565865	1.565826	1.565788	1.565749	1.565710	1.565672	1.565633	1.565594	1.565555	1.565517
10100	1.565863	1.565824	1.565785	1.565746	1.565707	1.565669	1.565630	1.565591	1.565552	1.565514	1.565475	1.565436	1.565397
10200	1.565745	1.565706	1.565667	1.565628	1.565590	1.565551	1.565512	1.565473	1.565434	1.565396	1.565357	1.565318	1.565279
10300	1.565628	1.565589	1.565550	1.565511	1.565473	1.565434	1.565395	1.565356	1.565317	1.565279	1.565240	1.565201	1.565162
10400	1.565512	1.565473	1.565434	1.565395	1.565357	1.565318	1.565279	1.565240	1.565201	1.565163	1.565124	1.565085	1.565046
10500	1.565396	1.565357	1.565318	1.565279	1.565241	1.565202	1.565163	1.565124	1.565085	1.565047	1.565008	1.564969	1.564930
10600	1.565282	1.565243	1.565204	1.565165	1.565127	1.565088	1.565049	1.565010	1.564971	1.564933	1.564894	1.564855	1.564816
10700	1.565167	1.565128	1.565089	1.565051	1.565012	1.564973	1.564934	1.564895	1.564856	1.564817	1.564779	1.564740	1.564701
10800	1.565054	1.565015	1.564976	1.564938	1.564899	1.564860	1.564821	1.564782	1.564743	1.564704	1.564666	1.564627	1.564588
10900	1.564941	1.564902	1.564863	1.564825	1.564786	1.564747	1.564708	1.564669	1.564630	1.564591	1.564553	1.564514	1.564475
11000	1.564829	1.564790	1.564752	1.564713	1.564674	1.564635	1.564596	1.564557	1.564518	1.564479	1.564441	1.564402	1.564363
11100	1.564718	1.564679	1.564641	1.564602	1.564563	1.564524	1.564485	1.564446	1.564407	1.564368	1.564329	1.564291	1.564252
11200	1.564607	1.564569	1.564530	1.564491	1.564452	1.564413	1.564374	1.564335	1.564296	1.564257	1.564218	1.564179	1.564141
11300	1.564497	1.564459	1.564420	1.564381	1.564342	1.564303	1.564264	1.564225	1.564186	1.564147	1.564108	1.564069	1.564031
11400	1.564388	1.564349	1.564310	1.564271	1.564232	1.564193	1.564154	1.564115	1.564076	1.564037	1.563998	1.563959	1.563920
11500	1.564280	1.564241	1.564202	1.564163	1.564124	1.564085	1.564046	1.564007	1.563968	1.563929	1.563890	1.563851	1.563812
11600	1.564172	1.564133	1.564094	1.564055	1.564016	1.563977	1.563938	1.563899	1.563860	1.563821	1.563782	1.563743	1.563704
11700	1.564064	1.564025	1.563986	1.563947	1.563908	1.563869	1.563830	1.563791	1.563752	1.563713	1.563674	1.563635	1.563596
11800	1.563958	1.563919	1.563880	1.563841	1.563802	1.563763	1.563724	1.563685	1.563646	1.563607	1.563568	1.563529	1.563490
11900	1.563851	1.563812	1.563773	1.563734	1.563695	1.563656	1.563617	1.563578	1.563539	1.563500	1.563461	1.563422	1.563383

TABLE 1. *Refractive indices of potassium bromide*—Continued

[Computed from equations 1 and 2]

Wavelength	Refractive index at —												
	16° C	17° C	18° C	19° C	20° C	21° C	22° C	23° C	24° C	25° C	26° C	27° C	28° C
A													
5500	1.563746	1.563707	1.563668	1.563629	1.563590	1.563551	1.563512	1.563473	1.563434	1.563395	1.563356	1.563317	1.563278
5520	1.563537	1.563498	1.563459	1.563420	1.563381	1.563342	1.563303	1.563264	1.563225	1.563186	1.563147	1.563108	1.563069
5540	1.563330	1.563291	1.563252	1.563213	1.563174	1.563135	1.563096	1.563057	1.563018	1.562979	1.562940	1.562901	1.562862
5560	1.563127	1.563087	1.563048	1.563009	1.562970	1.562931	1.562892	1.562853	1.562814	1.562775	1.562736	1.562697	1.562657
5580	1.562925	1.562886	1.562846	1.562807	1.562768	1.562729	1.562690	1.562651	1.562612	1.562573	1.562534	1.562494	1.562455
5600	1.562726	1.562687	1.562648	1.562608	1.562569	1.562530	1.562491	1.562452	1.562413	1.562374	1.562334	1.562295	1.562256
5620	1.562529	1.562490	1.562451	1.562411	1.562372	1.562333	1.562294	1.562255	1.562216	1.562177	1.562137	1.562098	1.562059
5640	1.562334	1.562295	1.562256	1.562217	1.562177	1.562138	1.562099	1.562060	1.562021	1.561981	1.561942	1.561903	1.561864
5660	1.562142	1.562103	1.562064	1.562025	1.561985	1.561946	1.561907	1.561868	1.561829	1.561789	1.561750	1.561711	1.561672
5680	1.561952	1.561913	1.561874	1.561835	1.561795	1.561756	1.561717	1.561678	1.561639	1.561599	1.561560	1.561521	1.561482
5700	1.561765	1.561725	1.561686	1.561647	1.561608	1.561568	1.561529	1.561490	1.561450	1.561411	1.561372	1.561333	1.561294
5720	1.561579	1.561539	1.561500	1.561461	1.561422	1.561382	1.561343	1.561304	1.561264	1.561225	1.561186	1.561147	1.561107
5740	1.561395	1.561356	1.561316	1.561277	1.561238	1.561198	1.561159	1.561120	1.561080	1.561041	1.561002	1.560962	1.560923
5760	1.561213	1.561174	1.561134	1.561095	1.561056	1.561016	1.560977	1.560938	1.560898	1.560859	1.560820	1.560780	1.560741
5780	1.561034	1.560995	1.560955	1.560916	1.560877	1.560837	1.560798	1.560759	1.560719	1.560680	1.560640	1.560601	1.560562
5800	1.560856	1.560817	1.560778	1.560738	1.560699	1.560659	1.560620	1.560581	1.560541	1.560502	1.560462	1.560423	1.560384
5820	1.560681	1.560641	1.560602	1.560562	1.560523	1.560483	1.560444	1.560405	1.560365	1.560326	1.560286	1.560247	1.560207
5840	1.560508	1.560468	1.560429	1.560389	1.560350	1.560310	1.560271	1.560232	1.560192	1.560153	1.560113	1.560074	1.560034
5860	1.560336	1.560296	1.560257	1.560217	1.560178	1.560138	1.560099	1.560060	1.560020	1.559981	1.559941	1.559902	1.559862
5880	1.560166	1.560127	1.560087	1.560047	1.560008	1.559969	1.559929	1.559889	1.559850	1.559810	1.559771	1.559731	1.559692
5900	1.559998	1.559959	1.559919	1.559880	1.559840	1.559801	1.559761	1.559721	1.559682	1.559642	1.559603	1.559563	1.559524
5920	1.559832	1.559793	1.559753	1.559714	1.559674	1.559635	1.559595	1.559555	1.559516	1.559476	1.559437	1.559397	1.559358
5940	1.559669	1.559629	1.559589	1.559550	1.559510	1.559471	1.559431	1.559391	1.559352	1.559312	1.559273	1.559233	1.559193
5960	1.559506	1.559466	1.559426	1.559387	1.559347	1.559308	1.559268	1.559228	1.559189	1.559149	1.559110	1.559070	1.559030
5980	1.559346	1.559306	1.559267	1.559227	1.559187	1.559148	1.559108	1.559068	1.559029	1.558989	1.558949	1.558910	1.558870
6000	1.559187	1.559147	1.559108	1.559068	1.559028	1.558989	1.558949	1.558909	1.558870	1.558830	1.558790	1.558751	1.558711
6020	1.559029	1.558989	1.558950	1.558910	1.558870	1.558831	1.558791	1.558751	1.558712	1.558672	1.558632	1.558593	1.558553
6040	1.558874	1.558835	1.558795	1.558755	1.558715	1.558676	1.558636	1.558596	1.558557	1.558517	1.558477	1.558437	1.558398
6060	1.558720	1.558681	1.558641	1.558601	1.558561	1.558522	1.558482	1.558442	1.558403	1.558363	1.558323	1.558283	1.558244
6080	1.558568	1.558528	1.558488	1.558448	1.558409	1.558369	1.558329	1.558289	1.558249	1.558210	1.558170	1.558130	1.558090
6100	1.558418	1.558378	1.558338	1.558298	1.558259	1.558219	1.558179	1.558139	1.558099	1.558060	1.558020	1.557980	1.557940
6120	1.558269	1.558229	1.558189	1.558149	1.558110	1.558070	1.558030	1.557990	1.557950	1.557911	1.557871	1.557831	1.557791
6140	1.558121	1.558081	1.558041	1.558002	1.557962	1.557922	1.557882	1.557842	1.557802	1.557762	1.557723	1.557683	1.557643
6160	1.557975	1.557935	1.557896	1.557856	1.557816	1.557776	1.557736	1.557696	1.557656	1.557616	1.557576	1.557537	1.557497
6180	1.557831	1.557791	1.557752	1.557712	1.557672	1.557632	1.557592	1.557552	1.557512	1.557472	1.557432	1.557392	1.557353
6200	1.557689	1.557649	1.557609	1.557569	1.557529	1.557489	1.557449	1.557409	1.557369	1.557329	1.557289	1.557249	1.557209
6220	1.557547	1.557507	1.557467	1.557427	1.557387	1.557347	1.557307	1.557267	1.557227	1.557187	1.557147	1.557107	1.557067
6240	1.557407	1.557367	1.557327	1.557287	1.557247	1.557207	1.557167	1.557127	1.557087	1.557047	1.557007	1.556967	1.556927
6260	1.557269	1.557229	1.557189	1.557149	1.557109	1.557069	1.557029	1.556989	1.556949	1.556909	1.556869	1.556829	1.556789
6280	1.557132	1.557092	1.557052	1.557012	1.556972	1.556932	1.556892	1.556852	1.556812	1.556772	1.556732	1.556692	1.556652
6300	1.556996	1.556956	1.556916	1.556876	1.556836	1.556796	1.556756	1.556716	1.556676	1.556636	1.556596	1.556556	1.556516
6320	1.556863	1.556822	1.556782	1.556742	1.556702	1.556662	1.556622	1.556582	1.556542	1.556502	1.556462	1.556421	1.556381
6340	1.556730	1.556690	1.556649	1.556609	1.556569	1.556529	1.556489	1.556449	1.556409	1.556369	1.556329	1.556288	1.556248
6360	1.556598	1.556558	1.556518	1.556477	1.556437	1.556397	1.556357	1.556317	1.556277	1.556237	1.556196	1.556156	1.556116
6380	1.556468	1.556428	1.556388	1.556347	1.556307	1.556267	1.556227	1.556187	1.556147	1.556106	1.556066	1.556026	1.555986
6400	1.556339	1.556299	1.556259	1.556219	1.556178	1.556138	1.556098	1.556058	1.556018	1.555977	1.555937	1.555897	1.555857
6420	1.556211	1.556171	1.556131	1.556091	1.556050	1.556010	1.555970	1.555930	1.555889	1.555849	1.555809	1.555769	1.555729
6440	1.556085	1.556045	1.556005	1.555965	1.555924	1.555884	1.555844	1.555804	1.555764	1.555723	1.555683	1.555643	1.555603
6460	1.555960	1.555919	1.555879	1.555839	1.555799	1.555758	1.555718	1.555678	1.555637	1.555597	1.555557	1.555517	1.555476
6480	1.555836	1.555795	1.555755	1.555715	1.555675	1.555634	1.555594	1.555554	1.555513	1.555473	1.555433	1.555392	1.555352
6500	1.555714	1.555674	1.555633	1.555593	1.555553	1.555512	1.555472	1.555432	1.555391	1.555351	1.555311	1.555270	1.555230
6520	1.555592	1.555552	1.555511	1.555471	1.555431	1.555390	1.555350	1.555310	1.555269	1.555229	1.555189	1.555148	1.555108
6540	1.555472	1.555432	1.555392	1.555351	1.555311	1.555270	1.555230	1.555190	1.555149	1.555109	1.555068	1.555028	1.554988
6560	1.555353	1.555313	1.555273	1.555232	1.555192	1.555151	1.555111	1.555071	1.555030	1.554990	1.554949	1.554909	1.554869
6580	1.555236	1.555195	1.555155	1.555114	1.555074	1.555033	1.554993	1.554953	1.554912	1.554872	1.554831	1.554791	1.554750
6600	1.555119	1.555078	1.555038	1.554997	1.554957	1.554916	1.554876	1.554836	1.554795	1.554755	1.554714	1.554674	1.554633
6620	1.555003	1.554962	1.554922	1.554881	1.554841	1.554800	1.554760	1.554719	1.554679	1.554639	1.554598	1.554557	1.554517
6640	1.554888	1.554848	1.554807	1.554767	1.554726	1.554686	1.554645	1.554604	1.554564	1.554523	1.554483	1.554442	1.554402
6660	1.554775	1.554735	1.554694	1.554654	1.554613	1.554573	1.554532	1.554491	1.554451	1.554410	1.554370	1.554329	1.554289
6680	1.554662	1.554622	1.554581	1.554541	1.554500	1.554459	1.554419	1.554378	1.554338	1.554297	1.554257	1.554216	1.554176
6700	1.554552	1.554511	1.554470	1.554430	1.554389	1.554349	1.554308	1.554267	1.554227	1.554186	1.554146	1.554105	1.554064
6720	1.554442	1.554401	1.554360	1.554320	1.554279	1.554239	1.554198	1.554157	1.554117	1.554076	1.554035	1.553995	1.553954
6740	1.554332	1.554291	1.554251	1.554210	1.554169	1.554129	1.554088	1.554047	1.554007	1.553966	1.553925	1.553885	1.553844
6760	1.554224	1.554183	1.554143	1.554102	1.554061	1.554021	1.553980	1.553939	1.553899	1.553858	1.553817	1.553777	1.553736
6780	1.554117	1.554076	1.554036	1.553995	1.553954	1.553914	1.553873	1.553832	1.553792	1.553751	1.553710	1.553669	1.553629
6800	1.554010	1.553970	1.553929	1.553888	1.553847	1.553807	1.553766	1.553725	1.553685	1.553644	1.553603	1.553562	1.553522
6820	1.553905	1.553865	1.553824	1.553783	1.553743	1.553702	1.553661	1.553620	1.553579	1.553539	1.553498	1.553457	1.553416
6840	1.553802	1.553761	1.553720	1.553679	1.553639	1.553598	1.553557	1.553516	1.553475	1.553435	1.553394	1.553353	1.553312
6860	1.553699	1.553658	1.553617	1.553576	1.553536	1.553495	1.553454	1.553413	1.553372	1.553332	1.553291	1.553250	1.553209
6880	1.553596	1.553555	1.553514	1.553473	1.553433	1.553392	1.553351	1.553310	1.553269	1.553229	1.553188	1.553147	1.553106
6900	1.553495	1.553454	1.553413	1.553373	1.553332	1.553291	1.553250	1.553209	1.553168	1.553127	1.553087	1.553046	1.553005
6920	1.553394	1.553353	1.553313	1.553272	1.553231	1.553190	1.553149	1.553108	1.553067	1.553026	1.552985	1.552945	1.552904
6940	1.553295	1.553255	1.553214	1.553173	1.553132	1.553091	1.553050	1.553009	1.552968	1.552927	1.552886	1.552845	1.552805
6960	1.553197	1.553156	1.553115	1.553074	1.553033	1.552992	1.552951	1.552910	1.552869	1.552828	1.552787	1.552746	1.552705
6980	1.553099	1.553058	1.553017	1.552976	1.552935	1.552894	1.552853	1.552812	1.552771	1.552730	1.552689	1.552648	1.552607
7000	1.553002	1.552961	1.552920	1.552879	1.552838	1.552797	1.552756	1.552715	1.552674	1.552633	1.552592	1.552551	1.552510
7020	1.552906	1.552865	1.552824	1.552783	1.552742	1.552701	1.552660	1.552619	1.552578	1.552537	1.552496	1.552455	1.552414
7040	1.552811	1.552770	1.552729	1.552688	1.552647	1.552606	1.552565	1.552524	1.552483	1.552442	1.552401	1.552360	1.552319
7060	1.552717	1.552676	1.552635	1.552594	1.552553	1.552512	1.552471	1.552430	1.552389	1.552348	1.552307	1.552266	1.552225
7080	1.552623	1.552582	1.552541	1.552500	1.552459	1.552418	1.552377	1.552336	1.552295	1.552254	1.552213	1.552171	1.552130
7100	1.552532	1.552491	1.552449	1.552408	1.552367	1.552326	1.552285	1.552244	1.552203	1.552162	1.552121	1.552079	1.552038

TABLE 2. *Observed and computed refractive indices of potassium bromide at 22° C*

Character of source	Designation of line	Wavelengths in air	n (observed)	n (computed)	Residual (observed minus computed)
		μ			
Helium tube		0.7065188	1.552449	1.552447	$+2\times10^{-6}$
Mercury arc		.6907496	1.553207	1.553212	−5
Helium tube	He red	.6678149	1.554433	1.554430	+3
Cadmium arc	Cd red	.6438470	1.555853	1.555853	0
Helium tube	d	.5875618	1.559967	1.559966	+1
Mercury arc	e	.5460740	1.563928	1.563930	−2
Cadmium arc	Cd green	.5085824	1.568476	1.568479	−3
Mercury arc		.4916036	1.570945	1.570935	+10
Hydrogen tube	F	.4861327	1.571786	1.571789	−3
Mercury arc	g	.4358342	1.581474	1.581475	−1
Do	h	.4046563	1.589754	1.589753	+1

TABLE 3. *Temperature coefficients of refractive index of potassium bromide*

Wavelength	$-\frac{dn}{dt}$ (observed)	$-\frac{dn}{dt}$ (computed)	Residual (observed minus computed)
μ			
0.4047	36.75×10^{-6}	37.09×10^{-6}	-0.34×10^{-6}
.4358	37.10	37.50	−.40
.4861	38.37	38.16	+.21
.4916	37.29	38.24	−.95
.5086	39.43	38.46	+.97
.5461	39.20	38.95	+.25
.5876	40.03	39.50	+.53
.6438	39.67	40.24	−.57
.6678	41.58	40.56	+1.02
.6907	40.41	40.86	−0.45
.7065	40.83	41.07	−.24

Subsequent examination of two different samples of potassium bromide by the authors verifies the possibility of even larger differences between samples. More important, differences in dispersion between samples were indicated. Figure 10 shows plots of the differences between the two other crystals studied, and the one measured upon the two spectrometers. The values designated as P_1 represent the 60° sample upon which the most extensive series of measurements was made, P_2 is a 30° prism, and P_3 is another 60° prism. Prism P_3 gave very poor imagery, and double images of the collimator slit were detected. Upon examination, this prism appeared cracked along cleavage planes in the interior of the crystal. Single, but indistinct, images of the collimator slit appeared when the prism aperture was reduced by masking portions of the surfaces with black paper so that the radiation did not pass through the portion containing the flaws. Differences in indices amounting to as much as one unit in the third decimal place in the blue were noted for this crystal, together with a definite difference in dispersion, as indicated by the slope of the curve. The differences between P_2 and P_1 are much less pronounced, amounting to about $+6.7\times10^{-5}$ in the average. No difference in dispersion between these two samples was found.

5. Conclusion

The values of refractive indices in table 1 are thought to have errors not exceeding $\pm5\times10^{-6}$. It should be understood that these index values are for the particular sample measured. The values reported by other observers are on the whole distributed rather symmetrically around the values reported in this paper. Systematic differences between different samples appear more important than hitherto realized. The reasons for these differences are not clearly understood but probably have to do with different amounts and types of impurities in the samples. The effect of impurities

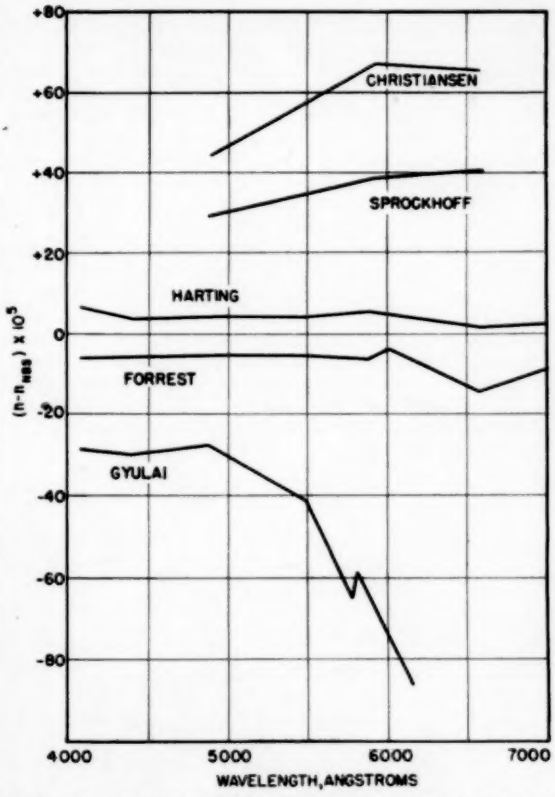

FIGURE 9. *Comparison of indices of potassium bromide reported by different observers.*

Harting's data and the NBS data are given for 20° C. Christiansen's data at 18° C, Sprockhoff's at 18° C, Forrest's at 26.4° C, and Gyulai's at 48° C were reduced to their 20° C equivalents by use of the temperature coefficients in table 3.

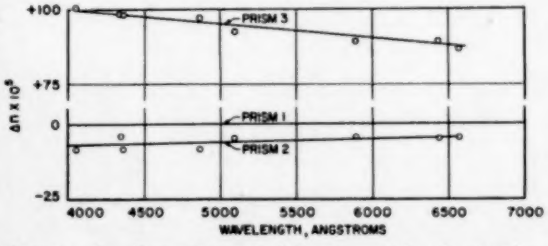

FIGURE 10. *Comparison of different crystals of potassium bromide at 23° C.*

upon the ultraviolet absorption band is well known. Melvin [14], for example, mentioned in 1931 that the transmission limits of four samples of lithium fluoride varied between 1080 and 1350A owing to slight traces of impurities. Shifting this absorption band, of course, influences the dispersion in this neighborhood, and it appears possible in the case of potassium bromide that this influence may extend into the visible region of the spectrum. Strain will also affect the refractive index, and it is possible that prism P_3 has some internal strain. This prism was one of the first to be made in this country, and it is possible that the same degree of care was not taken in purifying the salt and removing strain by annealing as is taken today in manufacturing such crystals. It is thought that the variation demonstrated between samples P_1 and P_2 is more nearly representative of the order of magnitude of the variation to be found between different samples of potassium bromide.

6. References

[1] W. S. Rodney, Dissertation, the Catholic University of America, Washington, D. C. (1951).
[2] H. Harting, Z. Instrumentenk. **63,** 125–136 (1943).
[3] J. W. Forrest, J. Opt. Soc. Am. **32,** 382 (1942).
[4] G. N. Ramachandran, Proc. Indian Acad. Sci. [A] **25,** (1947).
[5] T. Radhakrishnan, Proc. Indian Acad. Sci. [A] **31,** (1950).
[6] J. Guild and G. W. Watts, Proc. Opt. Conv. **II,** (1926).
[7] J. Guild, Proc. Phys. Soc. (London) **29,** 311 (1916).
[8] R. Glazebrook, Dictionary of Applied Physics **IV.**
[9] L. W. Tilton, BS J. Research **2,** 909 (1929) RP64.
[10] L. W. Tilton, J. Research NBS **14,** 393 (1935) RP393.
[11] H. Topsoe and C. Christiansen, Ann. chim. et phys. 5–99 (1874).
[12] M. Sprockhoff, Neues Jahr. Mineral. Geol., Beilage **18,** 117–154 (1904).
[13] Z. Gyulai, Z. Physik **46,** 80 (1927).
[14] E. Melvin, Phys. Rev. **37,** 1230 (1931).

Washington, D. C., July 30, 1952.

On Approximate Solutions of Systems of Linear Inequalities*

Alan J. Hoffman

Let $A\boldsymbol{x} \leqq \boldsymbol{b}$ be a consistent system of linear inequalities. The principal result is a quantitative formulation of the fact that if $\boldsymbol{x}$ "almost" satisfies the inequalities, then $\boldsymbol{x}$ is "close" to a solution. It is further shown how it is possible in certain cases to estimate the size of the vector joining $\boldsymbol{x}$ to the nearest solution from the magnitude of the positive coordinates of $A\boldsymbol{x}-\boldsymbol{b}$.

1. Introduction

In many computational schemes for solving a stem of linear inequalities

$$\begin{aligned} A_1 \cdot \boldsymbol{x} &= a_{11}x_1 + \ \ldots\ + a_{1n}x_n \leqq b_1 \\ &\cdot \\ &\cdot \\ &\cdot \\ A_m \cdot \boldsymbol{x} &= a_{m1}x_1 + \ \ldots\ + a_{mn}x_n \leqq b_m \end{aligned} \tag{1}$$

riefly, $A\boldsymbol{x} \leqq \boldsymbol{b}$), one arrives at a vector $\bar{\boldsymbol{x}}$ that lmost" satisfies (1). It is almost obvious geo- trically that, if (1) is consistent, one can infer at there is a solution $\boldsymbol{x}_0$ of (1) "close" to $\bar{\boldsymbol{x}}$. The urpose of this report is to justify and formulate recisely this assertion.[1] We shall use fairly general efinitions of functions that measure the size of ectors, since it may be possible to obtain better stimates of the constant c (whose important role described in the statement of the theorem) for me measuring functions than for others. We shall ake a few remarks on the estimation of c after mpleting the proof of the main theorem.

2. The Main Theorem

We require the following

efinitions:

For any real number a, we define

$$a^+ = \begin{cases} a & \text{if } a \geqq 0 \\ 0 & \text{if } a < 0. \end{cases}$$

or any vector $\boldsymbol{y} = (y_1, \ldots, y_k)$, we define

$$\boldsymbol{y}^+ = (y_1^+, \ldots, y_k^+). \tag{2}$$

A positive homogeneous function F_k defined on -space is a real continuous function satisfying

(i) $F_k(\boldsymbol{x}) \geqq 0$, $F_k(\boldsymbol{x}) = 0$ if, and only if, $\boldsymbol{x} = \boldsymbol{0}$

(ii) $\alpha \geqq 0$ implies $F_k(\alpha\boldsymbol{x}) = \alpha F_k(\boldsymbol{x})$ (3)

Theorem: *Let* (1) *be a consistent system of inequalities and let* F_n *and* F_m *each satisfy* (3). *Then there exists a constant* $c > 0$ *such that for any* $\boldsymbol{x}$ *there exists a solution* $\boldsymbol{x}_0$ *of* (1) *with*

$$F_n(\boldsymbol{x} - \boldsymbol{x}_0) \leqq cF_m\ (A\boldsymbol{x} - \boldsymbol{b})^+).$$

The proof is essentially contained in two lemmas (2 and 3 below) given by Shmuel Agmon.[2]

Lemma 1. *If* F_m *satisfies* (3), *there exists an* $e > 0$ *such that for every* $\boldsymbol{y}$ *and every subset* S *of the half spaces* (1)

$$F_m(\bar{\boldsymbol{y}}) \leqq eF_m(\boldsymbol{y})$$

where $\boldsymbol{y} = (y_1, \ldots, y_m)$, $\bar{\boldsymbol{y}} = (\bar{y}_1, \ldots, \bar{y}_m)$, *and*

$$\bar{y}_i = \begin{cases} y_i & \text{if the } i\text{th half space belongs to } S \\ 0 & \text{otherwise.} \end{cases}$$

Proof. It is clear from (3) (i) that any e will suffice for $y = 0$. By (3) (ii), we need only consider the ratio $F_m(\bar{\boldsymbol{y}})/F_m(\boldsymbol{y})$ for $\boldsymbol{y}$ such that $F(\boldsymbol{y}) = 1$, a compact set. Hence, for each subset S, $F_m(\bar{\boldsymbol{y}})/F_m(\boldsymbol{y})$ has a maximum e_S. Set $e = \max e_S$.

Lemma 2. *Let* Ω *be the set of solutions of* (1), *let* $\boldsymbol{x}$ *be a point exterior to* Ω, *and let* $\boldsymbol{y}$ *be the point in* Ω *nearest to* $\boldsymbol{x}$. *Let* S *be the subset of the half spaces* (1), *each of which contains* y *in its bounding hyperplane, and let* Ω_S *be the intersection of these half spaces.*

Then $\boldsymbol{x}$ *is exterior to* Ω_S *and* $\boldsymbol{y}$ *is the nearest point of* Ω_S *to* $\boldsymbol{x}$.

Lemma 3. *Let* M *be an* $m \times n$ *matrix obtained from* A *by substituting* 0 *for some of the rows of* A, *and let* Ω *be the cone of solutions of* $M\boldsymbol{z} \leqq 0$. *Let* E *be the set of all points* x *such that* (i) $\boldsymbol{x}$ *is exterior to* Ω, *and* (ii) *the origin is the point of* Ω *nearest to* $\boldsymbol{x}$.

Then there exists a $d_S > 0$ *such that* $\boldsymbol{x} \epsilon E$ *implies*

$$F_m((M\boldsymbol{x})^+) \geqq d_S F_n(\boldsymbol{x}).$$

Proof of the theorem. Let $\boldsymbol{x}$ be any vector exterior to the solutions Ω of (1), let $\boldsymbol{x}_0$ be the point of Ω nearest to $\boldsymbol{x}$, and let S be defined as in lemma 2.

Let M be the matrix obtained from A by substitut-

*This work was sponsored (in part) by the Office of Scientific Research, USAF.

[1] A. M. Ostrowski has kindly pointed out that part of the results given below is implied by the fact that if K and L are two convex bodies each of which is in small neighborhood of the other, then their associated gauge functions differ slightly.

[2] S. Agmon, The relaxation method for linear inequalities, National Applied Mathematics Laboratory Report 52-27, NBS (prepublication copy).

ing 0 for the rows not in S, and let $\bar{\boldsymbol{b}}$ be the vector obtained from $\boldsymbol{b}$ by substituting 0 for the components not contained in S.

Then lemma 2 says that $\boldsymbol{x}_0$ satisfies $M\boldsymbol{z}=\bar{\boldsymbol{b}}$, $\boldsymbol{x}$ is exterior to the solutions of $M\boldsymbol{z}\leqq\bar{\boldsymbol{b}}$, and $\boldsymbol{x}_0$ is the solution of $M\boldsymbol{z}\leqq\bar{\boldsymbol{b}}$ nearest to $\boldsymbol{x}$. Perform the translation $\boldsymbol{z}'=\boldsymbol{z}-\boldsymbol{x}_0$. Then $M\boldsymbol{z}\leqq\bar{\boldsymbol{b}}$ if, and only if,

$$M\boldsymbol{z}'=M\boldsymbol{z}-M\boldsymbol{x}_0=M\boldsymbol{z}-\bar{\boldsymbol{b}}\leqq\boldsymbol{0}.$$

Thus $\boldsymbol{x}-\boldsymbol{x}_0$ belongs to the set E of lemma 3, and

$$F_m((M\boldsymbol{x}-\bar{\boldsymbol{b}})^+)=F_m((M(\boldsymbol{x}-\boldsymbol{x}_0))^+)\geqq d_S F_n(\boldsymbol{x}-\boldsymbol{x}_0)\geqq dF_n(\boldsymbol{x}-\boldsymbol{x}_0),$$

where $d=\min_S d_S$.

Thus,

$$F_n(\boldsymbol{x}-\boldsymbol{x}_0)\leqq\frac{1}{d}F_m(M\boldsymbol{x}-\bar{\boldsymbol{b}})\leqq\frac{e}{d}F_m((A\boldsymbol{x}-\boldsymbol{b})^+),$$

using lemma 1. Setting $c=e/d$ completes the proof of the theorem.

3. Estimates of c for various norms

None of the estimates to be obtained is satisfactory, since each requires an inordinate amount of computation except in special cases. It is worth remarking, however, that even without knowledge of the size of c, the theorem is of use in insuring that any computation scheme that makes $(A\boldsymbol{x}-\boldsymbol{b})^+$ approach $\boldsymbol{0}$ will bring x close to the set of solutions of (1). This guarantees, for instance, that in Brown's method for solving games the computed strategy vector is approaching the set of optimal strategy vectors.

In what follows let

$|\boldsymbol{x}|$ =maximum of the absolute values of the coordinates of $\boldsymbol{x}$;

$||\boldsymbol{x}||$ =sum of the absolute values of the coordinates of $\boldsymbol{x}$;

$|||\boldsymbol{x}|||$=the square root of the sum of the squares of the coordinates of $\boldsymbol{x}$.

Note that if F_m is any one of these norms, then $e=1$. We consider these cases:

Case I. $F_n=|||\quad|||$, $F_m=|\quad|$. If $C=(c_{ij})$ is a square matrix of rth order, let

$$\Gamma(C)=\left[\sum_{j=1}^{r}\left(\sum_{i=1}^{r}|C_{ij}|\right)^2\right]^{\frac{1}{2}},$$

where the C_{ij}'s are the cofactors of the elements of c_{ij}. Using this notation, and assuming that the rows of (1) are normalized so that $\sum_{j=1}^{n}a_{ij}^2=1$, Agmon (see p. 9 of reference in footnote 2) has shown that if A is of rank r, then

$$C\leqq\frac{\left[\sum_{1\leq h<\cdots<j_r\leq n}(\Gamma^{j_1,\ldots,j_r}_{i_1,\ldots,i_r})^2\right]^{\frac{1}{2}}}{\left[\sum_{1\leq h<\cdots<j_r\leq n}|A^{j_1,\ldots,j_r}_{i_1,\ldots,i_r}|^2\right]^{\frac{1}{2}}},$$

where $i_1, \ldots, i_r$ are r (fixed) linearly independe rows of (a_{ij}); $A^{j_1,\ldots,j_r}_{i_1,\ldots,i_r}$ is the $r\times r$ submatr formed by the fixed rows and indicated columns, an where the summation is performed over all differe combinations of the j's.

Case II. $F_n=|\quad|$, $F_m=|\quad|$.

Case III. $F_n=|\quad|$, $F_m=||\quad||$.

For cases II and III, it is convenient to have description of E alternative to that contained i lemma 3. We shall use the notation of lemma 3.

Lemma 4. *Let K'=the cone spanned by the ro vectors of M, with the origin deleted. Then $K'=E$.*

Proof. Let $M_1, \ldots, M_m$ be the row vectors of M and let $\boldsymbol{x}=\lambda_1M_1+\ \ldots\ +\lambda_mM_m$, where $\boldsymbol{x}\neq\boldsymbol{0}$, an $\lambda_i\geqq0$, $i=1, \ldots, m$. Then $\boldsymbol{x}$ is exterior to Ω, an the origin is the point of Ω closest to $\boldsymbol{x}$; that is, $\boldsymbol{z}\in$ implies $(\boldsymbol{x}-\boldsymbol{z})\cdot(\boldsymbol{x}-\boldsymbol{z})-\boldsymbol{x}\cdot\boldsymbol{x}\geqq0$. For $\boldsymbol{z}\cdot\boldsymbol{x}=\boldsymbol{z}\cdot(\lambda_1M_1+\ \ldots\ +\lambda_mM_m)=\lambda_1\boldsymbol{z}\cdot M_1+\ \ldots\ +\lambda_m\boldsymbol{z}\cdot M_m\leqq0$. Hence $(\boldsymbol{x}-\boldsymbol{z})\cdot(\boldsymbol{x}-\boldsymbol{z})-\boldsymbol{x}\cdot\boldsymbol{x}=\boldsymbol{z}\cdot\boldsymbol{z}-2\boldsymbol{z}\cdot\boldsymbol{x}\geqq0$. This shows tha $K'\subset E$.

We now prove that $E\subset K'$. Assume $\boldsymbol{x}\in E$. Then

$$\boldsymbol{z}\in\Omega \text{ implies } \boldsymbol{z}\cdot\boldsymbol{x}\leqq0 \tag{4}$$

(otherwise let w be a sufficiently small positive num ber; then $w\,\boldsymbol{z}\in\Omega$ and $w\boldsymbol{z}\cdot w\boldsymbol{z}-2w\boldsymbol{z}\cdot\boldsymbol{x}<0$). Consider $\boldsymbol{z}$ as the coordinates of a half space whose bounding plane contains the origin. Then (4) says that all half spaces ("through" the origin) containing the row vectors of M also contain $\boldsymbol{x}$. It is a fundamental result in the theory of linear inequalities [2] that this later statement implies that $\boldsymbol{x}$ is in the cone generated by the rows of M. Hence $E\subset K'$.

4. Case II

It is clear from the proof of the theorem that all we need is to calculate $\min_{\boldsymbol{x}\in E}(|M\boldsymbol{x})^+|/|\boldsymbol{x}|)$, for each M corresponding to a subset S of the vectors $A_1, \ldots, A_m$. Let $A_1, \ldots, A_k$ (say) be the vectors of the subset S. Then by lemma 4, $\boldsymbol{x}\in E$ implies that there exist $\lambda_1, \ldots, \lambda_k$ with $\lambda_j\geqq0$ such that

$$\boldsymbol{x}=\lambda_1A_1+\ \ldots\ +\lambda_kA_k. \tag{5}$$

Hence,

$$|\boldsymbol{x}|\leqq a_S\sum_{j=1}^{k}\lambda_j, \tag{6}$$

where a_S is the largest absolute value of the co-ordinates of $A_1, \ldots, A_k$.

It follows from the homogeneity of $|(M\boldsymbol{x})^+|/|\boldsymbol{x}|$ that

[2] T. S. Motzkin, Beiträge zur Theorie der Linearen Ungleichungen. Jerusalem, 1936, with references to proofs by Minkowski and Weyl.

need only consider $x \in E$ such that if x is expressed in (5), $\sum_{j=1}^{k} \lambda_j = 1$.

Then

$$|Ax|^+| = \max_i (A_i \cdot x)^+ = \max_i (A_i \cdot x) =$$

$$\max_i \left(A_i \cdot \sum_{j=1}^{k} \lambda_j A_j \right) = \max_i \sum_{j=1}^{k} g_{ij} \lambda_j,$$

where $g_{ij} = A_i \cdot A_j, \lambda_j \geqq 0, \sum \lambda_j = 1$.

Hence,

$$\min |(Mx)^+| = \min_{\lambda} \max_i \sum_{j=1}^{k} g_{ij} \lambda_j = v_S, \tag{7}$$

where v_S is the value of zero sum two person game whose matrix is g_{ij}.

Therefore, from (6) and (7)

$$\min_{x \in E} \frac{|(Mx)^+|}{|x|} \geqq \frac{v_S}{a_S}.$$

When $v_S = 0$? Clearly, if, and only if, the origin is in the convex body spanned by $A_1, \ldots, A_k$. But this would imply that the set E is the entire space (except for the origin). And it follows from the proof of the main theorem that this can occur only for a subset that would never arise in lemma 2.

Therefore, using the language of the theorem

$$|x - x_0| \leqq c |(Ax - b)^+|, \tag{8}$$

where

$$c = \max_{v_S > 0} \frac{a_S}{v_S}.$$

A special case occurs when all $A_i \cdot A_j > 0$. Let $v = \min_{i,j} A_i \cdot A_j$, $a = \max_{i,j} |a_{ij}|$. Then,

$$|x - x_0| \leqq \frac{a}{v} |(Ax - b)^+|. \tag{9}$$

5. Case III

Reasoning, along the lines of case II, we need only estimate $\min_{\lambda} |\left(\sum_{j=1}^{k} g_{ij} \lambda_j \right)^+|$, and it is possible to derive from it an expression analogous to (8), which unfortunately does not seem to have a neat statement in terms of games or any other familiar object. An interesting special case occurs, however, if the matrix g_{ij} (for S all the rows of A), has the property that

$$w = \min_i \left(g_{ii} + \sum_{\substack{j=1 \\ g_{ij} < 0}}^{n} g_{ij} \right) > 0.$$

Then

$$\min |\left(\sum_{j=1}^{k} g_{ij} \lambda_j \right)^+| \geqq \min_{\lambda} \sum_{i=1}^{k} \sum_{j=1}^{k} g_{ij} \lambda_j$$

$$= \min_{\lambda} \sum_{j=1}^{k} \lambda_j \sum_{i=1}^{k} g_{ij} \geqq \min_{\lambda} \sum_{j=1}^{k} \lambda_j w = w.$$

Then we obtain, with a having the same meaning as in (9)

$$|x - x_0| \leqq \frac{a}{w} |(Ax - b)^+|. \tag{10}$$

WASHINGTON, June 5, 1952.

rnal of Research of the National Bureau of Standards Vol. 49, No. 4, October 1952 Research Paper 2363

Deuterium and Hydrogen Electrode Characteristics of Lithia-Silica Glasses

Donald Hubbard and Given W. Cleek

The pH and pD responses of a series of lithia-silica glasses have been investigated and compared with the hygroscopicity, deuteroscopicity, and chemical durability of the glasses in aqueous and deuterium oxide buffers. The curves for pH and pD response as a function of composition pass through an optimum electrode response that is limited on the low percentage of silica end by poor chemical durability and a strong tendency to devitrify upon reheating the glasses for the purpose of blowing the electrodes. The optimum also falls off on the high-silica end where opalescence appears and the hygro- and deuteroscopicities decrease.

The pH and pD response, hygroscopicity, and deuteroscopicity, as well as the chemical durability in aqueous and deuterium oxide solutions, appear to reflect some of the critical features of the Li_2O-SiO_2 phase equilibrium diagram, with the optimum electrode response occurring in the composition range in which tridymite is the primary phase.

Indices of refraction and expansion data for these Li_2O-SiO_2 glasses exhibit breaks at the same compositions indicated by the physicochemical properties.

1. Introduction

Electrodes prepared from silicate glasses whose mpositions include substantial percentages of i2O have become commercially accepted in recent ars because of their favorable voltage response to drogen-ion activity in aqueous solutions over an tended range of pH, alkaline salt concentrations, d temperature [1 to 4].[1] Considerable confusion, wever, still prevails in the readily available literare concerning the use of Li_2O in electrode glasses to 10]. The present investigation was undertaken ascertain whether a series of Li_2O-SiO_2 glasses exibited any unusual features in regard to the normal pendence of pH response upon the properties of itable chemical durability and adequate hygropicity [11 to 13]. In addition, a study of the deuroscopicity,[2] chemical durability to deuterium xide solutions, and the electrode response (pD) of ese Li_2O-SiO_2 glasses to deuterium-ion activity ere undertaken.

The experimental procedures employed for dermining the deuteroscopicity, pD response, and the emical durability to deuterium buffers of this series glasses were similar to the procedures reported in evious investigations on other glass series for hygropicity, pH response, and chemical durability to queous solutions [11 to 13].

2. Hygroscopicity and Deuteroscopicity

The hygroscopicity and deuteroscopicity values sted in table 1 and plotted in figure 1 were obtained n two series of Li_2O-SiO_2 glasses. One of these eries (○) was that studied for density and reported y Young and his colleagues [14]. Their glasses had een analyzed and carefully annealed by a cooling schedule designed to place each member of the series in a comparable condition. The hygroscopicity and deuteroscopicity composition curves for these glasses demonstrated abrupt changes at the same compositions indicated by the density composition curve [14] and by other hygroscopicity composition data obtained by a different procedure and reported in an earlier publication [15]. Data for index of refraction [3] and expansion [4] obtained on this same series of glasses are presented in table 2 and figure 2 because they emphasize the same composition features shown by the hygroscopicity and deuteroscopicity curves.

For all properties studied on this analyzed and carefully annealed series of glasses, including the amounts of H_2O and D_2O retained upon reheating at 110° C after the completion of the hygroscopicity and deuteroscopicity experiments, distinct changes in the slopes are indicated near 82 and 77 percent of SiO_2. The break at the higher percentage of SiO_2 corresponds very closely to the eutectic composition between the compounds $Li_2O.2SiO_2$ and tridymite, while the other is approximately 2 percent lower in SiO_2 than the transition point reported between $Li_2O.SiO_2$ and $Li_2O.2SiO_2$ [19].

The compositions for the members of the new series of Li_2O-SiO_2 glasses whose hygroscopicity and deuteroscopicity are plotted (+) in figure 1 were calculated from the batch compositions. No definite schedule had been observed in cooling through the annealing range.

The exaggerated difference in the two series of glasses can probably be ascribed to the extent of the departure from randomness of the silica network. This is strongly supported by the fact that the lithia-silica glasses show a marked tendency to crystallize in the composition ranges in which $Li_2O.SiO_2$ and SiO_2 are the primary phases.

[1] Figures in brackets indicate the literature references at the end of this paper.

[2] "Deuteroscopicity" is the expression applied to D_2O sorption corresponding to the term "hygroscopicity."

[3] These index of refraction values were obtained by C. A. Faick, using an immersion method [16, 17].

[4] These expansion data were taken by L. H. Maxwell, using the Saunders' modified Fizeau interferometric procedure [18].

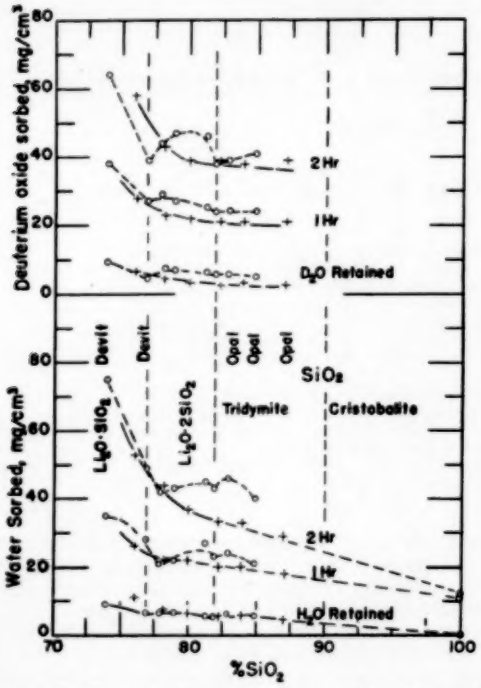

FIGURE 1. *Hygroscopicity and deuteroscopicity of two series of* Li_2O-SiO_2 *glasses.*

(o), glasses annealed and analyzed [14]; (+), glasses having no definite annealing schedule and whose compositions were calculated from batch compositions.

TABLE 1. *Hygroscopicity and deuteroscopicity of two series of* Li_2O–SiO_2 *glasses*

Glasses		Water (H_2O)			Deuterium oxide (D_2O)		
Li_2O	SiO_2	Sorbed 1 hr	Sorbed 2 hr	Retained	Sorbed 1 hr	Sorbed 2 hr	Retained
%	%	mg/cm²	mg/cm²	mg/cm²	mg/cm²	mg/cm²	mg/cm²
A. Annealed and analyzed glasses of Young, Glaze, Faick, and Finn [14]							
26.13	73.87	33	75	8.8	38	64	9.7
23.18	76.82	27	49	6.4	27	39	4.6
22.20	77.80	21	42	6.5	29	44	7.7
21.09	78.91	22	43	6.7	27	47	7.0
18.73	81.27	27	45	5.5	25	46	6.1
18.11	81.89	23	43	5.2	24	38	5.9
17.05	82.95	24	46	6.0	24	39	5.9
15.12	84.88	21	40	5.6	24	41	5.0
Fused SiO_2		11	12	0	----	----	-----
B. Glasses whose compositions were calculated from the batch composition							
23.9	76.1	26	53	11.0	28	57	6.9
21.8	78.2	22	44	7.4	23	43	4.3
20.0	80.0	22	37	6.3	22	39	3.4
17.8	82.2	20	33	5.4	21	39	2.5
16.1	83.9	20	33	5.9	21	38	3.1
12.9	87.1	19	28	4.2	21	39	2.3
Corning 015 [a]		104	108	-------	----	----	-----

[a] A commercial electrode glass included for comparison.

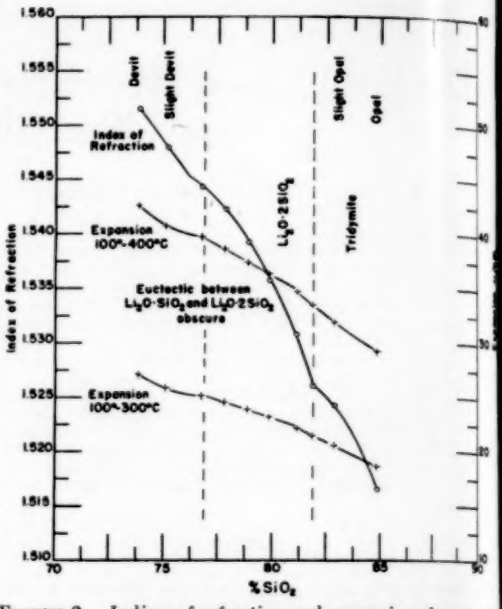

FIGURE 2. *Indices of refraction and expansion characteristi of a series of* Li_2O-SiO_2 *glasses.*

TABLE 2. *Index of refraction* (Na λ=5889) *and expansi characteristics of a series of* Li_2O-SiO_2 *glasses*

Glasses		Expansion				Critical temperature	Softening temperature	Index of refraction
Li_2O	SiO_2	100° to 300° C	100° to 400° C	100° CT [a]	100° ST [b]			
%	%	μ/cm	μ/cm	μ/cm	μ/cm	°C	°C	
26.13	73.87	27.1	42.6	50.7	60.7	445	475	1.5313
24.81	75.19	25.9	40.7	48.0	58.0	445	475	1.5480
23.18	76.82	25.1	39.7	48.7	54.7	450	475	1.5443
22.20	77.80	24.5	38.6	48.5	56.0	460	485	1.5423
21.09	78.91	23.8	37.3	46.2	56.7	460	490	1.5392
20.06	79.94	23.1	36.3	45.0	56.0	460	490	1.5357
18.73	81.27	22.1	34.7	44.1	46.6	465	480	1.5307
18.11	81.89	21.4	33.5	42.8	49.8	465	495	1.5290
17.05	82.95	20.5	31.8	39.7	47.7	455	480	1.5242
15.12	84.88	18.6	29.2	36.7	43.2	460	490	1.5165
Fused SiO_2		----	----	----	----	----	----	1.4567

[a] CT, critical temperature. [b] ST, softening temperature.

3. Chemical Durability

The chemical durabilities of the Li_2O-SiO_2 glasses over an extended pH range are listed in table 3 and plotted in figure 3. These durability data, obtained by an interferometer procedure [20, 21], illustrate the familiar swelling in the acid range (represented as negative attack in the figure), and the usual solution of the glass in the alkaline buffers. These durability features are characteristic of many silicate glasses exposed to the Britton-Robinson universal buffer mixtures at 80° C [11 to 13].

TABLE 3. *Chemical durability and* pH *response of* Li_2O-SiO_2 *glasses in Britton-Robinson universal buffers*

Glasses [a]		Chemical durability (6 hr, 80° C) at pH						pH response, 4.1 to 8.2 after soaking			Working characteristics
Li_2O	SiO_2	2.0	4.1	6.0	8.2	10.2	11.8	15 min	6 hr	24 hr	
Wt %	*Wt %*	*Fringes*	*Fringes*	*Fringes*	*Fringes*	*Fringes*	*Fringes*	*mv*/pH	*mv*/pH	*mv*/pH	
23.9	76.1	30 swell	30 swell	30 swell	24 swell	30 attack	72 attack	(e)	------	------	Devitrified.
21.8	78.2	9 swell	9 swell	9 swell	9 swell	6 attack	21 attack	(e)	------	------	Slight devitrification.
20.0	80.0	1½ swell	1½ swell	1½ swell	2− swell	1½ attack	7 attack	32.5	------	14.0	Clear.
17.8	82.2	1− swell	1− swell	½+ swell	½+ swell	SC [d]	2 attack	56.5	54.0	44.5	Do.
16.1	83.9	¼ swell	¼ swell	¼ swell	$^{3}/_{10}$ swell	SC [d]	1½ attack	57.5	57.5	57.5	Slight opal.
12.9	87.1	$^{1}/_{10}$+ swell	$^{1}/_{10}$+ swell	$^{1}/_{10}$+ swell	D [c] swell	SC [d]	1+ attack	------	55.5	55.5	Opal.
Fused SiO_2		ND [b]	ND [b]	ND [b]	ND [b]	ND [b]	½ attack	(f)	(f)	(f)	

[a] Series B of table 1. [b] ND, not detectable. [c] D, detectable. [d] SC, surface cut. [e] Devitrified. [f] No definite pH response.

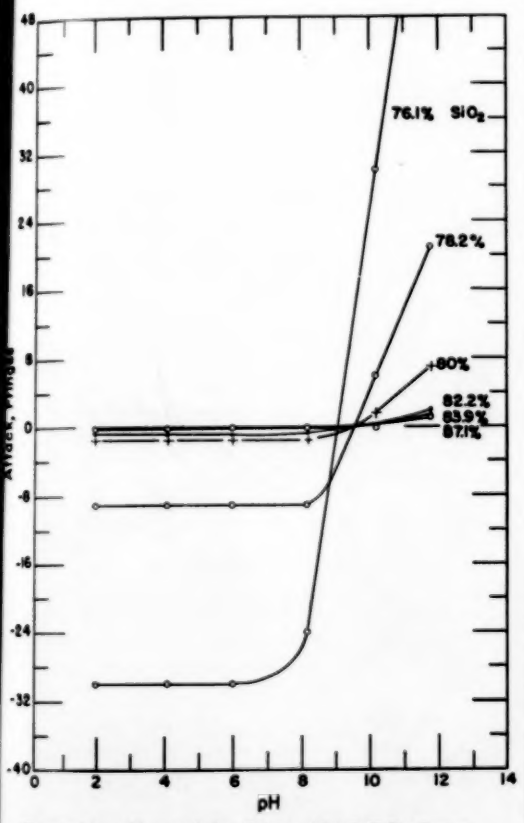

FIGURE 3. *Chemical durability of* Li_2O-SiO_2 *glasses.*

Britton-Robinson universal buffer mixtures, 6 hours, 80° C.

4. Relation Between pH Response, Hygroscopicity, and Chemical Durability

An over-all picture of the dependence of pH response of the Li_2O-SiO_2 glasses on their chemical durability and hygroscopicity is shown in figure 4. The pronounced decline in the chemical durability for members of this series having increased Li_2O

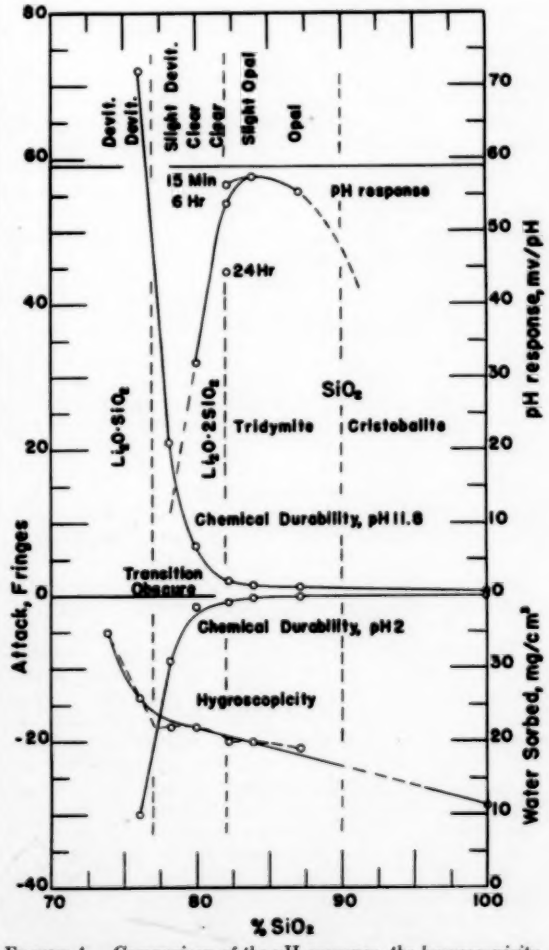

FIGURE 4. *Comparison of the* pH *response, the hygroscopicity, and the chemical durability at* pH 2 *and* 11.8 *of a series of* Li_2O-SiO_2 *glasses.*

The approximate compositions at which a new primary phase appears in the equilibrium diagram are indicated by vertical lines. Hygroscopicity values (1-hr exposure) are for glasses "B" table 1, except for 73.8 percent SiO_2—two possible curves are drawn through the resulting composite data.

content, as indicated by the curves for attack and swelling at pH 11.8 and pH 2, respectively, is associated with an equally pronounced failure in the pH response of electrodes prepared from these glasses. Although the composition range over which successful electrodes can be prepared is restricted by the appearance of coarse devitrification for the glasses of lower percentages of SiO_2 upon reheating for the purpose of blowing the electrode bulbs, and by the appearance of opals in the higher SiO_2 members, the pH response–composition curve obviously indicates an optimum similar to those found for all other series of glasses previously investigated [11, 12, 13].

The correspondence between the departures of the pH response–composition curve and some of the critical compositions of the phase equilibrium diagram is rather striking, with the optimum performance appearing in the composition range in which tridymite is the primary phase [19].

Perhaps the most interesting and possibly the most significant feature of these data is the fact that the optimum pH response for the Li_2O-SiO_2 glasses occurs at much lower values of hygroscopicity than do the optima for Na_2O-SiO_2 and K_2O-SiO_2 glasses [13]. Whether this has any significant bearing on an ultimate acceptable theory for the glass electrode can only be ascertained in light of much additional data on other series of glasses.

5. Comparison of pD Response and pH Response of Li_2O-SiO_2 Glasses

In an effort to obtain some information concerning the response of silicate glasses to deuterium ions, the difference in potential for electrodes prepared from the glasses of the Li_2O-SiO_2 series was determined between two solutions of limited buffer capacity prepared from D_2O by the use of P_2O_5 and CaO.[5] These materials were chosen because they did not introduce hydrogen ions, and at the same time they produced buffers, from inexpensive compounds, having a wide pD interval. The apparent values (obtained with a calibrated glass electrode) of the resulting buffers were pD 0.65 for the D_3PO_4 and pD 12.4 for $Ca(OD)_2$.

The results obtained for pD response and chemical durability of the Li_2O-SiO_2 glasses in these deuterium oxide buffers are given in table 4 and plotted (○) in figure 5. A comparison of these results with the data obtained with the Britton-Robinson universal buffers (fig. 4) indicates that the response to deuterium ions is superior to the response to hydrogen ions. However, a glance at the respective durability curves reveals that there is a marked superiority in durability of the glasses, especially at high alkalinity, in the special deuterium buffers over the aqueous Britton-Robinson buffers.

In order to obtain a more rigorous comparison, a set of parallel experiments were performed using water buffers prepared with the same constituents and of equal concentration as the deuterium oxide

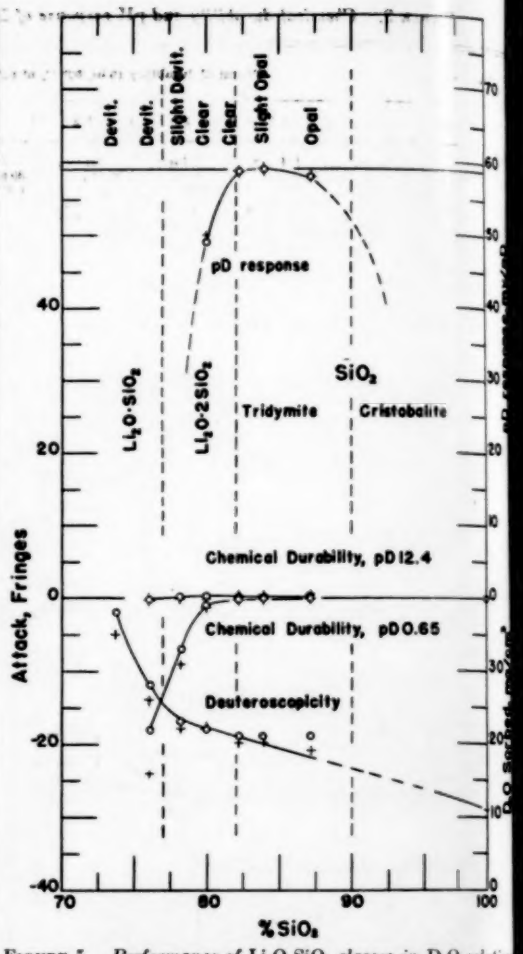

FIGURE 5. *Performance of Li_2O-SiO_2 glasses in D_2O solutions compared with the performance in H_2O solutions.*

(○), the pD response and chemical durability in deuterium oxide solutions of D_3PO_4, pD 0.65; and saturated $Ca(OD)_2$, pD 12.4 (+), the pH response and chemical durability in aqueous solutions of H_3PO_4, pH 0.65 and saturated $Ca(OH)_2$, pH 12.3.

solutions (Data listed in table 4 and plotted (+) in fig. 5.). When this was done, no significant differences in pH and pD response were detected. However, the impression remained that the electrode performances were slightly steadier in the deuterium oxide than in the aqueous solutions. In accordance with this, the amount of swelling observed in the acid deuterium oxide was less than in the corresponding aqueous solutions. It is also interesting to note that three of the glasses showed swelling in the saturated solution of $Ca(OH)_2$ above pH 12, while only one of them did so in the saturated solution of $Ca(OD)_2$. It should also be pointed out that the saturated solution of $Ca(OD)_2$ had an apparent pH approximately 0.1 of a unit higher than the pH of the $Ca(OH)_2$.

[5] The deuterium oxide having a certified purity of 99.8 percent of D_2O was obtained from stock available in the Bureau's Mineral Products Division, originally purchased from the Stuart Oxygen Co. of San Francisco, Calif., by permission of the Atomic Energy Commission.

TABLE 4. *pH and pD response, hygroscopicity, and deuteroscopicity, chemical durability in aqueous and deuterium oxide buffers prepared from P_2O_5 and CaO, of a series of Li_2O-SiO_2 glasses*

Glasses (B) table 1, except for glass containing 73.87 percent of SiO_2									
Glasses		Vapor sorbed 1 hr		Electrode response between—		Chemical durability (attack)			
Li_2O	SiO_2	H_2O	D_2O	pH 0.65 and 12.3	pD 0.65 and 12.4	H_3PO_4 pH 0.65	D_3PO_4 Apparent pD 0.65	$Ca(OH)_2$ pH 12.3	$Ca(OD_2)$ Apparent pD 12.4
%	%	mg/cm²	mg/cm²	mv/pH	mv/pD	*Fringes*	*Fringes*	*Fringes*	*Fringes*
26.13	73.87	35	38	(a)	.....	.....	.....	.....	.....
23.9	76.1	26	28	(a)	.....	24 swell.....	18 swell.....	¼ swell, pitted..	⅓₀ swell.
21.8	78.2	22	23	(b)	.....	9 swell.....	7 swell.....	8well, pitted.....	¼ attack.
20	80	22	22	50	49	1+ swell.....	1 swell.....	¼ swell, pitted..	¼− attack.
17.8	82.2	20	21	58.7	58.7	¼ swell.....	¼− swell.....	⅔₀ attack.....	⅔₀ attack.
16.1	83.9	20	21	59	59	⅔₀− swell.....	⅓₀ swell.....	⅓₀ attack.....	⅓₀ attack.
12.9	87.1	19	21	58	58	D[d] swell.....	D[d] swell.....	⅓₀ attack.....	⅓₀− attack.
Fused SiO_2....		11	.....	(c)	(c)	ND[c] swell.....	ND[c] swell.....	⅔₀ attack.....	⅓₀+ attack.
Corning 015....		104	111	58.4	58.1	⅔₀ swell.....	D[d] swell.....	¼− attack.....	⅔₀ attack.

[a] Devitrified while blowing electrodes. [b] Slight devitrification. [c] No definite electrode response. [d] D, detectable. [e] ND, not detectable.

Lithium Ion Response of Electrodes Prepared From Li_2O-SiO_2 Glasses

The question is often raised concerning the equivitive response of glass electrodes to positive ions ther than hydrogen, especially to ions common to oth the solution and to the glass. In the present se the response to lithium ions of an electrode prered from the lithium silicate glass (Li_2O, 12.9%; iO_2, 87.1%) was determined over the range pLi 1 3 in solutions containing $LiNO_3$ to which 1 ml of acial acetic acid per 50 ml of solution was added to aintain a constant pH during the observations. f one assumes that all of the voltage change observed etween the glass electrode and the saturated calomel reference cell over this pLi range can be attributed to the response of the glass electrode to Li^+ ions, he pLi response of the Li_2O-SiO_2 glass was less than mv per pLi. For all practical purposes it can be tated that a pLi response of electrodes prepared rom this Li_2O-SiO_2 glass is essentially absent, hereas a full pH and pD response is present.

It would be interesting to extend these investigaons to a study of the response of the glass electrode o tritium ions.

7 Summary

The pH and pD response of electrodes prepared rom a series of Li_2O-SiO_2 glasses have been compared ith the hygroscopicity, dueteroscopicity, and chemical durability of the glasses in aqueous and deuterium xide buffers. The curves for pH and pD response s a function of composition passed through an ptimum electrode response that was limited on the ow-silica end by poor chemical durability and a trong tendency toward devitrification of the glasses hile the electrodes were being blown. The optimum also fell off on the high-silica end where palescence appeared and the hygroscopicities and euteroscopicities decreased. The optimum electrode performance was attained by those glasses hat most nearly approximated the properties of Corning 015. However, this optimum appeared at lower sorption values than were found for Corning 015 and other glass systems previously investigated.

Electrodes prepared from the Li_2O-SiO_2 glasses apparently respond to deuterium ions as readily as to hydrogen ions.

In the present experiments the Li_2O-SiO_2 glasses showed detectably more swelling in the acid qaueous than in the acid deuterium oxide solutions. Interesting examples of swelling in alkaline buffers above pH and pD values of 12 were observed. The apparent pD values for saturated Ca $(OD)_2$ were slightly higher than for the corresponding Ca $(OH)_2$ buffer.

The pH and pD response, hygroscopicity, and deuteroscopicity, as well as the chemical durabilities in aqueous and deuterim oxide solutions, appear to reflect some of the critical features of the Li_2O-SiO_2 phase-equilibrium diagram with the optimum electrode response occurring in the composition range in which tridymite is the primary phase.

8. References

[1] Henry H. Cary, Warren P. Baxter, U. S. Patent 2,462,843 March 1949.
[2] G. A. Perley, U. S. Patent 2,444,845, July 1948.
[3] G. A. Perley, Composition of pH responsive glasses, Anal. Chem. **21**, 391 (1949).
[4] G. A. Perley, pH response of glass electrodes, Anal. Chem. **21**, 559 (1949).
[5] D. A. MacInnes and M. Dole, The behaviour of glass electrodes of different compositions, J. Am. Chem. Soc. **52**, 29 (1930).
[6] S. I. Ssokolof and A. H. Passynsky, On glass electrodes, Z. physik. Chem. **160**A, 366 (1932).
[7] J. L. Gabbard and M. Dole, Additional notes on the glass electrode: I. Glass electrode errors at 30° C; II. Properties of lithium glass electrodes, Trans. of Electrochem. Soc. **72**, 129 (1937).
[8] Malcolm Dole, The glass electrode, (John Wiley & Sons, Inc., New York, N. Y. 1941).
[9] Malcolm Dole, Recent advances in the theory and use of glass electrodes for pH determinations. Symposium on pH measurements, ASTM Technical Publication No. 73, p. 45 (1946).
[10] G. A. Perley, Discussion. Symposium on pH measurements, ASTM Technical Publication No. 73, p. 55 (1946).

[11] Donald Hubbard, Given W. Cleek, and Gerald F. Rynders, Electrode function (pH response), hygroscopicity, and chemical durability of Na_2O–CaO–SiO_2 glasses, J. Research NBS **44,** 247 (1950) RP2076.
[12] Donald Hubbard, Mason H. Black, and Gerald F. Rynders, Electrode function (pH response), hygroscopicity, and chemical durability of soda-lead oxide-silica glasses, J. Research NBS **45,** 430 (1950) RP2154.
[13] Donald Hubbard, Mason H. Black, Sylvanus F. Holley, and Gerald F. Rynders, Electrode function (pH response), hygroscopicity and chemical durability of soda-potash-silica glasses, J. Research NBS **46,** 168 (1951) RP2189.
[14] J. C. Young, F. W. Glaze, C. A. Faick, and A. N. Finn, Density of some soda-potash-silica glasses as a function of the composition, J. Research NBS **22,** 453 (1939) RP1197.
[15] Donald Hubbard, Hygroscopicity of optical glasses as an indicator of serviceability, J. Research NBS **36,** 511 (1946) RP1719.
[16] C. A. Faick and A. N. Finn, The index of refraction of some soda-lime-silica glasses as a function of the composition, J. Am. Cer. Soc. **14,** 518 (1931).
[17] C. A. Faick and Bernard Fonoroff, A precision apparat for the rapid determination of indices of refraction a dispersion by immersion, J. Research NBS 32, 67 (19 RP1575.
[18] J. B. Saunders, Improved interferometric proced with application to expansion measurements, Research NBS **23,** 179 (1939) RP1227.
[19] F. C. Kracek, System SiO_2-$2Li_2O$·SiO_2, J. Phys. Ch **34** (2) 2645 (1930).
[20] E. Berger, Grundsatzliches uber die chemische angr barkeit von glasen I. Glastech. Ber. dent. ch Ges. **14,** 351 (1936).
[21] Donald Hubbard, Edgar H. Hamilton, and Alfred Finn, Effect of the solubility of glass on the behav of the glass electrode, J. Research NBS **22,** 339 (19 RP1187.

Washington, June 16, 1952

Journal of Research of the National Bureau of Standards Vol. 49, No. 4, October 1952 Research Paper 2364

Calorimetric Properties of Polytetrafluoroethylene (Teflon) from 0° to 365° K[1]

George T. Furukawa, Robert E. McCoskey, and Gerard J. King

The thermal properties of polytetrafluoroethylene (Teflon) samples were investigated, using an adiabatic-vacuum calorimeter. The effect of the annealing and quenching processes on the heat capacity of a molded Teflon sample was studied. The heat-capacity data were used to compute the heat capacity, enthalpy, and entropy of the polymer samples at 5-deg intervals from 0° to 365° K. The heat-capacity results with the molded, annealed, and quenched samples of Teflon show the possibility of a glass transformation at about 160° K. The lack of a more definite glass-transformation effect is attributed to inter- and intramolecular hindrances to configurational changes in the Teflon polymer. The existence of first-order transitions at 293° and 303° K, previously reported by Quinn, Roberts, and Work, was confirmed.

1. Introduction

The examination of current scientific and industrial literatures indicates that the investigation and application of fluorine and fluorine compounds are becoming increasingly broader. Products containing fluorine are being used in such applications as heat-transfer agents, pest control, fire control, lubricants, pharmaceuticals, plastics, intermediates in synthesis, and many others. Although the fluorocarbons have molecular structure somewhat similar to their hydrocarbon analogs, their chemical and physical properties are greatly different. Similarly, fluorine-containing compounds have been found in many instances to behave very differently from the other halogen analogs. From these considerations it seems a systematic experimental investigation of "key" fluorine compounds would aid in the present far-reaching studies involving fluorine and its compounds.

The Bureau has undertaken a program for the study of thermodynamic properties of both simple and more complicated fluorocarbons. In the recent years the fluorocarbon plastic, polytetrafluoroethylene, has come into wide use, on account of its remarkable thermal and chemical stability, as gasket, packing, electrical insulation, and protective coating for vessels handling corrosive materials. Obviously, thermodynamic study of this material and its monomer, tetrafluoroethylene, would be highly desirable in the further understanding of polymerization processes and fundamental structure of polymers in general. This report deals with the heat-capacity investigations of two polytetrafluoroethylene samples. One sample was in the form of powder and the other in molded sheets. The enthalpy and entropy values were calculated from the heat-capacity data. The investigation confirmed the existence of two first-order transitions [1][2], one at 293° K and a much less pronounced one at 303° K. The heat-capacity results show the possibility of a glass transformation at about 160° K.

[1] This paper is based on the work sponsored by the Ordnance Corps, U. S. Department of the Army.

[2] Figures in brackets indicate the literature references at the end of this paper.

2. Experimental Procedure and Sample

The calorimetric apparatus and experimental procedures were essentially the same as used in the investigation of the thermal properties of diphenyl ether [2]. The details of the design and operation of a similar calorimeter are given in the paper on 1,3-butadiene by R. B. Scott, et al. [3]. Briefly, the experimental method was as follows: Each of the samples was placed in a copper container provided with vanes to promote the rapid attainment of thermal equilibrium and with a central well for a platinum resistance thermometer and heater assembly. The sample was pumped (vacuum about 10^{-4} mm Hg) for 2 days at room temperature and for 1 day at about 50° C to eliminate volatile impurities. There was no indication of continuous evolution of gases or loss of material during the pumping process. After the container was sealed with a small quantity of helium gas, it was suspended within the adiabatic shield system. At all times during the calorimetric experiments the shield was maintained at the same temperature as the container by means of differential thermocouples and shield heaters. The outer surface of the container and the adjacent shield surface were polished to minimize heat transfer by radiation. The vacuum surrounding the container was 10^{-5} mm Hg or better. The electric-power input to the calorimeter heater (about 100 ohms) was measured by means of a Wenner potentiometer in conjunction with a standard resistor and a volt box. The resistance of the platinum resistance thermometer was measured by using a Mueller-type bridge. The length of a heating period was determined with an interval timer run on standard 60 cycles furnished by the Radio Section of the Bureau. The timer was periodically compared with the time signals from the Time Section and was found to vary not more than 0.02 sec for a heating period, which was never less than 2 min. All electric instruments were recently calibrated at the Bureau.

The experimental measurements were usually made by first cooling the material to the lowest temperature attainable with the particular refrigerant. During this process the space surrounding the sus-

pended sample container was filled with a few centimeters of helium gas to permit rapid cooling. For slow cooling, however, the space was maintained at a high vacuum. Upon attaining the desired temperature, the helium gas was pumped out, and the experiments were made continuously up the temperature scale, the final temperature of the first heating period being the initial temperature of the second and so on. At the lower temperatures, where the slope of the heat-capacity curve changes rapidly, the temperature rise for a heating period was made as small as 2 to 3 deg to make negligible the curvature correction in the heat-capacity value obtained. At the higher temperatures, where the curvature is small, temperature intervals of about 5 to 10 deg were taken.

The heat-capacity measurements were made in the temperature range 15° to 370° K;[3] first, with the empty container, and then with the container plus the samples. The net heat capacities were obtained by subtracting the smoothed heat capacities of the empty container from the observed gross heat capacities. The net heat capacities so obtained are given in section 3.

Four series of experimental measurements were made with two samples of polytetrafluoroethylene, or Teflon.[4] One sample was a powder, and the other was in the form of $\frac{1}{16}$-in. sheet. The latter sample was prepared by molding the powder material. These materials are considered to be typical of the products currently made by the E. I. du Pont de Nemours Co. The Teflon powder was transferred directly into the copper container without further treatment, but the Teflon sheet was cut into small cubes of about $\frac{1}{16}$ in. on the edge before placing it in the container. This latter material without any further treatment will be designated as molded Teflon in order to distinguish it from the Teflon samples that were subjected to heat treatments prior to the heat-capacity experiments. In order to determine the extent to which an annealing process would increase the crystallinity in the Teflon sheet, the latter material was heated at 350° C under vacuum for 4 hr and cooled slowly to room temperature. This material will be designated as annealed Teflon. The fourth series of experiments was made with the Teflon sheet that had been heated to about 350° C until clear and quenched in liquid nitrogen. Renfrew and Lewis [4] obtained clear Teflon film by heating the film until clear and subsequently quenching it in water. The quenched $\frac{1}{16}$-in. Teflon sheet used in this investigation, however, was not clear. The heat-capacity experiments with the quenched Teflon were made only over a limited temperature range, about 120° to 330° K.

3. Results and Discussion

The experimental results, net heat capacities, from the four series of heat-capacity measurements with the powder, molded, annealed, and quenched Teflon samples are plotted in figures 1, 2, 3 and 4, respectively. The heat-capacity measurements with the Teflon powder were made after rapidly cooling the polymer (run 2) from room temperature to liquid nitrogen temperature. This was followed by experiments with the sample slowly cooled (run 4). Similar series of experiments were carried out with the molded Teflon (runs 1 and 2 were after cooling rapidly; run 5 was after cooling slowly). The heat-capacity results were not affected significantly by the rate of cooling. The experiments with the annealed and quenched Teflon samples were therefore made without varying the rate of cooling. The experimental values with the powder, molded, annealed samples were smoothed graphically, and the smoothed values are given in tables 1, 2, and respectively, at 5-deg intervals from 0° to 365° K. The values below 15° K were obtained by extrapolating a Debye function [2], which was fitted to the experimental values in the temperature range 15° to 30° K. The heat-capacity values between 280° and 310° K, where Teflon undergoes two first-order transitions, have been omitted in the tables. The smoothed heat capacities from the four series of experiments are compared in figure 5. No table of smoothed heat capacity of the quenched sample is given.

During the heat-capacity measurements persistent upward thermal drifts of about 1 mdeg min^{-1} were observed in the range 160° to 170° K with the Teflon powder. Similar upward drifts were found with the molded, annealed, and quenched Teflon samples in the range 145° to 175° K. The thermal drift is probably related to the much larger drifts observed with the rubber polymers [5] in the temperature range of glass transformation. The heat-capacity curves with the Teflon samples, however, do not exhibit the steep rise found with rubber polymers and other polymers, supercooled liquids, and noncrystalline solids at the glass-transformation temperature [6]. However, the results with the molded Teflon do show a slightly more rapid rise in the curve at about 160° K. The Teflon powder does not exhibit any unusual behavior in this temperature range. The quenched sample, in which greater amorphous character was expected to be frozen-in, does not exhibit any more pronounced rise in the curve at this temperature. Actually, the molded and quenched samples give almost identical heat-capacity values (fig. 5). This would indicate that the polymeric chain segments in Teflon are not sufficiently flexible or capable of rotation [6] to make a significant contribution to glass transformation. Also it is likely that the heating and the subsequent quenching processes did not freeze in sufficient amorphous character [4] or open structure in the polymer on account of its high melt viscosity [8]. Renfrew and Lewis [4] found, according to X-ray diffraction photographs, almost as much crystallinity in a Teflon sample heated above its high-temperature transition point and quenched in water as in a sample cooled slowly. According to the theory of viscous flow [7] the polymer segments cooperate in the flow by a simultaneous configurational change involving rotation of the polymer

[3] The temperatures expressed in degrees Kelvin were obtained from the relation °K = °C + 273.16°.

[4] The authors are indebted to W. D. Bowersox of the E. I. du Pont de Nemours Co. for the samples.

ments. As pointed out by Hanford and Joyce [8], rigidity of the Teflon polymer to rotation is nifested in the high melt viscosity and in the lity of the polymer to be form-stable under its own ght above its melting temperature (about 327° C). ese considerations seem to corroborate the non-stence of a pronounced glass-transformation effect Teflon. The annealing process, on the other hand, ms to have lowered the rise in the heat-capacity ve found for the molded and quenched Teflon mples at 160° K. This would indicate that the nealing process has increased the order in the fon polymer and that what little glass-trans-rmation effect that was present was decreased. fon is considered to exist in a high degree of rstallinity [4, 8, 11], and thus the polymer has a sed, well-packed structure that would further hibit glass transformation. The lowering of the at capacity with the annealed Teflon supports this ect of crystallization on the glass transformation.

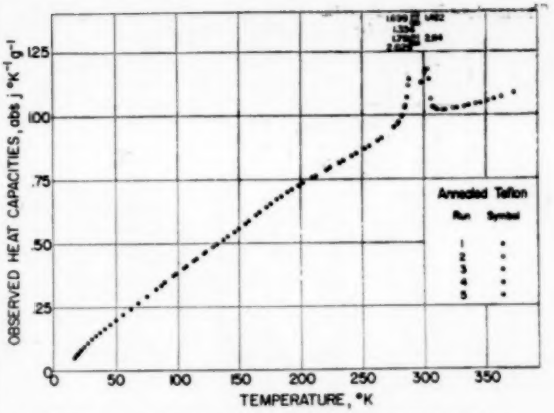

FIGURE 3. *Observed heat capacities of annealed Teflon.*

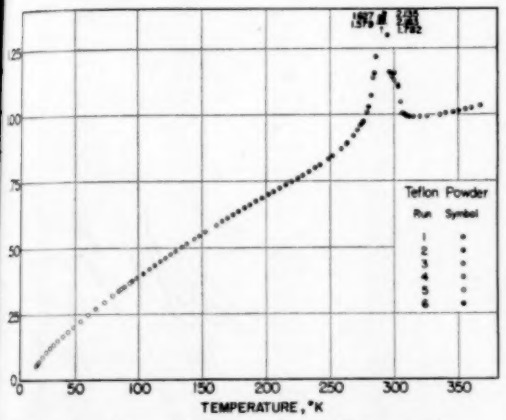

FIGURE 1. *Observed heat capacities of Teflon powder.*

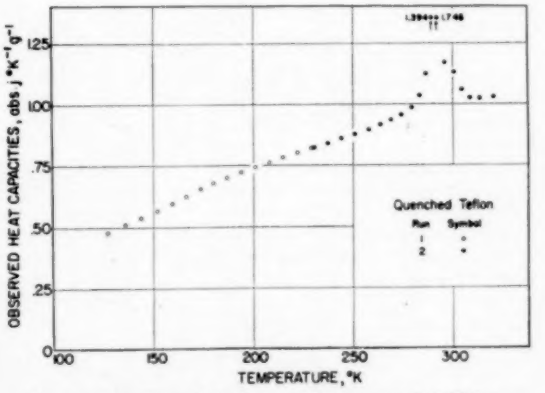

FIGURE 4. *Observed heat capacities of quenched Teflon.*

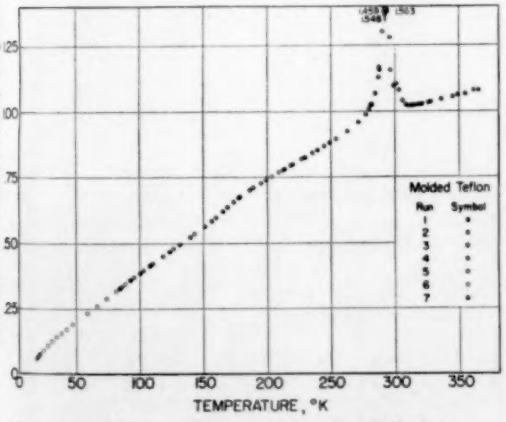

FIGURE 2. *Observed heat capacities of molded Teflon.*

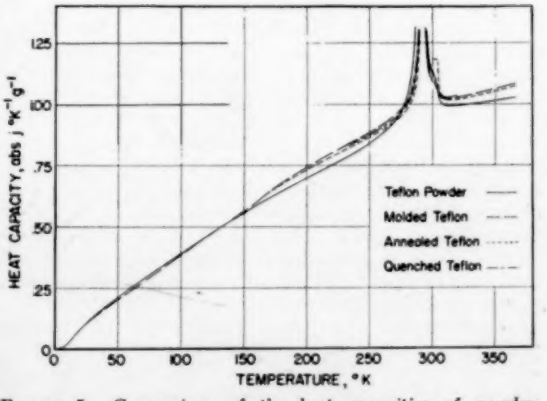

FIGURE 5. *Comparison of the heat capacities of powder, molded, annealed, and quenched Teflon samples.*

TABLE 1.—*Heat capacity, enthalpy, and entropy of Teflon powder at intergal temperatures*

T	C	$H_T-H_0^a$	$S_T-S_0^a$
°K	abs j °K^{-1} g^{-1}	abs j g^{-1}	abs j °K^{-1} g^{-1}
0	0	0	0
5	0.0024	0.003	0.0008
10	.0179	.046	.0062
15	.0472	.206	.0188
20	.0767	.519	.0355
25	.1033	.966	.0565
30	.1271	1.544	.0775
35	.1486	2.233	.0987
40	.1696	3.030	.1200
45	.1871	3.922	.1410
50	.2054	4.903	.1616
55	.2258	5.980	.1821
60	.2458	7.159	.2026
65	.2651	8.437	.2231
70	.2836	9.809	.2434
75	.3017	11.27	.2636
80	.3205	12.83	.2837
85	.3385	14.48	.3036
90	.3561	16.21	.3235
95	.3731	18.04	.3432
100	.3897	19.94	.3628
105	.4069	21.93	.3822
110	.4240	24.01	.4015
115	.4410	26.17	.4207
120	.4578	28.42	.4399
125	.4743	30.75	.4589
130	.4905	33.16	.4778
135	.5066	35.66	.4966
140	.5224	38.23	.5153
145	.5378	40.88	.5339
150	.5529	43.61	.5524
155	.5677	46.41	.5708
160	.5825	49.28	.5890
165	.5975	52.23	.6072
170	.6123	55.26	.6253
175	.6270	58.36	.6432
180	.6410	61.53	.6610
185	.6556	64.77	.6788
190	.6688	68.08	.6965
195	.6819	71.46	.7140
200	.6950	74.90	.7315
205	.7083	78.41	.7488
210	.7217	81.98	.7660
215	.7354	85.63	.7832
220	.7492	89.34	.8002
225	.7629	93.12	.8172
230	.7770	96.97	.8341
235	.7914	100.9	.8510
240	.8063	104.9	.8678
245	.8221	109.0	.8846
250	.8393	113.1	.9014
255	.8579	117.3	.9182
260	.8794	121.7	.9351
265	.9041	126.1	.9520
270	.9339	130.7	.9692
275	.9771	135.5	.9867
280	1.036	140.5	1.005
310	.9959	178.6	1.134
315	.9925	183.5	1.150
320	.9932	188.5	1.166
325	.9940	193.5	1.181
330	.9979	198.5	1.196
335	1.002	203.5	1.211
340	1.006	208.5	1.226
345	1.010	213.5	1.241
350	1.014	218.6	1.256
355	1.018	223.7	1.270
360	1.022	228.8	1.284
365	1.026	233.9	1.298

TABLE 2. *Heat capacity, enthalpy, and entropy of molded Teflon at integral temperatures*

T	C	$H_T-H_0^a$	$S_T-S_0^a$
°K	abs j °K^{-1} g^{-1}	abs j g^{-1}	abs j °K^{-1} g^{-1}
0	0	0	0
5	0.0021	0.003	0.0008
10	.0182	.047	.0063
15	.0477	.209	.0190
20	.0764	.524	.0359
25	.1016	.975	.0570
30	.1247	1.542	.0776
35	.1455	2.218	.0984
40	.1647	2.994	.1191
45	.1833	3.864	.1395
50	.2017	4.827	.1598
55	.2198	5.881	.1799
60	.2380	7.025	.1998
65	.2562	8.261	.2196
70	.2745	9.588	.2392
75	.2929	11.01	.2588
80	.3120	12.52	.2783
85	.3312	14.13	.2978
90	.3500	15.83	.3173
95	.3680	17.62	.3367
100	.3857	19.51	.3560
105	.4035	21.48	.3752
110	.4212	23.54	.3944
115	.4390	25.69	.4135
120	.4566	27.93	.4326
125	.4740	30.26	.4516
130	.4910	32.67	.4706
135	.5080	35.17	.4894
140	.5250	37.75	.5081
145	.5423	40.42	.5269
150	.5598	43.18	.5455
155	.5775	46.02	.5642
160	.5975	48.96	.5828
165	.6180	51.99	.6015
170	.6385	55.14	.6203
175	.6587	58.38	.6391
180	.6772	61.72	.6579
185	.6940	65.15	.6766
190	.7102	68.66	.6954
195	.7257	72.25	.7141
200	.7408	75.91	.7326
205	.7556	79.66	.7511
210	.7701	83.47	.7695
215	.7842	87.36	.7878
220	.7982	91.31	.8060
225	.8120	95.34	.8241
230	.8257	99.43	.8421
235	.8394	103.6	.8600
240	.8533	107.8	.8778
245	.8673	112.1	.8955
250	.8818	116.5	.9132
255	.8971	120.9	.9308
260	.9133	125.5	.9484
265	.9315	130.1	.9659
270	.9526	134.8	.9835
275	.9765	139.6	1.001
280	1.012	144.6	1.019
310	1.021	179.3	1.137
315	1.023	184.4	1.153
320	1.027	189.5	1.169
325	1.032	194.7	1.185
330	1.038	199.8	1.201
335	1.044	205.1	1.217
340	1.049	210.3	1.232
345	1.055	215.5	1.248
350	1.061	220.8	1.263
355	1.068	226.2	1.278
360	1.074	231.5	1.293
365	1.081	236.9	1.308

In the range 280° to 310° K, the Teflon samples exhibit a transformation involving a large enthalpy change. The heat-capacity curve rises sharply and falls with a small "shoulder." The experiments with the annealed sample resolved the "shoulder" into a small peak. These effects are shown and compared in different samples in figures 1 to 5. The authors believe that, from the nature of the two peaks, two first-order transitions are present. During the heat-capacity experiments persistent downward thermal drifts were observed in this temperature range. These thermal drifts are quite similar to those observed in the investigation of crystallization in rubber polymers [5]. The thermal drifts are believed to arise as the bulky macromolecules slowly alter their configuration. The heat-capacity results would be thus dependent somewhat on the time allowed for thermal equilibrium. As experience with rubber polymers [5] show that these thermal drifts can continue for an undesirably long period, the thermal drifts were not followed for longer than 30 min. The existence and the long duration of the thermal drifts in this temperature range are substantiated by the long periods required for volume

TABLE 3. *Heat capacity, enthalpy, and entropy of annealed Teflon at integral temperatures*

T	C	$H_T - H_0^S$	$S_T - S_0^S$
°K	abs j °K^{-1} g^{-1}	abs j g^{-1}	abs j °K^{-1} g^{-1}
0	0	0	0
5	0.0024	0.0030	0.0008
10	.0182	.0470	.0063
15	.0483	.2089	.0190
20	.0759	.5204	.0367
25	.1012	.9641	.0564
30	.1244	1.529	.0770
35	.1453	2.204	.0977
40	.1642	2.978	.1184
45	.1833	3.847	.1388
50	.2020	4.811	.1591
55	.2200	5.866	.1792
60	.2378	7.010	.1991
65	.2560	8.245	.2189
70	.2744	9.571	.2385
75	.2929	10.99	.2581
80	.3119	12.50	.2776
85	.3313	14.11	.2971
90	.3500	15.81	.3166
95	.3682	17.61	.3360
100	.3858	19.49	.3553
105	.4037	21.47	.3746
110	.4215	23.53	.3938
115	.4391	25.68	.4129
120	.4565	27.92	.4320
125	.4738	30.25	.4509
130	.4910	32.66	.4699
135	.5080	35.16	.4887
140	.5250	37.74	.5075
145	.5418	40.41	.5262
150	.5587	43.16	.5449
155	.5756	45.99	.5634
160	.5971	48.92	.5821
165	.6164	51.96	.6007
170	.6350	55.09	.6194
175	.6531	58.31	.6381
180	.6704	61.62	.6567
185	.6866	65.01	.6753
190	.7019	68.48	.6938
195	.7164	72.03	.7122
200	.7306	75.64	.7306
205	.7445	79.33	.7488
210	.7583	83.09	.7669
215	.7720	86.91	.7849
220	.7854	90.81	.8028
225	.7986	94.77	.8206
230	.8115	98.79	.8383
235	.8244	102.9	.8559
240	.8373	107.0	.8734
245	.8504	111.3	.8908
250	.8639	115.5	.9081
255	.8776	119.9	.9253
260	.8918	124.3	.9425
265	.9060	128.8	.9596
270	.9256	133.4	.9768
275	.9482	138.1	.9940
280	.9761	142.9	1.011
310	1.023	179.4	1.135
315	1.021	184.5	1.151
320	1.023	189.6	1.168
325	1.027	194.7	1.183
330	1.031	199.9	1.199
335	1.036	205.0	1.215
340	1.042	210.2	1.230
345	1.048	215.4	1.245
350	1.052	220.7	1.260
355	1.061	226.0	1.275
360	1.068	231.3	1.290
365	1.075	236.7	1.305

equilibrium found in dilatometer experiments [11, 12]. The first peak, or the transition involving the greater enthalpy change, is estimated to be at about 293° K, and the second peak to be at 303° K. Rigby and Bunn [11], using a dilatometer method, observed a single first-order transition in Teflon at 20° C. These authors also obtained X-ray diffraction photographs of the polymer at various temperatures, and reported a change from a more ordered to a less ordered crystal structure as the temperature was increased. These authors mentioned further that the two states are not sharp and distinct. More

TABLE 4. *Comparison of the enthalpy and entropy change in the interval 280° to 310° K*

Sample and run	ΔH	ΔS
	abs j g^{-1}	abs j °K^{-1} g^{-1}
Teflon powder:		
Run 4	38.02	0.1293
Run 6	38.04	.1294
Molded Teflon:		
Run 3	34.68	.1177
Run 4	34.75	.1180
Annealed Teflon:		
Run 2	36.42	.1236
Run 4	36.53	.1240
Quenched Teflon:		
Run 2	35.49	.1205

recently, Quinn, et al. [1], using a volume dilatometer method, observed two first-order transitions in their volume-temperature curve at 20° and 30° C. Their results give evidences of large hysteresis in the volume-temperature curve. Similarly, Pierce, et al. [12] obtained X-ray diffraction photographs with Teflon and attributed the first change in crystal order, occurring from 17° to 20° C, to first-order transition. However, the second change occurring in the range of temperature above 20° C was reported as being from second-order transition (glass transformation). The three investigations [10, 11, 12] mentioned above show that the transitions involve a change in the volume of about 1 to 1.2 percent. Renfrew and Lewis [4], using both time-temperature cooling and heating curves, found two first-order transitions in the range of temperature from 318° to 327° C. These authors suggested the possibility of the existence of two crystalline forms with their melting points closely spaced. The existence of two crystalline forms would seem possible on the basis that both left- and right-handed helical polymers exist due to the high rotational hindrance. Probably the two forms exist independently even within the same polymer molecule. Furthermore, each helical form probably can exist in two crystalline states as found by Bunn and Garner [13] with polyamides, either of the two states being obtained by relative translation along the chain axes [11]. The two room-temperature transitions in Teflon probably can be attributed to the crystal-crystal transformation in each of the helical forms.

The enthalpy change between 280° and 310° K is compared in table 4 for the four Teflon samples. The results show that Teflon powder has the largest enthalpy change. Both annealing and quenching processes seem to have increased the enthalpy change in this temperature interval, the annealing more so than the quenching process. Assuming the average heat capacity over the range 280° to 310° K to be 1 abs j °K^{-1} g^{-1}, the heat of transition associated with the two first-order transitions would be about 4 to 8 abs j g^{-1}, depending upon the physical state of the polymer.

The enthalpy and entropy values, given in tables 1, 2, and 3, were obtained by tabular integration of the heat capacities using the four-point Lagrangian integration coefficients [14]. The values at 15° K and below were obtained by evaluating the Debye function [2] fitted to the heat-capacity results in the

temperature range 15° to 30° K. Between 280° and 310° K, the experimental net heat capacities were used to evaluate the enthalpy and entropy change. The enthalpy change was obtained by summing the products of the net heat capacity and the temperature change for the intervals. The entropy change was obtained similarly by summing the $C\Delta T/T$'s, where C is the net heat capacity, ΔT the temperature change, and T the corresponding midtemperature of the interval. As in the case of rubber polymers [4], the Teflon polymer may be expected to have a residual entropy at the absolute zero of temperature due to its being a mixture of polymers of varying molecular weights, and to the random orientation of the polymer chains.

It is interesting to note (tables 1, 2, and 3), in comparing the enthalpies and entropies at 310° K of the powder, molded, and annealed Teflon samples, that these thermal quantities are almost equal. The large differences in these quantities at 280° K are offset by the adjusting effect of the two first-order transitions occurring between 280° and 310° K. The molded and annealed Teflon samples exhibit heat-capacity values quite similar above 310° K, and thus the enthalpy and entropy values continue to be close. On the other hand, the Teflon powder has considerably lower heat-capacity values above 310° K, and thus the thermal quantities above 310° K differ more.

The experimental results with the four Teflon samples show that the heat capacity of a Teflon specimen would be dependent upon its mechanical and thermal history. The heat treatment with respect to the high-temperature transition points (about 318° to 327° C) affects the heat capacity significantly. On the other hand, as pointed out previously, rapid or slow cooling of the polymer from room temperature does not show a significant effect upon the heat-capacity values. The deviation plot of the net heat capacities, except in the range 280° to 310° K, showed that above 50° K the results have a maximum spread of 0.1 percent, regardless of the rate at which the sample was cooled. In most cases the spread is much less than this value. From various considerations, the authors believe that the results for the same Teflon sample have an error[5] of 0.2 percent.

The authors are indebted to W. Bruenner and M. L. Reilly for some of the measurements and calculations.

4. References

[1] F. A. Quinn, Jr., D. E. Roberts and R. N. Work, J. Applied Phys. **22,** 1085 (1951).
[2] G. T. Furukawa, D. C. Ginnings, R. E. McCoskey, and R. A. Nelson, J. Research NBS **46,** 195 (1951) RP2191.
[3] R. B. Scott, C. H. Meyers, R. D. Rands, Jr., F. G. Brickwedde, and N. Bekkedahl, J. Research NBS **35,** 39 (1945) RP1661.
[4] M. M. Renfrew and E. E. Lewis, Ind. Eng. Chem. **38,** 870 (1946).
[5] G. T. Furukawa, R. E. McCoskey and Gerard J. King, NBS Reports 1016 (CR No. 2704), 1118 (CR No. 2804) and 1520 (CR No. 2961) to the Reconstruction Finance Corporation, Synthetic Rubber Division.
[6] W. Kauzmann, Chem. Rev. **43,** 219 (1948).
[7] W. Kauzmann and H. Eyring, J. Am. Chem. Soc. **62,** 3113 (1940).
[8] W. E. Hanford and R. M. Joyce, J. Am. Chem. Soc. **68,** 2082 (1946).
[9] H. C. Raine, R. B. Richards, and H. Ryder, Trans. Faraday Soc. **41,** 56 (1945).
[10] E. Hunter and W. G. Oakes, Trans. Faraday Soc. **41,** 49 (1945).
[11] H. A. Rigby and C. W. Bunn, Nature **164,** 583 (1949).
[12] R. H. H. Pierce, Jr., W. M. D. Bryant and J. F. Whitney, American Chemical Society Meeting (Buffalo, New York, March 23 to 27, 1952).
[13] C. W. Bunn and E. V. Garner, Proc. Roy. Soc. (London) [A] **189,** 39 (1947).
[14] Tables of Lagrangian Interpolation Coefficients (Columbia University Press, New York, N. Y., 1944).

WASHINGTON, D. C., June 13, 1952.

---

[5] For these experiments a true probable error cannot be statistically computed. The value given is an estimate arrived at by examining contributions to the inaccuracy from all known sources, and it is to be considered as the authors' best estimate of the error, which is just as likely to be exceeded as not.